ERDC/GSL TR-22-24

Geotechnical and Structures Laboratory

US Army Corps
of Engineers®
Engineer Research and
Development Center

ERDC
ENGINEER RESEARCH & DEVELOPMENT CENTER

U.S. Air Force Rapid Airfield Damage Recovery (RADR) Program

Evaluation of a Prototype Integrated Pavement Screed for Screeding Asphalt or Concrete Crater Repairs

Ben C. Cox, Nolan R. Hoffman, and Thomas A. Carr

September 2022

Approved for public release; distribution is unlimited.

The U.S. Army Engineer Research and Development Center (ERDC) solves the nation's toughest engineering and environmental challenges. ERDC develops innovative solutions in civil and military engineering, geospatial sciences, water resources, and environmental sciences for the Army, the Department of Defense, civilian agencies, and our nation's public good. Find out more at www.erdc.usace.army.mil.

To search for other technical reports published by ERDC, visit the ERDC online library at https://erdclibrary.on.worldcat.org/discovery.

ERDC/GSL TR-22-24
September 2022

Evaluation of a Prototype Integrated Pavement Screed for Screeding Asphalt or Concrete Crater Repairs

Ben C. Cox, Nolan R. Hoffman, and Thomas A. Carr

Geotechnical and Structures Laboratory
U.S. Army Engineer Research and Development Center
3909 Halls Ferry Road
Vicksburg, MS 39180-6199

Final report

Approved for public release; distribution is unlimited.

Prepared for Headquarters, Air Force Civil Engineer Center
139 Barnes Avenue, Suite 1
Tyndall AFB, FL 32403-5319

Under Project 471376, U.S. Air Force Rapid Airfield Damage Recovery (RADR) Program

Abstract

Finishing, or screeding, the hot mix asphalt or rapid-setting concrete surface of a crater repair is important for rapid airfield damage recovery (RADR) since it determines the aircraft ride surface quality. The objective of RADR repairs is to expediently produce a flush repair, defined as ±0.75 in. of the surrounding pavement surface, with minimal logistical and personnel burden. Multiple screeds were previously evaluated; the most recent project proposed a prototype design of a telehandler-operated integrated screed for both small and large repairs using asphalt or concrete. This project's objective was to finalize the prototype design and fabricate and test the prototype RADR screed.

The prototype RADR screed was successful for small repairs (8.5×8.5 ft). Large repairs (30×30 ft) were generally successful with modest repair quality criteria (RQC) issues being the only notable deficiencies. Large concrete repair RQC issues were attributed to plastic formwork movement, and large asphalt repair RQC issues were attributed to compaction issues or improper roll-down factors. Methods to mitigate these factors were investigated but should be further evaluated. Overall, the RADR screed was successful from technical perspectives but, functionally, is 600-800 lb overweight. Weight reduction should be considered before entering production.

DISCLAIMER: The contents of this report are not to be used for advertising, publication, or promotional purposes. Citation of trade names does not constitute an official endorsement or approval of the use of such commercial products. All product names and trademarks cited are the property of their respective owners. The findings of this report are not to be construed as an official Department of the Army position unless so designated by other authorized documents.

DESTROY THIS REPORT WHEN NO LONGER NEEDED. DO NOT RETURN IT TO THE ORIGINATOR.

Contents

Abstract ii

Figures and Tables v

Preface ix

1 Introduction 1

1.1 Background 1

1.1.1 Rapid Airfield Damage Recovery (RADR) 1

1.1.2 Pavement screeds and screeding operations 1

1.2 Objectives and scope 2

1.3 Outline of chapters 2

2 Literature Review 3

2.1 Concrete screeds 3

2.2 Asphalt screeds 5

2.3 Integrated screeds 7

3 Prototype RADR Screed 11

3.1 Overview of design 11

3.2 Screed bar 13

3.2.1 Initial finite element analysis and design 13

3.2.2 Final screed bar 16

3.3 Screed frame 18

3.4 Asphalt screed attachments 25

3.4.1 Grade control skis 26

3.4.2 Automatic grade control system (AGCS) 27

3.4.3 Manual grade control system (MGCS) 30

3.4.4 Ride track for grade control systems 31

3.4.5 End gates 32

3.4.6 Cutoff wheel 33

4 Experimental Program 35

4.1 Materials tested 35

4.1.1 Rapid-setting flowable fill 35

4.1.2 Rapid-setting concrete 43

4.1.3 Hot mix asphalt 43

4.2 Field test site 44

4.3 Test crater preparation 45

4.4 Equipment 50

4.4.1 Compact track loader 50

4.4.2 Telehandlers 50

4.4.3 Simplified volumetric mixer 51

4.4.4 Double drum vibratory roller 52

4.5 Crater repair methods 53
4.5.1 Concrete repairs 54
4.5.2 Asphalt repairs 55
4.6 Data collection 61
4.6.1 Surface profile surveys 61
4.6.2 Asphalt coring 65

5 Operation and Use of the RADR Screed 66
5.1 Connecting the screed and telehandler 66
5.1.1 Detailed description 66
5.1.2 Simplified steps 67
5.2 Concrete repair 67
5.2.1 Detailed description 67
5.2.2 Simplified steps 71
5.3 Asphalt repair 72
5.3.1 Detailed description 72
5.3.2 Simplified steps 79

6 RADR Screed Test Results 82
6.1 Large concrete repair 82
6.2 Small concrete repair 91
6.3 Large asphalt repair 93

7 Discussion of Results 108
7.1 RADR screed strengths 108
7.2 RADR screed areas of concern 109
7.2.1 Weight and telehandler capacity 109
7.2.2 Large repair finish quality 112

8 Conclusions and Recommendations 113
8.1 Conclusions 113
8.2 Recommendations 115

References 117

Unit Conversion Factors 119

Report Documentation Page

Figures and Tables

Figures

Figure 2.1. Concrete screeds tested in Carruth (2019). 3
Figure 2.2. Modified Autoskreed prototypes tested in Cox and Hoffman (2019). 4
Figure 2.3. CTL with Simex ST 200 screed attachment (Jackson and Hall 2014). 5
Figure 2.4. ARA prototype telehandler attachment asphalt screeds. 6
Figure 2.5. ASTH asphalt screeding attachments (Cox and Hoffman 2019). 8
Figure 2.6. Original ASTH design vs. new integrated screed design concept. 10
Figure 3.1. RADR screed overview–concrete configuration. 11
Figure 3.2. RADR screed overview–asphalt configuration. 12
Figure 3.3. Example screed bar design and FEA boundary and loading conditions. 14
Figure 3.4. Screed bar FEA results for ASTH screed. 15
Figure 3.5. Screed bar FEA results for RADR screed. 16
Figure 3.6. Final truss design of RADR screed bar. 17
Figure 3.7. Overview of RADR screed bar. 17
Figure 3.8. RADR screed-bar extension wings shown down (left) and up (right). 18
Figure 3.9. RADR screed frame overview. 19
Figure 3.10. RADR screed suspension system (right side) and support legs. 20
Figure 3.11. Use of leveling jacks to control RADR screed bar roll. 21
Figure 3.12. RADR screed travel springs at rest and partially compressed. 21
Figure 3.13. RADR screed crash rack and fork pocket extension adapter. 22
Figure 3.14. RADR screed cam action draw latch. 23
Figure 3.15. RADR screed power cord and connections. 24
Figure 3.16. RADR screed control pendant. 24
Figure 3.17. RADR screed swinging level indicators. 25
Figure 3.18. RADR screed attachment mounting locations. 26
Figure 3.19. RADR screed grade control ski. 27
Figure 3.20. RADR screed automatic grade control system (AGCS). 28
Figure 3.21. RADR screed AGCS–transition from existing pavement into repair. 29
Figure 3.22. RADR screed AGCS–transition out of repair to existing pavement. 30
Figure 3.23. RADR screed manual grade control system (MGCS). 31
Figure 3.24. RADR screed ride track for AGCS or MGCS. 32
Figure 3.25. RADR screed end gate. 33
Figure 3.26. RADR screed cutoff wheel. 34
Figure 4.1. Percolation observations for dry-placed flowable fill. 37
Figure 4.2. Dry-placed flowable fill DCP testing and coring setup. 37
Figure 4.3. Example DCP plot showing CBR vs. depth. 38

Figure 4.4. Dry pockets of flowable fill along formwork edges. 38
Figure 4.5. Attempted cores from dry-placed flowable fill. 39
Figure 4.6. CBR values determined from DCP testing. 39
Figure 4.7. Compressive strength and flow consistency of wet-placed flowable fill. 41
Figure 4.8. Photographs of flowable fill cylinders showing voids. 42
Figure 4.9. Aerial views of ERDC test sections. 45
Figure 4.10. Producing test craters. 46
Figure 4.11. Plastic formwork for large crater C1. 46
Figure 4.12. Placement plan for large crater C6 backfill. 47
Figure 4.13. Crater C6 flowable fill backfill–dry placement method (stage 1). 48
Figure 4.14. Crater C6 flowable fill backfill–wet placement method (stage 2). 48
Figure 4.15. Final crater C6 backfill profile and surveying. 49
Figure 4.16. Crater C6 surface profile showing depth (in.). 49
Figure 4.17. Caterpillar 277C compact track loader. 50
Figure 4.18. Caterpillar telehandlers. 51
Figure 4.19. Simplified volumetric mixer. 52
Figure 4.20. Double drum steel wheel roller. 53
Figure 4.21. Overview of concrete repair process. 54
Figure 4.22. Overview of asphalt repair process. 56
Figure 4.23. Illustration of asphalt placement in three paving lanes. 58
Figure 4.24. Excess asphalt cleanup prior to compaction. 59
Figure 4.25. Asphalt compaction. 60
Figure 4.26. Roller pattern for asphalt compaction. 60
Figure 4.27. Cutting back asphalt longitudinal joints. 61
Figure 4.28. Survey point layout illustration for large repairs. 62
Figure 4.29. Coring layout for large asphalt repairs. 65
Figure 5.1. Illustration of telehandler alignment with large concrete repair. 68
Figure 5.2. Illustration of telehandler outrigger deployment. 69
Figure 5.3. Illustration of telehandler alignment with large asphalt repair. 74
Figure 5.4. Illustration of screed roll due to telehandler boom sag. 75
Figure 6.1. Repair R1 overview photographs. 83
Figure 6.2. Repair R1 detail photographs. 84
Figure 6.3. Repair R1 surface profile survey map. 85
Figure 6.4. Dip in R1 quadrant 1 surface due to sagging forms. 85
Figure 6.5. Example mag bar surface profile survey map. 88
Figure 6.6. Example ASTH surface profile survey map. 89
Figure 6.7. Histogram comparing screed elevation deviations. 90
Figure 6.8. Box and whisker plot comparing screed elevation deviations. 90
Figure 6.9. Example overview photographs of small repair (R2 shown). 91

Figure 6.10. Surface profile survey maps for repairs R2 to R5. 92
Figure 6.11. Repairs R6 and R7 timing data. 93
Figure 6.12. Repairs R6 and R7 temperature data. 94
Figure 6.13. Repair R6 and R7 overview photographs. 96
Figure 6.14. Excess AC overflowing RADR screed inside end gate. 97
Figure 6.15. Second telehandler assisting with lifting screed. 97
Figure 6.16. Scuffing from grade control ski during repair R6. 98
Figure 6.17. Scuffing and joints on completed repair R6. 98
Figure 6.18. Depression at end of repair R6, L1 from over-rolling. 99
Figure 6.19. Detail of repair R6 pavement surface. 99
Figure 6.20. Effect of trimming joints on repair R7. 99
Figure 6.21. Tracking from AGCS during repair R7. 100
Figure 6.22. Tracking and scuffing on completed repair R7. 101
Figure 6.23. Transverse compaction of repair R7. 101
Figure 6.24. Repair R6 surface profile survey map. 102
Figure 6.25. Repair R7 surface profile survey map. 103
Figure 6.26. Repair R6 and R7 elevation histogram. 104
Figure 6.27. Profile view of repairs R6 and R7 elevations by lane. 105
Figure 6.28. Flushness vs. roll-down factor ratio for repair R7. 106
Figure 6.29. Air void data for repairs R6 and R7. 106
Figure 7.1. CAT TL1055C load chart. 110
Figure 7.2. Genie GTH-1256AF load chart. 111

Tables

Table 3.1. RADR screed physical properties. 12
Table 3.2. Screed bar FEA results. 15
Table 4.1. MIL-DTL-32527 flowable fill performance specifications. 35
Table 4.2. Draft revised flowable fill performance specifications. 36
Table 4.3. Hot mix asphalt concrete mix design properties. 44
Table 4.4. Crater properties for RADR screed testing. 45
Table 4.5. Telehandler specifications. 51
Table 4.6. Double drum vibratory roller specifications. 53
Table 4.7. RADR screed test plan by crater ID. 53
Table 4.8. Proposed RADR repair quality categories. 64
Table 6.1. Repair R1 placement data. 82
Table 6.2. Repair R1 survey results (by quadrant). 86
Table 6.3. Repair R1 survey results (by longitudinal profile line). 87
Table 6.4. Supplemental mag bar and ASTH survey data for large concrete repairs. 89

Table 6.5. Repair R2 to R5 survey results..... 92
Table 6.6. Repairs R6 and R7 parameters and dimensions..... 95
Table 6.7. Repairs R6 and R7 survey results..... 104

Preface

This study was conducted for the U.S. Air Force Civil Engineer Center (AFCEC), Tyndall Air Force Base, FL, under Project 471376, U.S. Air Force Rapid Airfield Damage Recovery (RADR) Program. The program manager was Dr. Robert Diltz of AFCEC. Mr. Jeb S. Tingle provided technical oversight of the project for the U.S. Army Engineer Research and Development Center (ERDC).

The work was performed by the Airfields and Pavements Branch (GMA) of the Engineering Systems and Materials Division (GM), U.S. Army Engineer Research and Development Center, Geotechnical and Structures Laboratory (ERDC-GSL). At the time of publication, Ms. Anna M. Jordan was Chief, GMA; Mr. Justin S. Strickler was Chief, GM; and Ms. Pamela G. Kinnebrew, GZT, was Technical Director for Military Engineering. Mr. Charles W. Ertle II was Deputy Director, ERDC-GSL, and Mr. Bartley P. Durst was Director.

COL Christian Patterson was the Commander of ERDC, and Dr. David W. Pittman was the Director.

1 Introduction

1.1 Background

1.1.1 Rapid Airfield Damage Recovery (RADR)

Rapid airfield damage recovery (RADR) includes recovery activities in response to an airbase attack to re-establish safe aircraft operations. Completing repairs in an expedient manner is key. Further, those repairs must utilize suitable materials, equipment, and construction techniques to reduce the need for subsequent repairs to maintain an operable pavement surface. Carruth (2019) provides a comprehensive summary of approximately two decades of prior work that has been conducted to modernize airfield damage repair technologies.

The present U.S. Air Force (USAF) RADR program has a specific focus on lighter and leaner equipment, materials, and tactics. Pieces of equipment that are smaller (more easily deployable), more versatile (able to perform the role of and replace multiple pieces of equipment), or require fewer personnel to operate are examples of lighter, leaner equipment.

1.1.2 Pavement screeds and screeding operations

The finishing, or screeding, of the surface material used for crater repairs (i.e., hot mix asphalt or rapid-setting concrete) is an important task in the RADR process since it determines the aircraft ride surface quality. As prescribed in the AFCEC *Interim RADR Tactics, Techniques, and Procedures (TTPs)* report (USAF-AFCEC 2019), final repair surfaces are assessed using repair quality criteria (RQC) as defined in Air Force Technical Order (TO) 35E2-5-1 (USAF 1992). Therein, a repair must be within ±0.75 in. of the surrounding existing pavement to be considered a flush repair, which is the objective for RADR repairs.

Multiple screeds have previously been evaluated for RADR applications over the years, each having some limitations or operational drawbacks. One recurring issue is that screeds may work adequately for small repairs (e.g., 8.5-ft square) but not for large repairs (e.g., 30-ft square). Traditionally, screeds have been specific to material type, being either a concrete screed or an asphalt screed, meaning unique pieces of equipment are required; more recent efforts have focused on the development of screeds that integrate both

concrete and asphalt screeding capabilities into a single device. Previous screed development and testing efforts are further described in Chapter 2. This report describes the development and evaluation of an integrated pavement screed prototype that was derived from the information learned from previous projects as well as the incremental improvement of promising screeds previously tested.

1.2 Objectives and scope

The overall objective of this project was to design, build, and test a single, integrated screed device that meets the following criteria.

1. It can be telehandler-operated by two persons (operator and spotter).
2. It can perform small (8.5×8.5 ft) and large (30×30 ft) repairs.
3. It is universal to both rapid-setting concrete (RSC) and hot mix asphalt concrete (AC) materials.

The objective of this project was accomplished through contract partnership with a fabrication shop to build the screed prototype and through full-scale field testing at ERDC of small and large crater repairs with both RSC and AC. The prototype screed is referred to throughout this report as the RADR screed.

1.3 Outline of chapters

Chapter 2 provides a literature review of previous screed testing for RADR applications. Chapter 3 describes the design process for the RADR screed and introduces the fabricated prototype. Chapter 4 describes the experimental program utilized in this project. Chapter 5 details operation and use of the screed. Chapter 6 presents results from screed tests. Chapter 7 provides discussion of results, and Chapter 8 presents conclusions and recommendations.

2 Literature Review

This literature review focuses on summarizing previous development and testing of screeds for airfield damage repair applications. This review is not intended to be exhaustive; rather, it is intended to be a high-level summary of general work conducted and key outcomes to aid in understanding the current work described in this report.

2.1 Concrete screeds

Several screeds have been previously evaluated by the U.S. Army Engineer Research and Development Center (ERDC) for rapid-setting concrete (RSC) applications. Carruth (2019) describes the testing of five commercially available screeds shown in Figure 2.1, including the manual vibratory screed (Wyco Screed King), which is utilized in the Interim RADR TTPs (USAF-AFCEC 2019).

Figure 2.1. Concrete screeds tested in Carruth (2019).

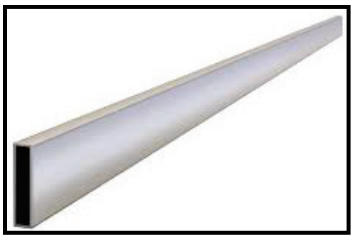

(a) Magnesium bar screed

(b) Wyco Screed King

(c) Spin screed

(d) Multiquip WSHE50KIT11H truss screed

(e) Original Autoskreed

The Figure 2.1 screeds exhibited a wide range of attributes with respect to cost, ease of use, quality of finish, and time requirements. As observed in prior RADR work, the screeds could all generally meet RQC requirements, but most required at least three personnel to effectively operate and have been described as cumbersome during after action reviews (AARs) in other troop demonstrations. Carruth (2019)

recommended that the Autoskreed, which is a hydraulic compact track loader (CTL) attachment, be pursued further with modifications.

Modifications to the original Autoskreed by the manufacturer led to the development of two new Autoskreed prototypes, the hydraulic Autoskreed (ASHyd) and the telehandler Autoskreed (ASTH) (Figure 2.2). Both screeds were evaluated in Cox and Hoffman (2019). The ASHyd was very similar to the original Autoskreed in that it was a hydraulically operated system, but it differed in that it was a stand-alone system rather than a CTL attachment. The ASTH was a simpler system with no power supply or major mechanical parts and was intended to utilize a 10,000-lb capacity telehandler as the prime mover.

Figure 2.2. Modified Autoskreed prototypes tested in Cox and Hoffman (2019).

a) Hydraulic Autoskreed (ASHyd) b) Telehandler Autoskreed (ASTH)

Both screeds were used to finish small and large crater repairs where large repairs were conducted in 15×15-ft quadrants. Both screeds alleviated the physical labor demands of earlier manual screeds and were less cumbersome. Relative to previously tested screeds that were not well-suited for large repairs, both the ASHyd and ASTH handled large repairs fairly well due to screed-bar extension wings that increased the screed width from 12 to 17 ft.

The ASHyd presented a greater maintenance and operations burden due to the onboard motor and hydraulics system, but it did not provide any performance benefits relative to the ASTH. As a result, the ASTH was put forward as the leading screed option at the time and was included in the RADR demonstration at the Silver Flag Exercise Site at Tyndall Air Force Base, FL, in September 2017 (Bell et al. 2019). In that demonstration, the ASTH was utilized in addition to the Screed King and magnesium bar screed. Comparatively, the ASTH performed favorably in that it was

straightforward and simple to use, exhibited operator forgiveness for newly trained operators, and reduced overall manpower requirements.

2.2 Asphalt screeds

Unlike concrete, there is no currently established screed for asphalt repairs, though research work has been performed. The existing method described in the Interim RADR TTPs (USAF-AFCEC 2019) utilizes a front-end loader (FEL) to both place and strike off asphalt, often requiring considerable handwork as well. This method has been adequate, though not ideal, for small repairs (e.g., 8.5-ft square) but not for large repairs (e.g., 30-ft square). The TTPs specifically state that asphalt screeds are currently being tested for CTLs or telehandlers; there are no TTPs for large crater repair but, according to the report, research is still underway.

Applied Research Associates (ARA) has performed the bulk of asphalt RADR research, particularly regarding TTP development but also with respect to screed evaluations. Figure 2.3 shows a Simex ST 200 screed attachment for a CTL that ARA frequently uses to create asphalt windrows and has successfully used for small repair screeding.

Figure 2.3. CTL with Simex ST 200 screed attachment (Jackson and Hall 2014).

Jackson and Hall (2014) worked to develop TTPs for large crater repairs using asphalt. This effort was not specifically a study of screeds but did speak to the issue. The approach therein was to utilize the Simex CTL screed and pave a large repair in six alternating 5-ft lanes. While feasible, it was concluded that the Simex CTL screed limits capability, increases repair complexity, and introduces opportunities for delays and RQC issues. It was recommended that alternative asphalt screed equipment be investigated.

ARA has evaluated a number of other asphalt screed options beyond the Simex CTL screed[1]. A market survey of potential screeds was first conducted, and then six screeds were tested. Three of the screeds were commercially available and included a CTL paver attachment, a self-propelled miniature paver, and a self-propelled road widener. Prototype screeds were also tested, including two telehandler attachment screeds named the simple strike off (SSO) and the bucket strike off (BSO) shown in Figure 2.4. Of all six screeds tested, it was concluded that the most promising screeds for RADR applications were the SSO and BSO.

Figure 2.4. ARA prototype telehandler attachment asphalt screeds.

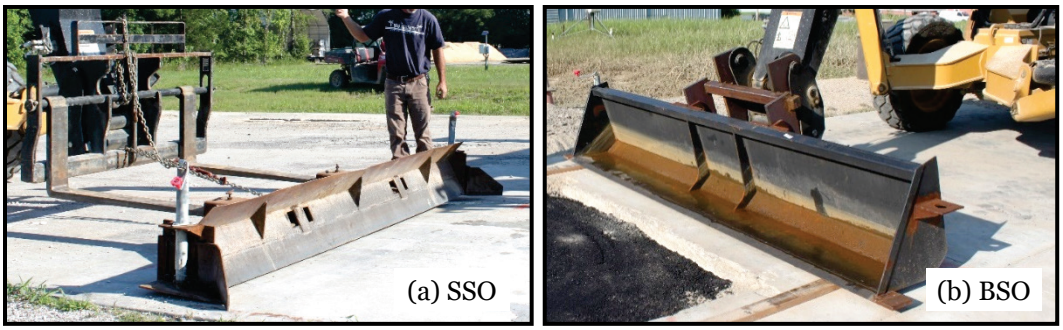

Cox and Hoffman (2019) further evaluated the SSO and BSO for small and large asphalt repairs. Some of both the testing procedures and the findings were similar between Cox and Hoffman (2019) and the ARA work. As in other work with either concrete or asphalt, small crater repairs were much less of a challenge compared to large repairs, so this discussion focuses on large repairs.

The SSO was favored over the BSO for several reasons. First, the SSO was very basic in design, and its integrated fork pockets made lifting with a telehandler simple. The BSO required the forks to be removed from the telehandler to be directly connected, meaning a longer setup time. The bucket of the BSO was intended to provide a buffer by maintaining a larger head of material to fill in low spots while screeding; however, this material was simply retained by the bucket, was wasted, and increased cleanup efforts.

For either screed, the greatest challenge during use related to grade control, particularly for large repairs as the screed extended into the repair

[1] Pullen, A. B., C. L. Wilbur, C. Ishee, and J. Hall. 2016. Draft report. *Rapid airfield damage repair asphalt concrete placement: Development of prototype asphalt concrete screeds*. Vicksburg, MS: U.S. Army Engineer Research and Development Center.

and then again as it transitioned out of the repair on the far side. The SSO was better equipped for this, and the procedure involved setting the screed grade height at an initial 1.5-in. mark on the existing pavement. As the screed was extended into the repair, one grade control ski remained on the existing pavement (outside the repair), while the other extended into the repair. The grade control ski height had to be manually adjusted just as the screed entered the crater in order to adjust the total overall height from 1.5 in. to 5.5 in. (1.5-in. roll-down factor plus 4-in. repair thickness). The process was performed in reverse once the screed reached the far end of the repair. This procedure provided adequate results, but the oversight and care required were less than ideal.

2.3 Integrated screeds

Cox and Hoffman (2019) describe efforts to develop an integrated pavement screed, starting with the initial evaluations of the two concrete screeds (ASHyd and ASTH) and two asphalt screeds (SSO and BSO). In this work, each screed was used to perform both concrete and asphalt repairs with the intent of identifying one screed that could be modified to create an integrated screed, perhaps using various components or aspects from multiple screeds tested.

Full details of the work and findings can be found in Cox and Hoffman (2019). For brevity herein, it is sufficient to state that SSO and BSO worked relatively well for all small repairs but fell short when used for large concrete repairs. This was primarily due to the nominal 11-ft width of these screeds, which cannot span the 15-ft width of a typical large concrete repair formed into quadrants. Therefore, the SSO and BSO had to be manually floated across the concrete surface, requiring considerable telehandler operator skill, rather than being able to span the entire width and ride on the forms or existing pavement like the ASHyd and ASTH.

In contrast, the ASHyd did not work well for large asphalt repairs due to the force required to push a large head of material. This was ultimately abandoned due to concerns of potential damage to the hydraulic system. The ASTH experienced no difficulty in pushing the asphalt, but it lacked some of the necessary components, such as grade control systems, to screed a repair without meticulous oversight and care. However, of the screeds tested, the ASTH was deemed the most versatile and most promising as a base platform when moving forward to an integrated screed. It already performed well for concrete repairs

and would be the easiest to create additional attachments for or otherwise modify for asphalt repairs.

Four key components were designed and fabricated as ASTH asphalt screeding attachments (Figure 2.5). These were an automatic grade control system (AGCS) for the inside repair end of the screed, a grade control ski for the outside repair end of the screed, end gates to control placement width, and a ride track for the AGCS (to be placed inside the repair on the flowable fill base surface).

Figure 2.5. ASTH asphalt screeding attachments (Cox and Hoffman 2019).

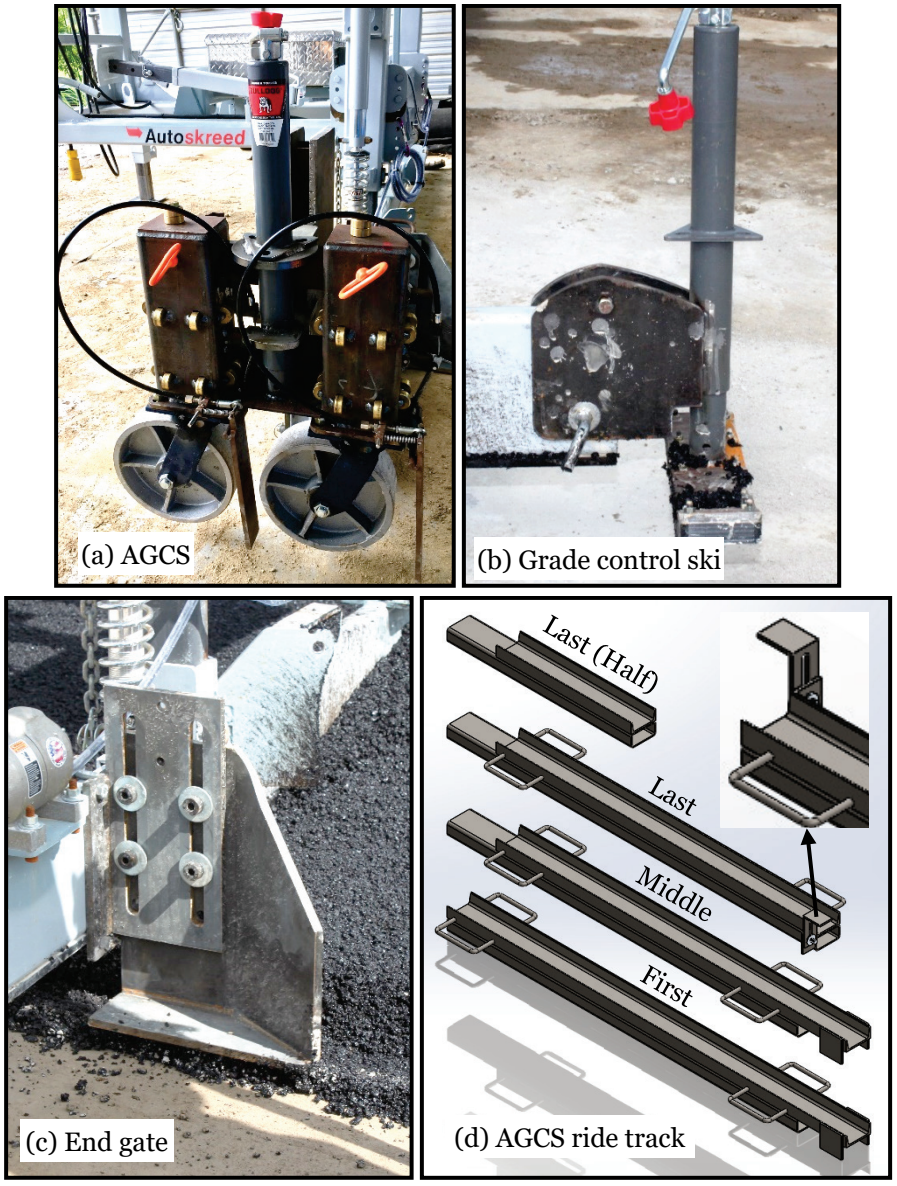

The prototype attachments worked moderately well but required improvement. It also became apparent that improvements to the ASTH design itself would be required to yield a fully capable screed not only for asphalt repairs but also for concrete repairs. A summary of key issues and recommendations for a final integrated screed prototype follows.

- The ASTH frame size was unnecessarily large both in height and length, increasing its logistical footprint. It was recommended to decrease the frame size by approximately 50%.
- The screed bar location at the front of the ASTH frame made it challenging to keep the screed level when pre-loading the travel springs. Instead, the ASTH tended to roll backward due to the momentum created. It was recommended to move the screed bar to the back of the screed.
- The travel springs, which provide vertical travel and make it easier for the operator to control the screed, were too stiff for the intended purposes. It was recommended to use lighter springs.
- The screed bar (2×8-in. steel tubing, ¼-in. wall thickness) did not possess the torsional stiffness needed to adequately support the asphalt attachments and was not tall enough to maintain a head of material during screeding without overtopping. It was recommended to redesign a stiffer, taller screed bar.
- It was recommended to add storage locations for asphalt attachments so that they could be kept onboard the screed frame.
- Minor improvements were required to the asphalt attachments:
    - Providing positive locking mechanisms on the grade control jacks to prevent them from unwinding when the screed vibrators were on,
    - Simplifying the AGCS and strengthening its latch release assembly, and
    - Reducing the weight of ride track sections.

The list of issues and recommended changes provided herein is not exhaustive but illustrates the key improvements required. Figure 2.6 illustrates the design of the ASTH relative to the integrated RADR screed design proposed for consideration in Cox and Hoffman (2019). The overall format of the screed was retained, but key areas for improvement were addressed. This conceptual integrated screed design was the final deliverable in Cox and Hoffman (2019); this report documents efforts to finalize the design, build a new prototype, and evaluate it.

Figure 2.6. Original ASTH design vs. new integrated screed design concept.

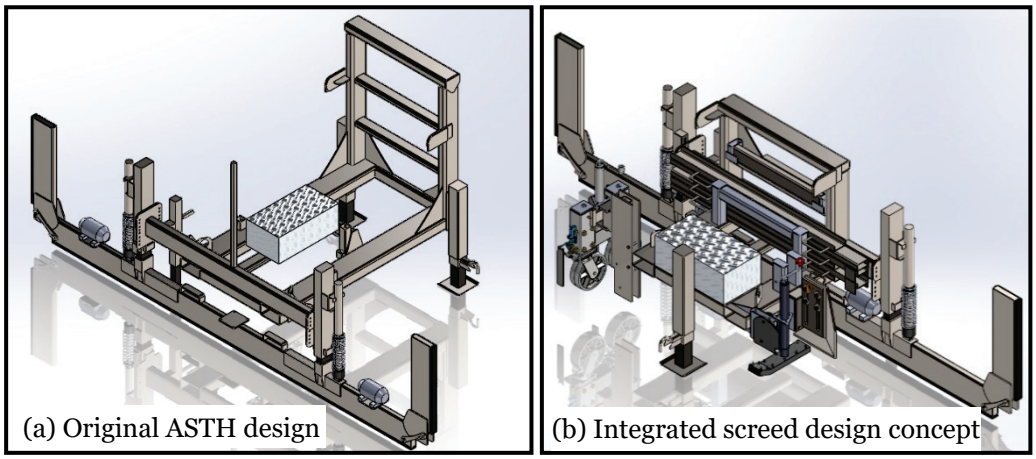

(a) Original ASTH design (b) Integrated screed design concept

3 Prototype RADR Screed

This chapter documents the key features of the RADR screed. Operation of the screed and results of screed testing are presented in Chapters 5 and 6.

3.1 Overview of design

Based on the preliminary design concept work performed in Cox and Hoffman (2019), a description of requirements was prepared and solicited for bids to build the new RADR screed prototype. This description of requirements was drafted with capacity for input from the contractor with the goal of marrying the contractor's expertise in machining and fabricating with ERDC's pavements and RADR experience.

This section presents an overview of the entire RADR screed as a complete system. Subsequent sections in this chapter provide details of each major component of the screed, including discussion of how recommendations from Cox and Hoffman (2019) were implemented.

Figures 3.1 and 3.2 show the overall RADR screed in the concrete and asphalt configurations, respectively. Key differences to note between these two figures are that the concrete configuration shown utilizes the fold-down extension wings necessary to perform large repairs. The asphalt configuration does not utilize the extension wings, which are shown stored, but does utilize other attachments of which the AGCS, end gates, and AGCS ride track are visible.

Figure 3.1. RADR screed overview–concrete configuration.

Figure 3.2. RADR screed overview–asphalt configuration.

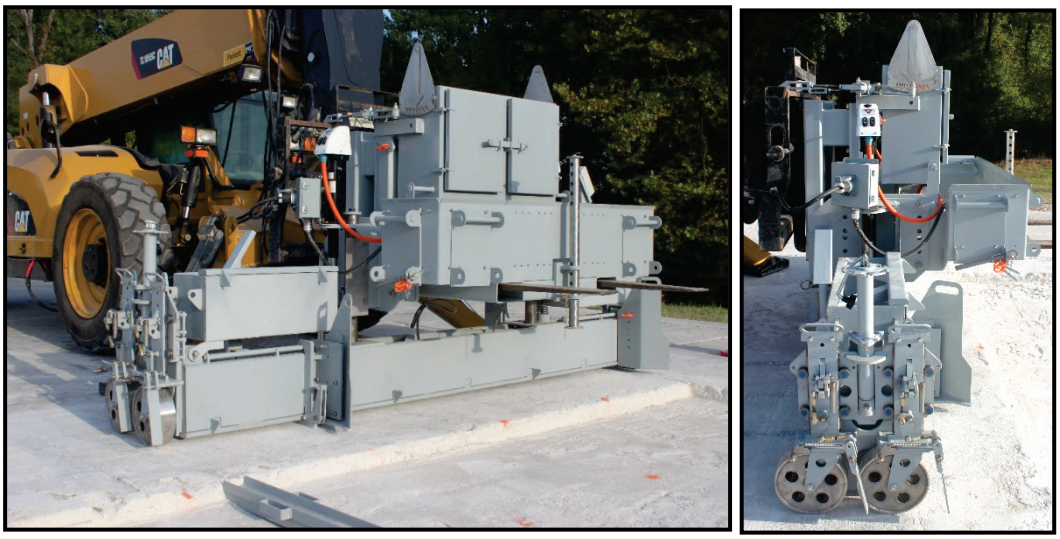

Table 3.1 provides a list of overall properties for the RADR screed. Relative to the ASTH in Cox and Hoffman (2019), the overall screed length and width (excluding screed bar) were reduced from 6.5 to 4.0 ft and 8.0 to 6.0 ft, respectively, but the height remained approximately the same if the swinging level indicators are not considered.

Table 3.1. RADR screed physical properties.

Dimensions	
Overall Height (ft)	6.0
Overall Length (ft)	4.0
Overall Width w/out Screed Bar (ft)	6.0
Screed Bar Width (ft)	12.0 to 17.0 (with 2.5-ft extensions)
Weights[a]	
Unloaded (no attachments on board) (lb)	3,125 [2,800][a]
Fully Loaded (all attachments on board (lb)	4,200 [3,875][a]
All Attachments[b] (lb)	1,075
Concrete Configuration (req. attachments only) (lb)	3,150 [2,825][a]
Asphalt Configuration (req. attachments only) (lb)	3,575 [3,250][a]
Controls	
Vibrators	(2) Vibco DC-500 Vibrators, 12 VDC, 4,000 VPM, 450 lb force
Screed Frame Leveling (front to back)	(2) Swinging level indicators
Screed Bar Leveling (side to side)	(2) Bulldog 500188 Powered Jacks, 12 VDC, 3,500 lb capacity
Screed Bar Suspension	(2) Springs, 32 lb/in.

a) Note that weights include the 325 lb fork pocket extension adapter. Values in brackets are without the adapter.

b) Attachments include the AGCS (215 lb), manual grade control system (MGCS), (185 lb), two grade skis (75 lb each), two end gates (65 lb each), six full-length and one half-length track sections (45 and 25 lb each, respectively), cutoff wheel (60 lb), and power cable (35 lb). Attachments are discussed in detail in subsequent sections of this chapter.

Maximum weights were not specified in the contract requirements for screed fabrication as they were not anticipated to be a prohibiting factor. However, the final screed was fairly heavy, which was primarily a result of the contractor's emphasizing strength and stiffness–factors that were stressed by ERDC in the initial kick-off meeting based on ASTH testing. As will be discussed in later chapters, the screed was successful from technical perspectives, but weight did pose functional challenges that will need to be addressed in future screed builds. Weight reduction should not be difficult to achieve (discussion with the contractor confirmed this.)

3.2 Screed bar

3.2.1 Initial finite element analysis and design

Cox and Hoffman (2019) noted stiffness issues with the original ASTH screed bar and recommended the screed bar be redesigned (though this was not done at the time as can be seen in Figure 2.6b). This project addressed screed bar design through the use of finite element analysis (FEA) to quickly and efficiently evaluate a range of alternative screed bar designs that would provide increased stiffness. Box designs (Figure 3.3) were the basis for FEA work in which eight design variations were evaluated.

FEA investigations were performed in Abaqus. Each box screed design evaluated was 12 in. tall by 12 in. wide and was analyzed in unit form in that a single 30-in. span was evaluated in each case rather than the full screed bar length. Boundary conditions were completely fixed on one end, and either a unit torsional or unit vertical load was applied to the other end (Figure 3.3). In this investigation, deflections were of greater interest than stresses, which are not shown for brevity, and torsional deflections were of greater interest than vertical deflections since torsional deficiencies were the primary motivator for a new screed bar design.

In all cases, a 0.25-in. steel plate was included on the front face and at either end of the screed bar section. Each design also included 2×2-in. steel tubing members that comprised the basic box frame shape. Variables considered in design variations included whether and where perpendicular (perp.) supports were to be used as well as whether and where angled truss supports were to be used. Truss supports were generally at 45°, but 30° and 60° were also considered. All tubing was 2×2-in. square with a 3/16-in. wall thickness. Note that because the FEA was a simplified representation of each design, the resulting

deflection values are not necessarily representative of a full-scale screed bar or test; however, the approach taken does provide comparative data between designs to assist in selecting a suitable design.

Figure 3.3. Example screed bar design and FEA boundary and loading conditions.

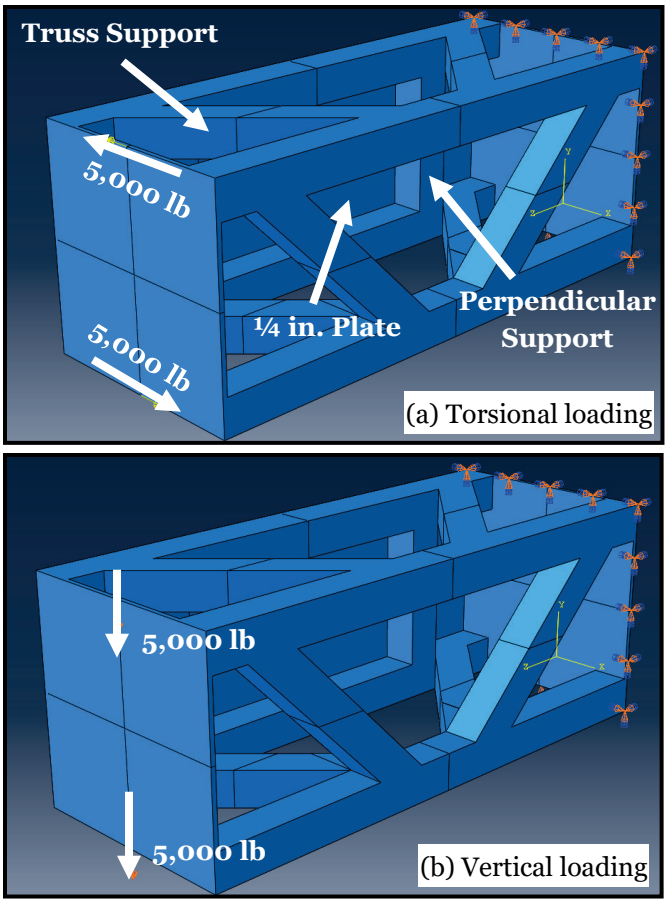

Table 3.2 provides a summary of all FEA results. Note that, in general, the design cases progress from simpler to more complex. Consequently, deflections decrease as additional support members are incorporated into the screed bar box design. With only the ¼-in. plate on the front of the primary box, torsional deflection is 142 mils. With the addition of only perpendicular supports, deflection decreases considerably. However, deflections further decrease as truss supports are incorporated. For the 45° truss designs, Case 6 yielded the stiffest structure.

Case 6 was further investigated by modifying the truss support angles to either 30° or 60° (Cases 7 and 8, respectively) to determine the effect of truss angle. Decreasing the truss angle to 30° stiffened the screed bar slightly, whereas increasing the truss angle to 60° decreased stiffness.

Since Case 7 exhibited only modest improvement, Case 6 was selected since 45° angles presented a slightly simpler scenario for fabrication.

Table 3.2. Screed bar FEA results.

	Screed Box Support Member Details by Face					Deflections (mils)	
Case	Front	Back	Top	Bottom	Truss Angle	Vertical	Torsional
1	¼ in. Plate	—	—	—	—	176	142
2	¼ in. Plate + Perp.	Perp.	Perp.	Perp.	—	49	36
3	¼ in. Plate	—	Truss	Truss	45	73	42
4	¼ in. Plate	Truss	Truss	Truss	45	24	10
5	¼ in. Plate + Truss	Truss	Truss	Truss	45	23	10
6	¼ in. Plate + Perp.	Truss	Truss	Truss	45	23	9
7	¼ in. Plate + Perp.	Truss	Truss	Truss	30	21	7
8	¼ in. Plate + Perp.	Truss	Truss	Truss	60	29	19

– All tubing was 2×2 in. square with 3/16-in. wall thickness.

– Perp. Refers to perpendicular supports.

For comparison to the original ASTH, Figures 3.4 and 3.5 illustrate FEA results for the ASTH screed bar and the Case 6 design chosen for the RADR screed, respectively. Recall that the ASTH screed bar consisted of 2×2-in. tubing with a 0.25-in. wall thickness. Figures 3.4 and 3.5 show that the torsional deflection decreased from 111 to 9 mils when comparing the Case 6 design to the ASTH screed bar. This is effectively an order-of-magnitude increase in torsional stiffness relative to the ASTH screed.

Figure 3.4. Screed bar FEA results for ASTH screed.

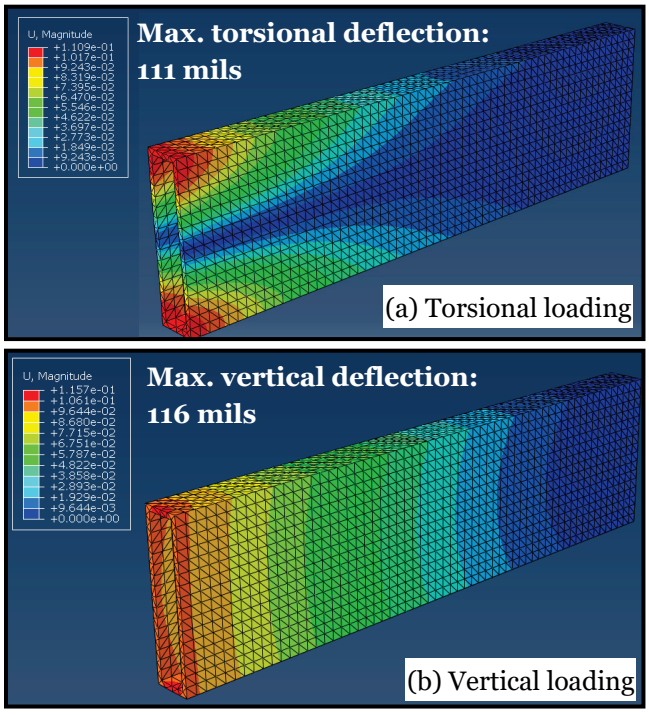

Figure 3.5. Screed bar FEA results for RADR screed.

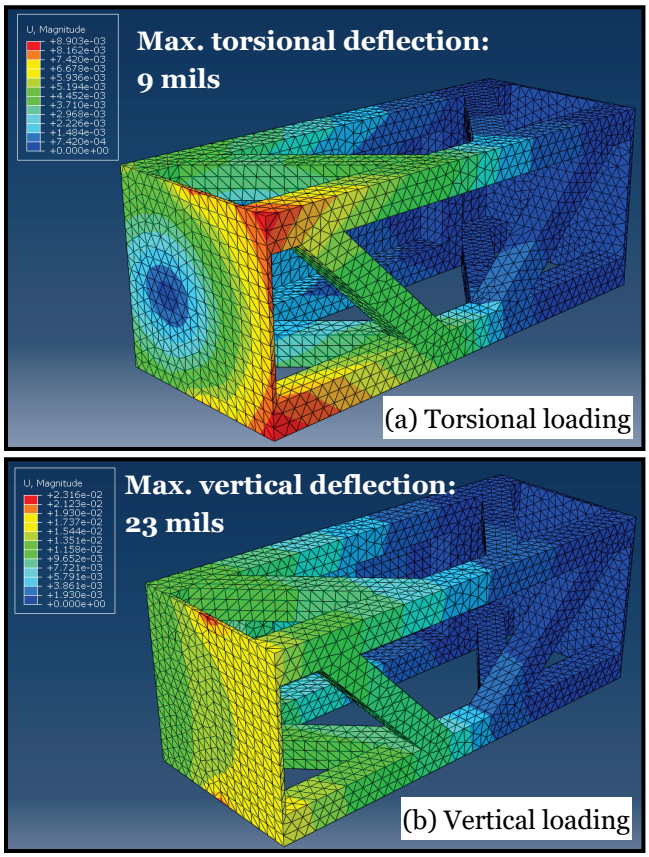

3.2.2 Final screed bar

The final screed bar design fabricated for the RADR screed was based on Case 6 in the FEA investigation. Slight but insignificant differences between the final screed bar and the Case 6 design were introduced during fabrication to account for factors such as the location of mounting plates or brackets. Gussets were also added in key areas to add support. Figure 3.6 shows a section of the final screed bar using 2×2-in. tubing. The design includes symmetrical top and bottom truss members at 45° angles, an identical truss structure on the back of the box frame, and perpendicular supports on the front of the box frame (including a ¼-in. plate).

Figure 3.6. Final truss design of RADR screed bar.

Figure 3.7 shows front and back views of the entire screed bar with extension wings folded down. The box truss design provides rigidity and stiffness and easily accommodates the mounting of asphalt attachments. The 12-in.-tall screed bar, which is taller than the 8-in. bar of the ASTH, is more effective at preventing overtopping of material, particularly asphalt.

Figure 3.7. Overview of RADR screed bar.

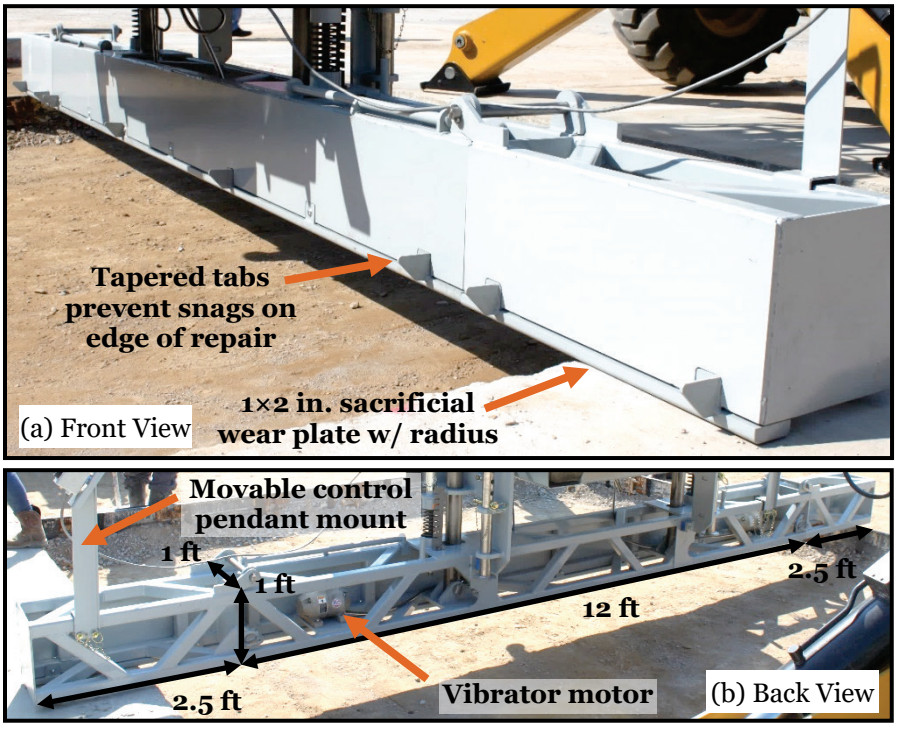

Figure 3.7a shows tapered tabs on the front of the screed bar that help it transition out of a crater repair without snagging on the crater edge, which often occurred with the ASTH. The screed plate that performs the finishing

is a 1×2-in. steel plate with ½-in. radii that aid the screed in floating over the repair material. The screed plate is a sacrificial piece that can be easily replaced, much like the blade on a CTL or FEL bucket.

Figure 3.7b shows the back of the screed bar, which is suspended from the screed frame (suspension system is discussed in the following section as part of the screed frame). Like the ASTH, the RADR screed has two Vibco 12 VDC vibrator motors that are housed within the screed bar truss and help provide some material consolidation.

Figure 3.8 illustrates the folding extension wings in the down and up positions. When folded down, the wings are locked in place using 1-in.-diam pinned connections to the main screed bar. These pins are simply inserted from the open back side of the screed bar and retained using wire-lock clevis pins, as shown in the Figure 3.8 inset.

Figure 3.8. RADR screed-bar extension wings shown down (left) and up (right).

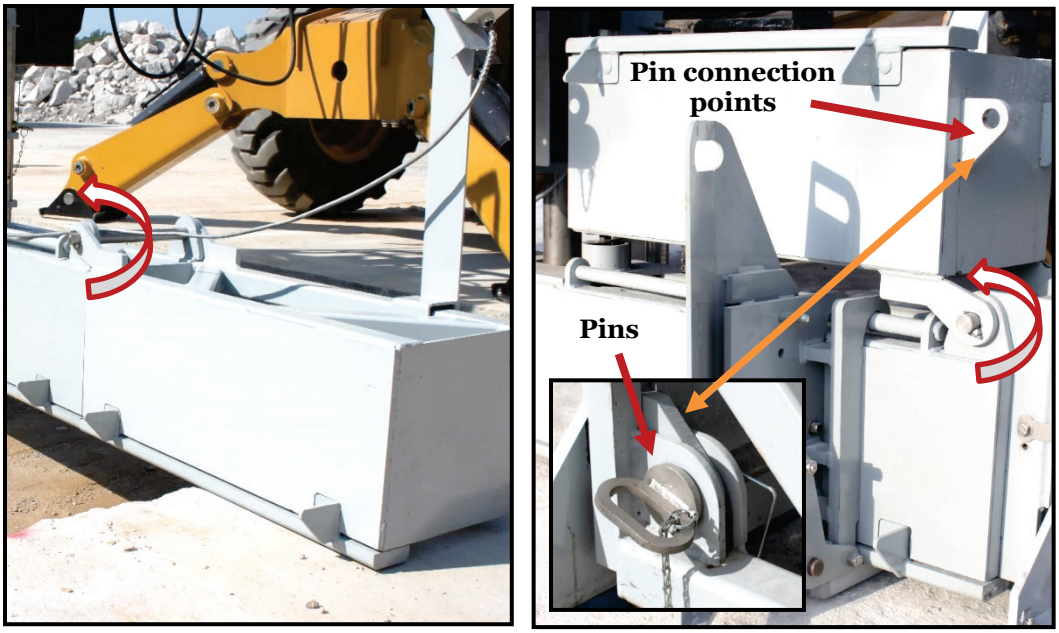

3.3 Screed frame

Figure 3.9 provides an overview of the RADR screed frame. Key components are the fork pockets, crash rack that butts against the telehandler mast, toolbox, storage bin for ride track pieces, support legs, and screed bar suspension system. The majority of these components are discussed with specific close-up photographs for better visualization, but generally speaking, the screed frame is the body of the screed by which it is

lifted with a telehandler. It provides support for the screed bar and also serves other functional purposes such as storage for tools and attachments.

Figure 3.9. RADR screed frame overview.

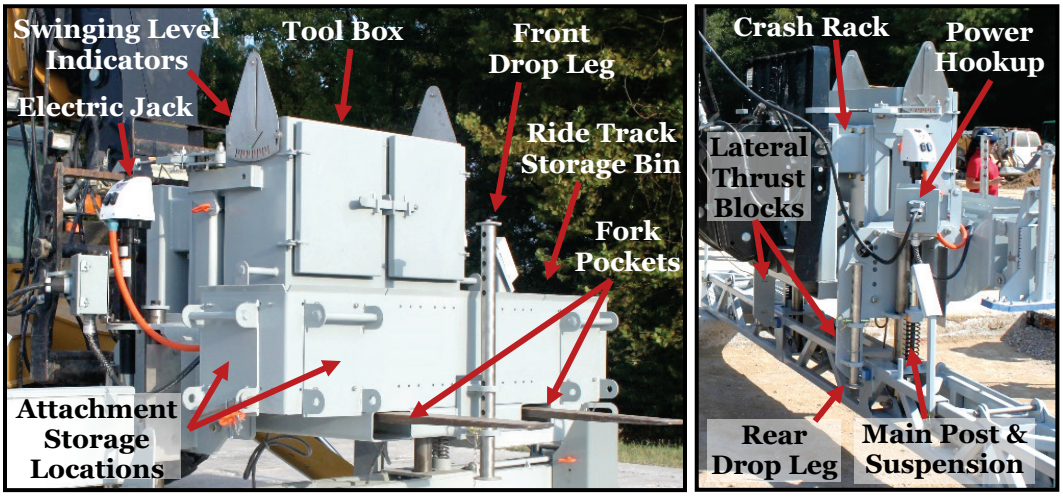

Figure 3.10 provides close-up detail of the screed support legs and screed bar suspension system. Both are significant improvements relative to the ASTH. The ASTH has four support legs that are raised and lowered by manual jacks. This makes picking up or dropping the ASTH with a telehandler time-consuming because the operator has to manually raise or lower four legs individually. The RADR screed has three legs in a tripod configuration (one front and two rear), and the legs are simple posts that can be quickly pinned up or dropped and pinned down.

The screed bar suspension system is comprised of three subcomponents: main posts, leveling jacks and travel springs, and lateral thrust blocks. The suspension system is intended to resist horizontal and torsional forces while allowing vertical travel, both by manual adjustment (electric leveling jacks) and by free floating during screeding (travel springs).

The main posts are 3-in.-diam solid steel shafts that are pinned to a plate at the bottom of the screed bar and attached to the screed frame with free movement up and down as shown in Figure 3.10. The screed bar's pinned connection and slotted upper plate also allow some degree of left-to-right rotation, or roll, of the screed bar. The lateral thrust blocks are made of a steel arm and low-friction block of ultra-high molecular weight (UHMW) polyethylene. They help to resist lateral forces so that the main posts are not required to carry all lateral forces during screeding.

Figure 3.10. RADR screed suspension system (right side) and support legs.

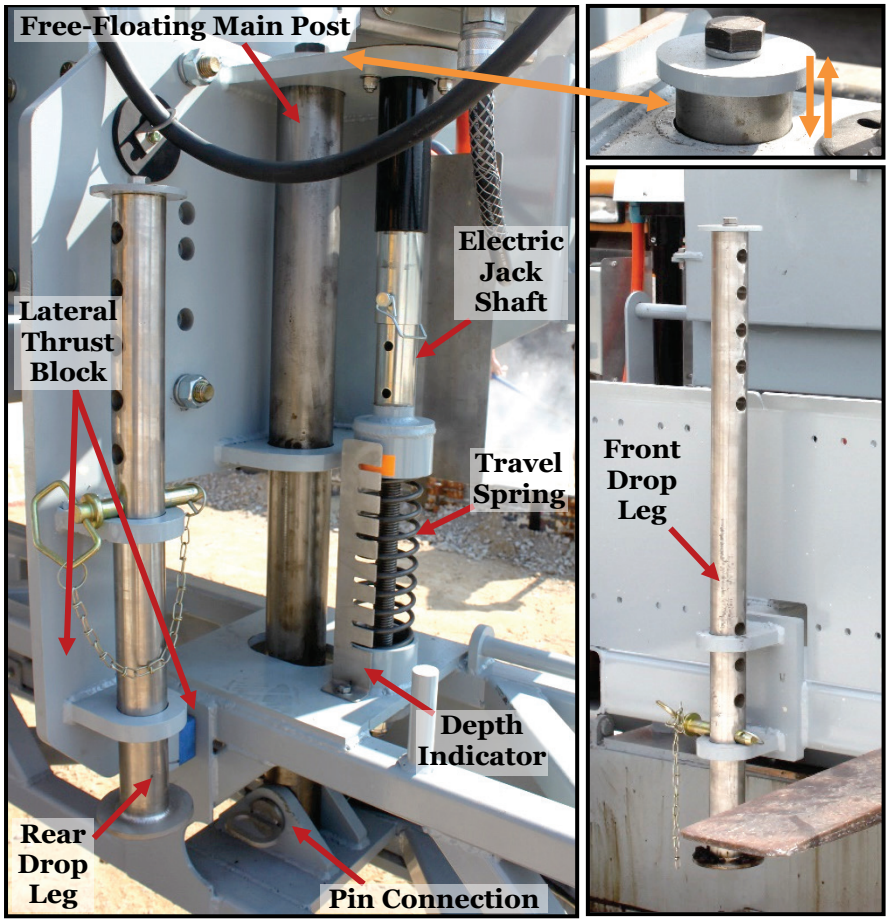

Vertical movement is managed by the electric jacks and travel springs. The electric jacks allow the ground spotter to manually adjust left-to-right roll of the screed bar before (or during) screeding (Figure 3.11). This is advantageous for large crater repairs where it may be beneficial to maintain a non-uniform contact load between the screed bar and grade references. In Figure 3.11 (one quadrant of a large concrete repair), the left screed bar end would be supported by existing concrete, which can support heavy load, whereas the right end would be riding the interior plastic formwork, which cannot support much load.

The travel springs (Figure 3.12) allow approximately 8 in. of vertical travel. Their primary purpose is to give the operator flexibility in adjusting the telehandler's boom angle throughout the screeding process. Unless the boom is perfectly level, which is unlikely, the boom will either climb or dive as it extends; without travel springs, the boom angle must be constantly adjusted to keep the screed in contact with grade references. Continual adjustment to maintain contact without applying too much

downward pressure is a challenge even for skilled operators. Alternatively, the travel springs can be partially depressed (e.g., to their midpoint) before screeding. The screed bar weight and minimal additional load of the springs maintain screed contact without overloading. As the operator extends the screed out, he can adjust the telehandler boom angle up and down with several inches of forgiveness. Indicators visible from the cab allow the operator to see his adjustments. These two features greatly reduce the operator skill required.

Figure 3.11. Use of leveling jacks to control RADR screed bar roll.

Figure 3.12. RADR screed travel springs at rest and partially compressed.

Figure 3.13 shows the screed crash rack as well as the fork pocket extension adapter as it mates to the telehandler mast. The fork pocket extension adapter was not in the original fabrication plan; however, due to an oversight by the contractor, the clearance between the lateral thrust block plates was not sufficient to permit the telehandler rack from fully mating with the screed. At the time this was realized, the best remediation plan was to add the bolt-on extension adapter that shifts the rear plane of the screed backward 10.75 in. and prevents the lateral thrust block plates from interfering with the telehandler mast. To avoid unworkable project delays, ERDC authorized the contractor to move forward with this plan.

Figure 3.13. RADR screed crash rack and fork pocket extension adapter.

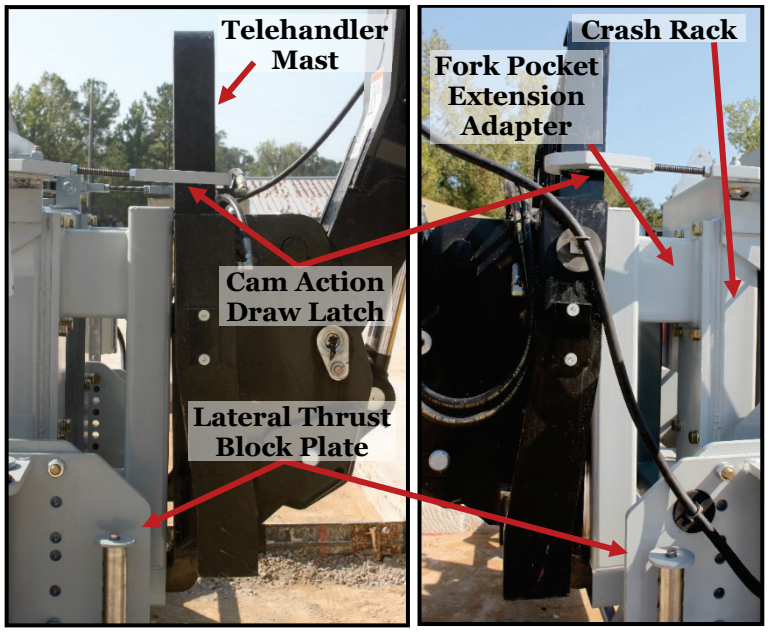

Mating the telehandler to the screed is a fairly simple and quick process, especially relative to the ASTH, due to two features. Figure 3.14 shows detail photographs of the cam action draw latches that secure the screed to the telehandler. These are mounted near the top rear of the screed frame and are adjustable in length to adapt to various telehandler mast frames. The latch is simply hooked over the mast frame (once the length is properly adjusted if using a new telehandler), and the latch handle is drawn over to secure the latch. The camming action of the latch will hold the latch closed under load. As an extra measure, wire-lock clevis pins are used to ensure the latch does not unintentionally release. The latches enable quick attachment or removal from the telehandler.

Figure 3.14. RADR screed cam action draw latch.

Figure 3.15 shows detail photographs of the power cord used to provide 12 VDC power from the telehandler to the screed for the jacks and vibrators. During setup, the power cord is suspended from the telehandler boom using magnets; loops in the cord allow the boom to extend freely. One end of the cord is connected to the telehandler's battery terminals using standard jumper-cable-style alligator clamps. The other end is plugged into the screed's power receptacle. This disconnect point enables the screed to be quickly removed from the telehandler without having to remove the entire power cord.

Figure 3.16 shows the control pendant for the screed's electronic jacks and vibrators. They are fairly simple with up-and-down controls for the left and right jacks and on-and-off control for the vibrators. The pendant is easily attached or detached from the pendant post by way of magnets attached to the back of the pendant. The pendant post slides over any of the 2-in. tubing that makes up the screed bar and is pinned

in place; this allows the pendant post to be repositioned to different locations depending on the current screed setup.

Figure 3.15. RADR screed power cord and connections.

Figure 3.16. RADR screed control pendant.

Figure 3.17 shows the swinging level indicators used as a reference when leveling the screed front-to-back using the telehandler's fork tilt control. This is necessary before screeding and, for large repairs, may be necessary

during screeding as most telehandler booms tend to sag at long extension distances. Each tick on the indicators is 2.5°, and a level is affixed to both sides of the screed for spotter convenience.

Figure 3.17. RADR screed swinging level indicators.

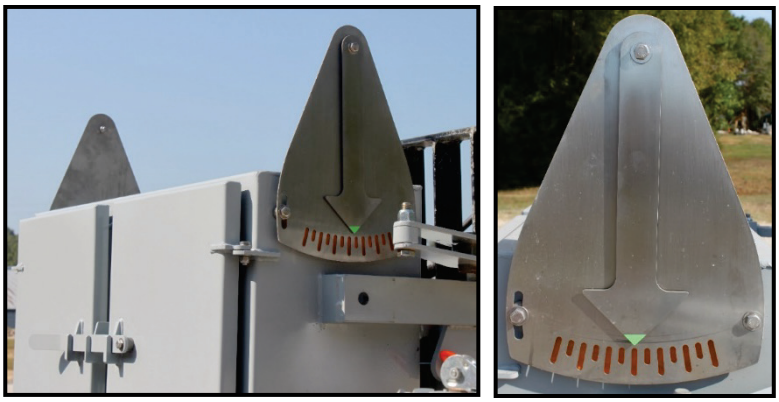

Other components not discussed in great detail include the ride track storage bin and the toolbox. The ride track bin holds all ride track pieces and contains two steel straps that prevent the track pieces from inadvertently bouncing out during transport. The toolbox can store the power cord when not in use but is primarily useful for storing common tools such as a hammer, wrenches, and gage blocks for setting screed bar height as well as spare parts such as replacement pins.

3.4 Asphalt screed attachments

Various attachment accessories are used when the screed is utilized for asphalt repairs. Grade control attachments including the AGCS, MGCS, and grade skis are mounted to the screed bar ends. End gates and the cutoff wheel are mounted to the accessory rail along the top of the screed bar. The ride track is laid out longitudinally inside the repair.

Figure 3.18 shows the mounting locations for each attachment. With the screed-bar extension wings folded, the end-mount attachments hook over the 1-in.-diam extension wing shaft (Figure 3.18a) and then pin in place at the bottom (Figure 3.18c). This design eliminates the need to entirely remove the wings for asphalt screeding. Front-mount attachments have hooks that hang on the mounting rail in Figure 3.18b and are secured using cam action latches at the bottom that hook securely over the 1×2-in. screed plate (Figure 3.18d). This design allows front-mount attachments to be positioned anywhere along almost the entire screed bar.

Figure 3.18. RADR screed attachment mounting locations.

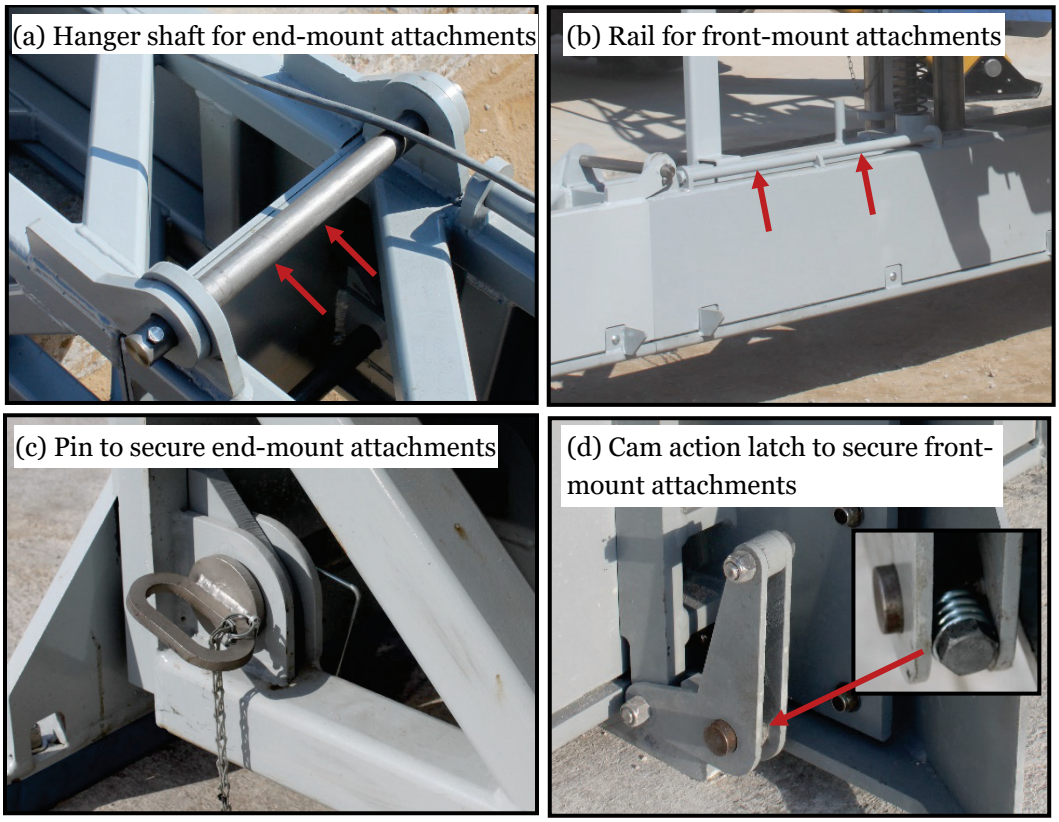

3.4.1 Grade control skis

The RADR screed is equipped with two grade control skis (left-hand and right-hand) as shown in Figure 3.19. Each ski is fairly simple, and its purpose is to allow the user to establish and maintain the proper screed bar height to provide the necessary asphalt compaction roll-down factor.

The grade control ski is intended for use on areas where the reference surface elevation is the same as that of the final repair (e.g., existing pavement outside of a large repair). The automatic or manual grade control systems are intended where grade control must transition into and out of the repair area.

The ski itself is 4 in. wide and 24 in. long with tapered leading and trailing ends to prevent snags on cracks, joints, or other pavement discontinuities. The ski is surfaced with a 1-in.-thick UHMW plate that can be replaced when worn. The ski is mounted on an adjustable fixture that is controlled by a heavy-duty leveling jack, which allows manual adjustment of the screed bar height. A scale and reference indicator are included so the user can easily determine the screed bar height. Once set, the jack handle locks

into an anti-rotation ring that prevents the jack from inadvertently unwinding due to the vibrators during screeding.

Figure 3.19. RADR screed grade control ski.

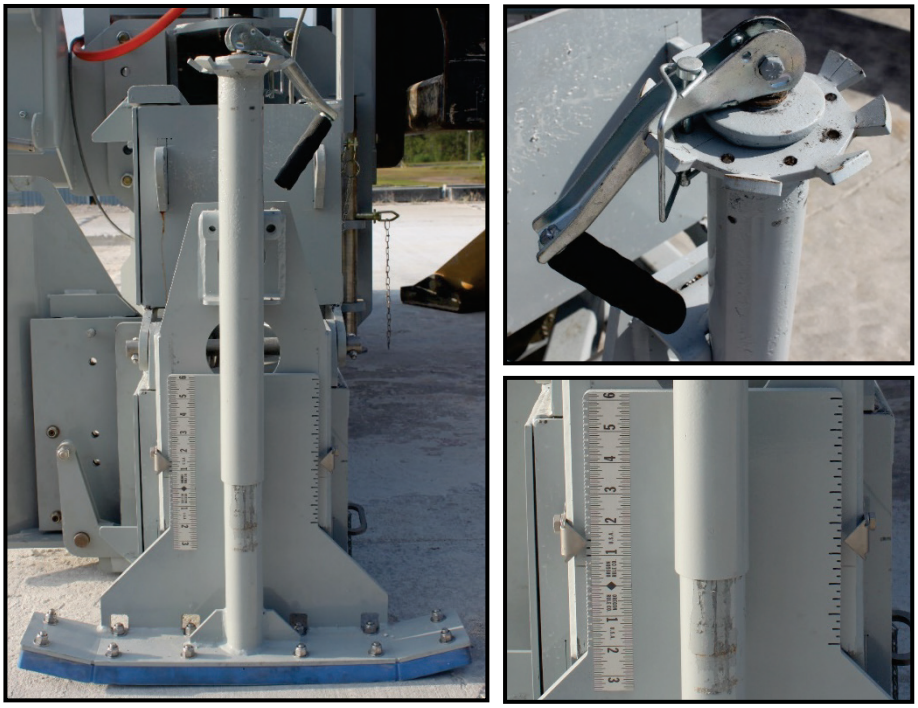

3.4.2 Automatic grade control system (AGCS)

The AGCS shown in Figure 3.20 is intended to provide automatically transitioning grade control on the inside edge of a large repair. Typical asphalt repair thickness is 4 in., meaning the screed bar must be maintained at a 1.5-in. height for proper roll-down when outside of the repair area but that it should be maintained at a 5.5-in. height when inside the repair area. The AGCS is a two-stage device that automatically accounts for this transition by keeping the screed bar at a consistent elevation with no operator intervention.

The AGCS consists of two 10.5-in.-diam wheels mounted on two independent sliding plates. Each sliding plate is attached by track rollers to a larger fixed plate. Between the sliding and fixed plates, a ratcheting gear rack is mounted on the fixed plate, and a pawl is mounted on the sliding plate. This ratcheting system allows each wheel and sliding plate to drop freely under gravity and then lock in place and not retract until the pawl is released via the release plate. A manual release lever can be used to

override the release plate and keep the pawl disengaged from the gear rack, which is useful during initial screed grade setup.

Figure 3.20. RADR screed automatic grade control system (AGCS).

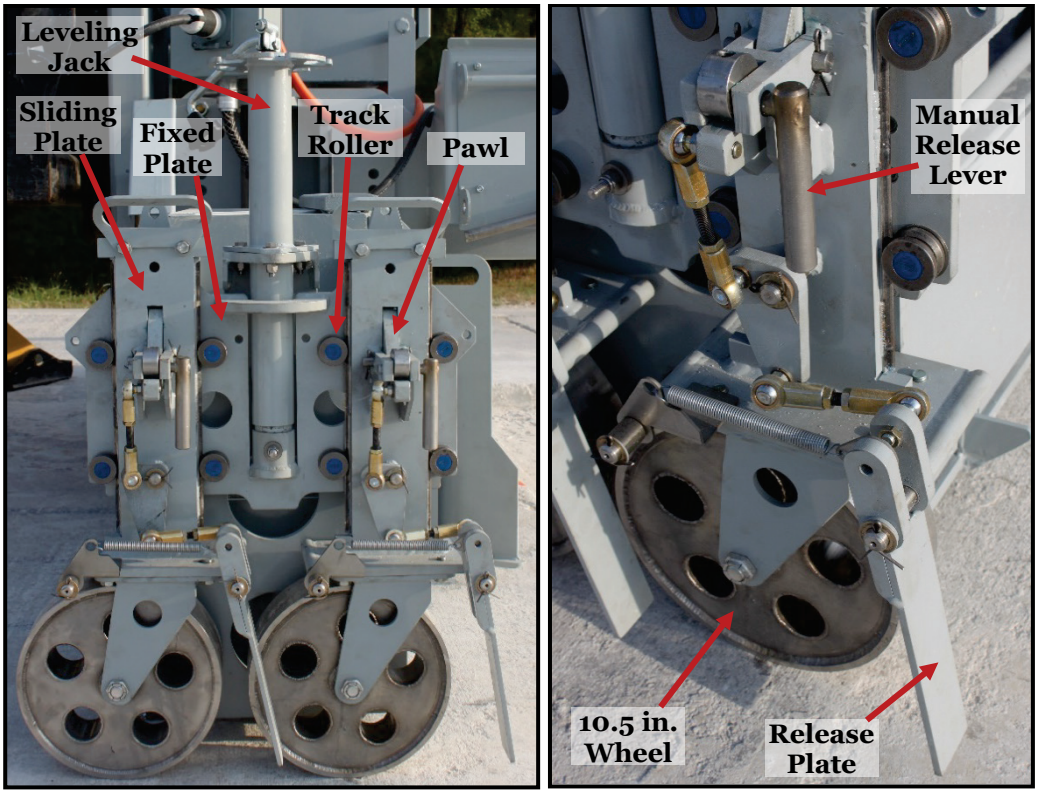

Figure 3.21 provides detail photographs of the screed as it transitions from outside the repair to inside the repair showing the action of the AGCS. In the left image, the leading AGCS wheel had already dropped approximately 2 in. as the screed was extended out into the repair. While the leading wheel dropped down to the ride track (described in Section 3.4.4), the trailing wheel supported the screed, keeping it at a constant elevation. In the right image, the leading wheel has locked in place at its new position and is supporting the screed, allowing the trailing wheel to drop to the ride track. This two-stage mechanism ensures the screed can adapt to the changing grade reference without affecting the screed bar elevation.

Figure 3.21. RADR screed AGCS–transition from existing pavement into repair.

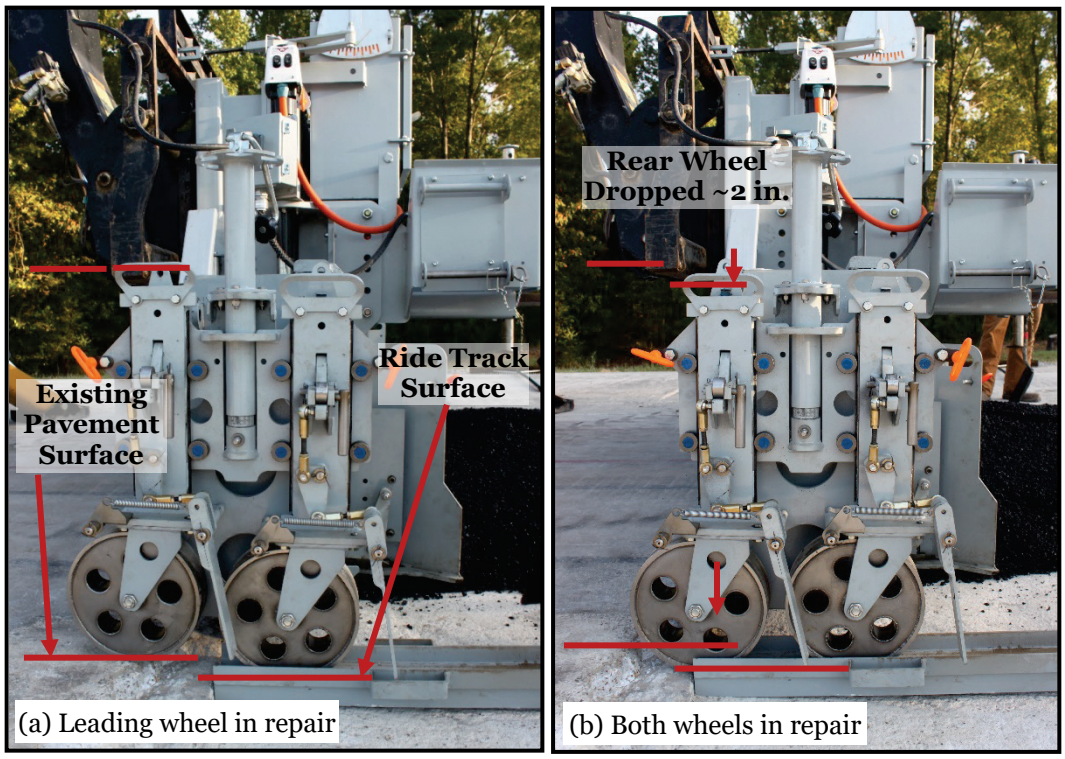

Figure 3.22 shows the AGCS as it transitions out of the repair and back onto the existing pavement surface. In Figure 3.22a, the leading wheel's release plate has just contacted the release tab at the end of the ride track. As the screed is pushed further forward, the release plate is swung backwards (Figure 3.22b), disengaging the pawl from the gear rack and permitting the wheel/sliding plate to move freely upwards. The ride track release tab holds the release plate back (Figure 3.22c) as the screed moves further forward, and the leading wheel simply rolls up and over the repair lip and back onto existing pavement while the trailing wheel supports the screed (Figure 3.22d). This same process would then take place with the trailing wheel while the leading wheel supports the screed.

The AGCS is the most technically complex attachment and does require the user to follow a simple checklist to ensure it performs properly. The procedures required are discussed in Chapter 5.

Figure 3.22. RADR screed AGCS–transition out of repair to existing pavement.

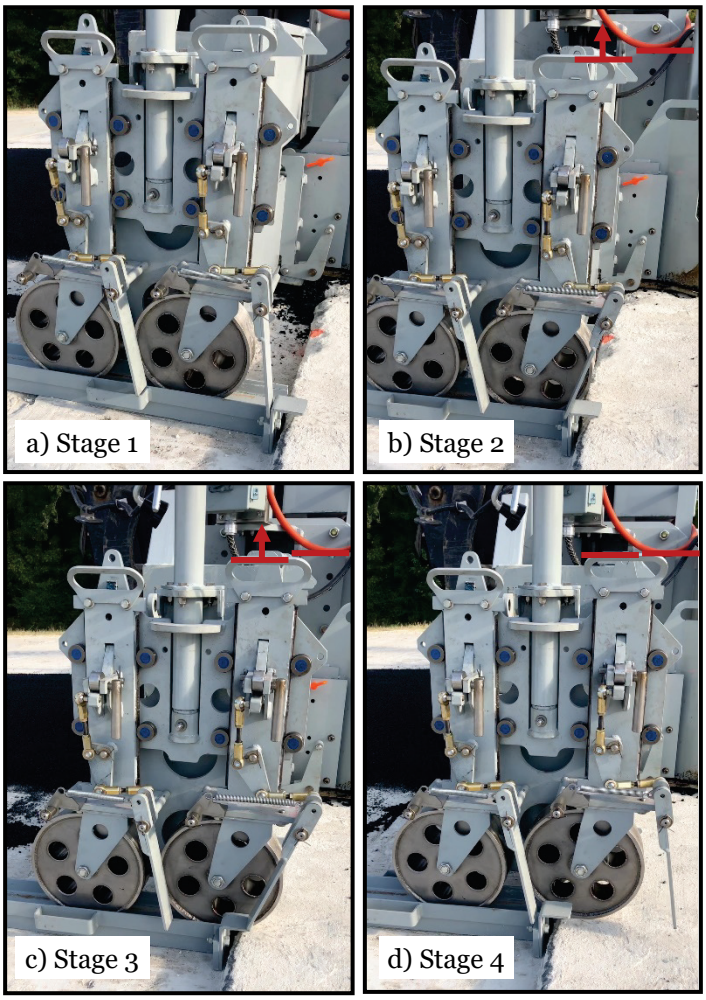

3.4.3 Manual grade control system (MGCS)

The MGCS shown in Figure 3.23 is conceptually similar to the AGCS except that it does not automatically transition to new grade references and, therefore, requires user interaction during screeding. The MGCS concept is similar in that its two adjustable wheels allow the user to manually lower the leading wheel down to the ride track as the screed enters the repair while the trailing wheel keeps the screed bar at its intended elevation. This process is repeated in reverse as the screed exits the repair.

While mechanically simpler, the MGCS does require greater attention from the spotter during screeding. It also requires greater coordination between the spotter and operator to ensure the operator provides time for the spotter to adjust the MGCS. Failure to do so could affect the repair quality or potentially damage the screed.

Figure 3.23. RADR screed manual grade control system (MGCS).

3.4.4 Ride track for grade control systems

Figure 3.24 shows the ride track for either the AGCS or MGCS grade control systems. The purpose of the ride track is two-fold. First, the track provides a smooth, solid foundation on which the grade control systems ride, which helps to bridge over any surface irregularities in the flowable fill base layer and spread out their effects on the final surface profile of the asphalt repair, yielding a more consistently smooth repair with fewer RQC violations. Second, the track surface sits 2 in. above the flowable fill base surface, dividing the repair depth of 4 in. in half. This provides an easier transition in and out of the repair for the grade control wheels.

The ride track is made up of six 65-in. sections and also includes a half-section that is 34 in. long. The track sections overlap each other so that they form a continuously linked track. The track was designed so that the degree of overlap is adjustable from 2 to 10 in. to allow the track to be sized exactly to a given repair size. For example, Figure 3.24 shows six track sections that are partially overlapped (approximately 6-in. overlap) to fill a 30-ft repair. Between the degree of overlap used and the half-section, many different track lengths can be produced up to 34 ft if all six

and a half sections are used. While there are unique first and last track sections, all middle sections are identical.

Figure 3.24. RADR screed ride track for AGCS or MGCS.

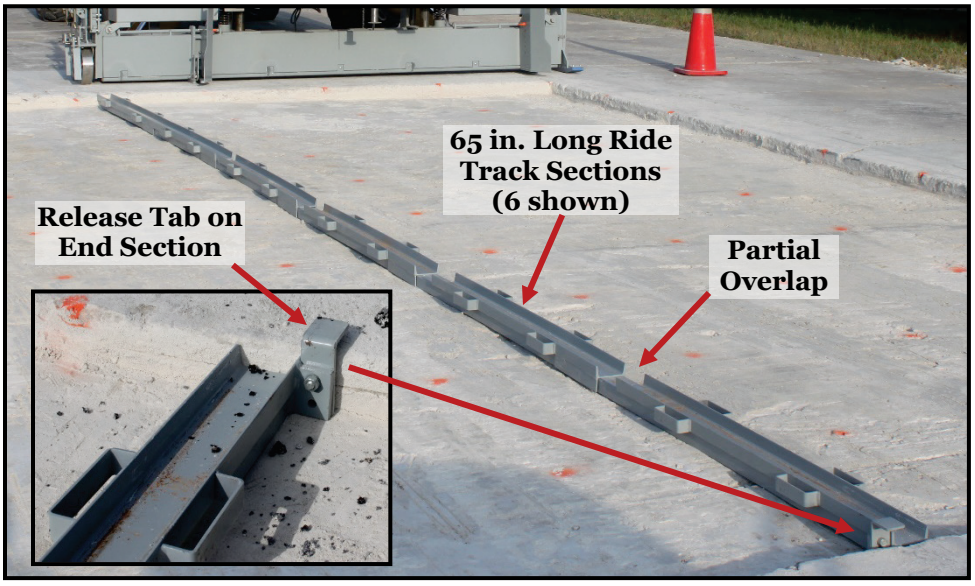

Each track section is 4 in. wide and 4 in. tall. The top half of the track is "C" channel where the web is the ride surface and the flanges serve as 2-in. tall guide rails that keep the grade control wheels on the track. The bottom 2-in. half of the track is made up of various pieces of flat bar welded together. Relative to the original prototype ride track in Cox and Hoffman (2019) that used rectangular tubing for the bottom half of the track, the Figure 3.24 track pieces are significantly lighter. Each track section has integrated handles for easy carrying, and the last track section has the AGCS release tab. The release tab is slotted with vertical adjustment to ensure it is positioned at the correct height to trigger the AGCS release plate.

3.4.5 End gates

Figure 3.25 shows one of two end gates for the screed that has both left- and right-hand end gates. The primary purpose of the end gates is to keep the head of material in front of the screed confined laterally and prevent excessive lateral spillage and movement. The end gates also help establish a clean vertical joint face prior to compaction. Being front-mounted attachments, the end gates can be positioned at any point along the width of the screed bar desired, offering flexibility with paving lane widths and screed placement.

Figure 3.25. RADR screed end gate.

Each end gate consists of a fixed portion and a sliding portion connected via track rollers. When not in use, a pin inserted through both portions prevents the sliding portion from moving. For screeding, the pin is removed, allowing the sliding portion to free-float on top of whatever surface it is on (existing concrete or flowable fill base). The nose of each end gate is rounded and tapered so that the end gate does not inadvertently cut into the surface on which it is riding.

3.4.6 Cutoff wheel

Figure 3.26 shows the cutoff wheel, a new attachment that was not prototyped in Cox and Hoffman (2019) but was added to the selection of attachments herein to aid in producing better repairs. The cutoff wheel is a front-mounting attachment that consists of a 16-in.-diam stainless steel disc blade mounted on a wheel hub.

The primary purpose of the cutoff wheel is to trim back the longitudinal joints of each paving lane prior to placing the adjacent lane. For a 30-by-30-ft large repair that requires three 10-ft-wide lanes, the two outside lanes would be paved, then trimmed back, and then the middle inside lane would be paved.

Figure 3.26. RADR screed cutoff wheel.

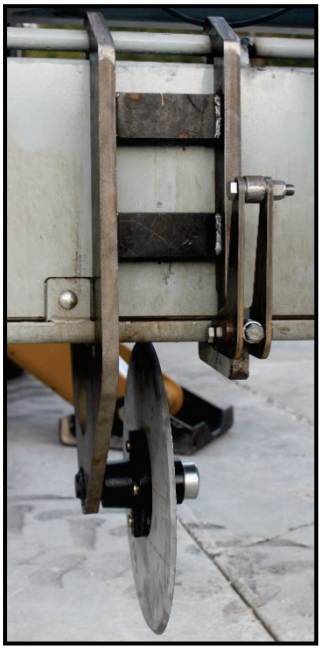

The cutoff wheel accomplishes three specific goals. First, it removes any low-density asphalt near the unconfined edge of a paving lane. Second, lateral shoving of the asphalt mix during compaction can be common with the RADR rolling pattern and 4-in.-thick lifts, reducing the asphalt thickness from 4 in. (sometimes dramatically); the cutoff wheel enables any feathered edges to be removed so that the adjacent lane is matching the correct thickness of asphalt. Third, lateral shoving, severe or not, can leave a wandering joint rather than a straight joint; the cutoff wheel creates a straight joint with a clean vertical face that is much easier to match when paving the adjacent lane.

4 Experimental Program

4.1 Materials tested

4.1.1 Rapid-setting flowable fill

Rapid-setting flowable fill (FF) is a highly fluid mixture of cement, fine aggregate, and water that uses rapid-setting cement (RSC) to quickly gain strength. Key advantages are that it is flowable, self-leveling, and self-consolidating. FF was used in this project as the backfill, or base, material for asphalt repairs.

Traditional RADR operations have exclusively utilized Utility Fill 1-Step 750 produced by Buzzi Unicem USA Inc. (further denoted FF-BU) for FF backfill. Recent efforts (Cox and Carr 2018; Cox and Hoffman 2019) have also evaluated other commercially available FF materials for the interest of expanding the list of technically acceptable products. This project presented the opportunity to evaluate additional untested materials since backfill characteristics were not pertinent to the project as long as they were reasonably representative of typical FF materials.

Cox and Carr (2018) and Cox and Hoffman (2019) evaluated two different CTS Flowable Fill (Mil. Spec.) mix designs from the CTS Cement Manufacturing Corporation, referred to as FF-CTS1 and FF-CTS2, respectively. This project evaluated a third mix design denoted FF-CTS3. Performance specifications governing the first two iterations were contained in MIL-DTL-32527 (DLA 2015b) (Table 4.1); a new set of specifications was drafted for the third iteration (Table 4.2). This report does not revisit evaluations of FF-CTS1 and FF-CTS2 in detail. It focuses only on FF-CTS3, and a stand-alone report that comprehensively documents all FF evaluations is forthcoming.

Table 4.1. MIL-DTL-32527 flowable fill performance specifications.

Test	Test Method	Placement Method	Criteria
Compressive Strength	ASTM D4832 (2016c)	Wet	≥ 750 psi at 28 days
		Dry	≥ 500 psi at 28 days
Initial Hardening	ASTM D6024/D6024M (2016a)	n/a	≤ 30 minutes
Segregation	ASTM C1610/C1610M (2017c)	Wet	< 5%
Linear Shrinkage	ASTM C426 (2016b)	Wet	< 2%

Table 4.2. Draft revised flowable fill performance specifications.

Test	Test Method	Cure Time	Criteria
Compressive Strength	ASTM C39 (2018)	2 hr	≥ 300 psi
		28 day	750 to 1,500 psi
Flow Consistency	ASTM D6103 (2017b)	—	10 to 18 in. spread
Segregation	ASTM C1610/C1610M (2017c)	—	< 5%
Linear Shrinkage	ASTM C426 (2016b)	—	< 2%

– Criteria in table are adaptations of MIL-DTL-32527 and are applicable for FF placed in normal RADR conditions (i.e., using a simplified volumetric mixer in a fluid consistency, also referred to as the wet method).

– Specifications for the dry placement method are a greater challenge to implement but, in general, the material should be permeable enough to allow the manufacturer's recommended batch water to percolate in approximately 5 min, and 28-day compressive strength should be a minimum of 65% relative to the wet method.

This project also evaluated FasTrac FastFill from Western Material & Design, further denoted FF-WM, which is believed to be very similar or perhaps identical to FF-BU.

All products were delivered in 3,000-lb supersacks (approximately 1 yd^3) for field testing with both dry and wet placement methods. Tests performed on these materials were either in situ (e.g., dynamic cone penetrometer) or from samples obtained during placement. This section presents results from these tests as material properties; the actual placements are not discussed here but are described in Section 4.2, which details test site preparation.

4.1.1.1 Dry placement method properties

FF materials placed with the dry method were evaluated visually for percolation characteristics during placement (two 4-in. lifts using 120 then 90 gal. of water, respectively, were placed for a total thickness of 8 in.). Following placement, dynamic cone penetrometer (DCP) tests were performed at 30 min, 2 hr, and 1 day. At 1 day, core sampling was attempted, but intact cores could not be retrieved.

Figure 4.1 shows four quadrants of dry-placed FF where the FF-BU and FF-WM were placed the previous day and the first lifts of FF-CTS2 and FF-CTS3 had just been wetted. FF-CTS2 and FF-CTS3 exhibited poorer percolation qualities compared to FF-BU and FF-WM. The latter absorbed almost all water to the point that the surface was mostly dry by the time 30 min DCP testing began. However, the CTS materials did not absorb water well, and approximately 1 in. of water remained standing on the surface when 30 min DCP testing began.

Figure 4.1. Percolation observations for dry-placed flowable fill.

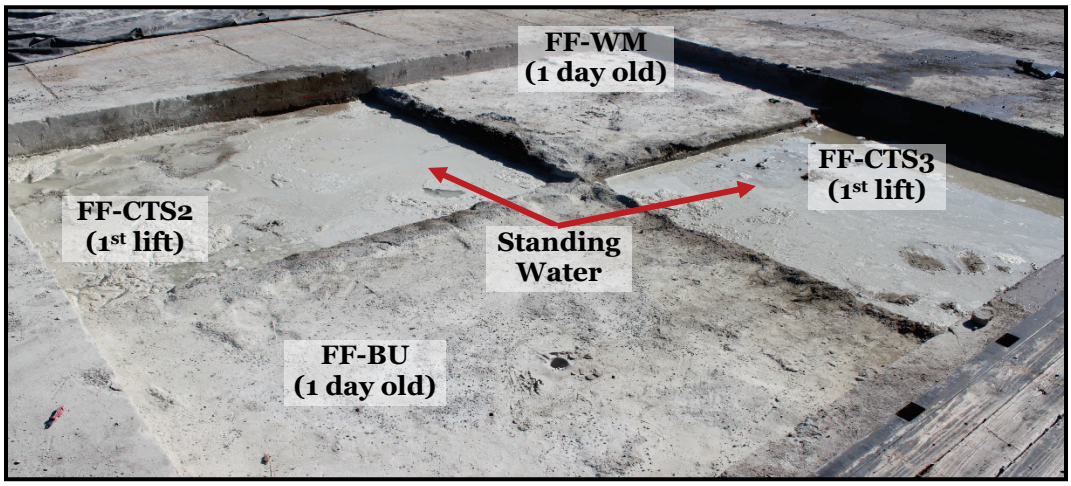

Figure 4.2 shows a typical DCP test and the 4-in. coring setup used. Note that FF-CTS2 was used primarily to provide additional material to fill the fourth quadrant but was not tested. Three replicate DCP tests were performed at each time interval for each material and were averaged.

Figure 4.2. Dry-placed flowable fill DCP testing and coring setup.

Figure 4.3 shows an example of a DCP plot for the first FF-BU replicate at 2 hr where California Bearing Ratio (CBR) is reported with depth. Generally, though not always, higher CBR values were observed at the very top of each lift (within the uppermost 1 in.), likely due to more hydration at the surface and less at greater depths where exposure to water was more difficult or required more time.

Figure 4.3. Example DCP plot showing CBR vs. depth.

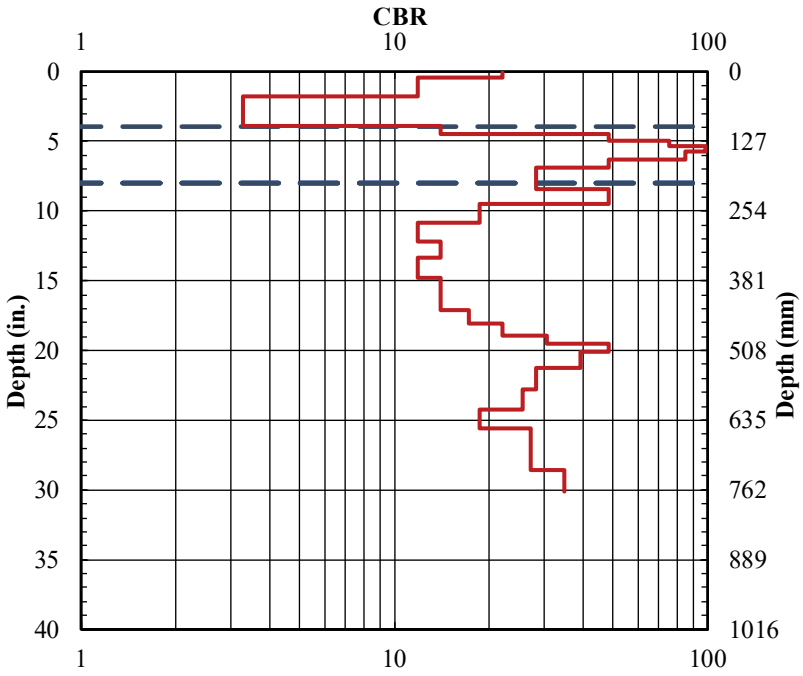

This assumption was also supported by visual inspection when the forms were stripped from the first two quadrants (FF-BU and FF-WM). Figure 4.4 shows there is a crust on each lift with a dry pocket of material underneath, creating a layered structure. It is not known how far the dry pockets extended from the quadrant edges, but attempts to cut cores from interior portions of each quadrant were unsuccessful. Figure 4.5 shows no complete core was able to be retrieved; the only recoverable pieces were from the top crust.

Figure 4.4. Dry pockets of flowable fill along formwork edges.

Figure 4.5. Attempted cores from dry-placed flowable fill.

Figure 4.6 shows a summary of CBR values from all DCP tests. Because it was found that the top surface of each placement formed somewhat of a crust with some dry pockets underneath, Figure 4.3 plots the top 1 in. of each lift compared to the lower 3 in. of each lift, alongside the average of each entire lift. Except for a few cases, CBR differences between the 1 in. crust and underlying 3 in. do not appear that meaningful.

Figure 4.6. CBR values determined from DCP testing.

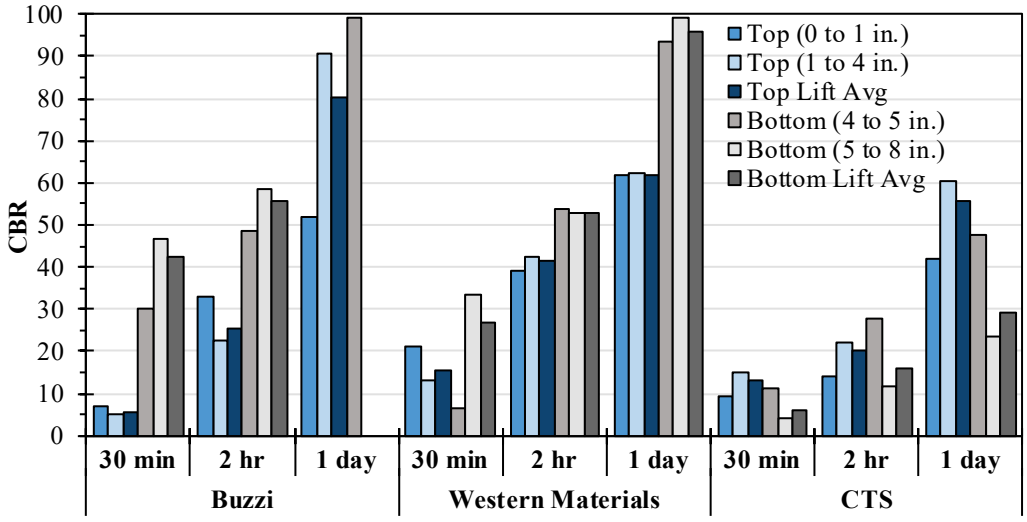

This discrepancy relative to visual observations of dry pockets, coring attempts, and individual DCP plots (e.g., Figure 4.3) is thought to be related to several factors. First, DCP results can be questionable at the very near surface of a test area (e.g., from 0 to 1 in.) due to the lack of confinement at the surface relative to at depth. Second, the exact interface between the top and bottom lifts (as well as the bottom lift and underlying materials) is not known. Both lifts were planned to be 4 in. thick; they

were overall fairly close to the target, but there were certainly variations. Figure 4.3 is a good illustration of this point. CBR is much higher at 5 in. deep than at 4 in.; it is possible that the bottom lift at this particular location was closer to 3 in. thick while the top lift was closer to 5 in. thick. These sorts of nuances would not be adequately represented in Figure 4.3. However, general trends are evident and useful.

CBR increased from 30 min to 2 hr to 1 day as would be expected. For FF-BU and FF-WM, the bottom lift always exhibited a higher average CBR than the top lift. It is interesting that the top lift for FF-CTS3 always exhibited higher average CBR values than the bottom lift; one possible explanation is that the top lift was placed while significant standing water remained on the bottom lift. This means that the top lift was effectively wetted from above and below, and as a result, at least some of the water that was intended to wet the bottom lift had no impact on the bottom lift.

At 1 day, FF-BU reached refusal, and FF-WM nearly reached refusal– both with approximate CBR values of 100. FF-BU and FF-WM were fairly similar, but FF-CTS3 exhibited about half the final average CBR (i.e., 55 CBR for top lift average). This may be partly due to reduced water percolation and therefore less hydration, but it is also likely that FF-CTS3 simply does not exhibit the same strength characteristics as FF-BU and FF-WM as discussed in the next section.

4.1.1.2 Wet placement method properties

FF materials placed with the wet method via the volumetric mixer described in Section 4.3.3 were evaluated for ASTM D6103 (2017b) flow consistency (two replicates) and ASTM C39 (2018) compressive strength (three replicates). These two tests represented a simplified screening method relative to the testing in Cox and Carr (2018) and were chosen primarily to assess flowability and strength in a balanced manner. Each FF material sample was obtained from the mixer's chute, and samples were obtained at various water-cement (w/c) ratios that are controlled by the mixer's flow gate setting.

Prior to the pour, the mixer's flow gate settings were checked, and it was determined that, when fully closed, the gate-setting dial indicator, which ranges from 0 to 12, read 4.75 rather than 0. It is believed that the mixer's gate-setting dial was inadvertently repositioned during manufacturer servicing, which occurred immediately prior to this test.

Normally, the gate setting is determined and visually fine-tuned during placement based on the FF consistency. The setting that provided normal FF consistency was 1.5, which was actually one full dial rotation and then a setting of 1.5; for simplicity here, dial settings greater than 12 are presented (e.g., one full rotation plus 1.5 equates to 13.5). Two additional gate settings of 12 and 15 were determined based on the outer limits of FF being too wet or too dry to place, respectively. For FF-BU, logistical issues prevented a sample from being obtained at the gate setting of 15. For FF-CTS3, the gate setting of 13.5 was found to produce a consistency too dry, so the gate setting of 15 was not attempted; instead, the third sample was taken at a gate setting of 11 to maintain three gate settings.

Figure 4.7 shows the flow and 2 hr, 1 day, and 28-day strength data for all three mixes at each gate setting. As in Figure 4.6, it is apparent that FF-BU and FF-WM exhibit very similar properties, especially compared to FF-CTS3. FF-CTS3 exhibits approximately half the strength and considerably lower flow numbers. However, this type of comparative assessment can be misleading. FF-CTS3 does still meet the Table 4.2 compressive strength criteria at 2 hr and 28 days, while FF-BU and FF-WM are so excessively strong that they are nearly double the maximum allowable compressive strength at 28 days.

Figure 4.7. Compressive strength and flow consistency of wet-placed flowable fill.

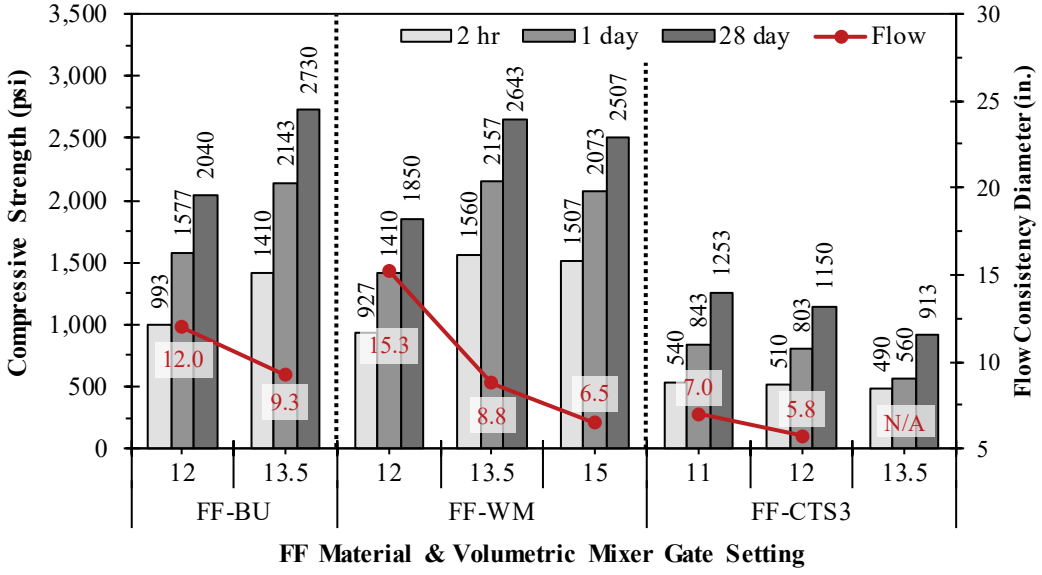

Flow numbers for each FF material appear lower than those for previously collected data. For example, FF-BU exhibited a 16 × 16-in. spread in Cox and Carr (2018) but only a 9.25 × 9.25-in. spread in Figure

4.7; the visual consistency in both cases would have been fairly similar, though probably not exactly identical. If the gate setting of 13.5 were taken to be the most appropriate gate setting for FF-BU and FF-WM, flow for both materials would fail the 10- to 18-in. spread requirement in Table 4.2. In past tests, FF-CTS1 exhibited a 9.5 × 9.5-in. spread and about 2,000 psi 28-day strength (Cox and Carr 2018), and FF-CTS2 exhibited an 11.4 × 11.4-in. spread and about 900 psi 28-day strength (Cox and Hoffman 2019). While 28-day strengths were reasonable for FF-CTS3 and fell between FF-CTS1 and FF-CTS2, the flow consistency results did not fall between the two; they were much lower. Overall, tests performed in this project (i.e., Figure 4.7) yielded lower flow results across the board, which is not currently understood at this point.

One issue that should be noted is that some FF-WM and almost all FF-CTS3 cylinders molded for compressive strength testing exhibited slight to severe honeycomb voids as shown in Figure 4.8. All sampling and testing were handled by a third-party laboratory, so it is unknown what caused the issue. All cylinders were molded within a few minutes of sampling, so timing would not be expected to be a contributing factor.

Figure 4.8. Photographs of flowable fill cylinders showing voids.

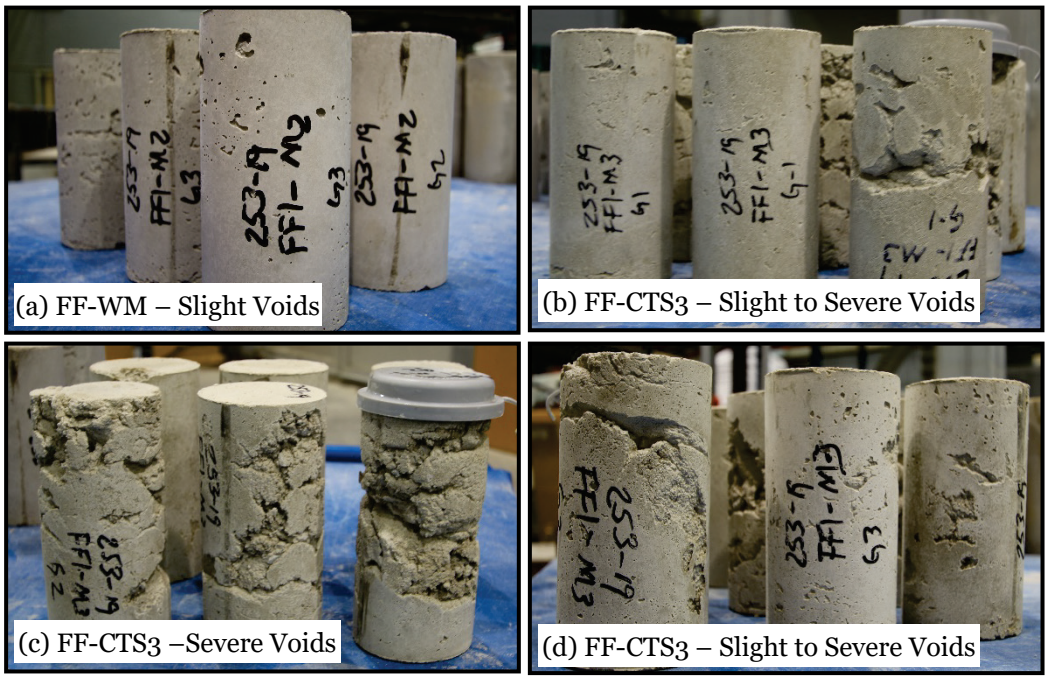

The drier mixes, like FF-CTS at a gate setting of 13.5, could have been too stiff to easily consolidate in the plastic mold, and this was not noticed; this does not, however, explain the occurrence of voids with wetter mixes, like

FF-CTS at a gate setting of 11. Regardless of the cause, Figure 4.7 results should be interpreted through this lens; the presence of voids would reduce compressive strength, but it is difficult to say to what degree.

4.1.2 Rapid-setting concrete

CTS Rapid Set® Concrete Mix (RSC) is a proprietary, pre-blended, rapid-setting concrete material that is used extensively in RADR operations for capping craters. Desirable attributes of RSC in the context of RADR are its fast set time (10 to 20 min) and its high early strength and load carrying capacity after only 2 hr of curing. RSC contains CTS's proprietary Rapid Set® Cement as well as 3/8-in. maximum size pea gravel. Military specification MIL-DTL-32536 (DLA 2015a) governs requirements for rapid-setting concrete capping materials. RSC was acquired in 3,000-lb supersacks.

4.1.3 Hot mix asphalt

Hot mix asphalt concrete (AC) was obtained from a local supplier, APAC Mississippi, from the Jackson, MS, plant. Two mixtures were used for field repairs in this project and are defined as AC1 and AC2 (Table 4.3).

AC1 (MT 9.5) was a Superpave-designed mixture approved for highway use by the Mississippi Department of Transportation (MDOT). The MDOT designation MT refers to medium traffic based on the 65-gyration design compactive effort. AC2 (SC-1 Commercial Surface) was a Marshall-designed mixture used for private paving work. Both utilized an unmodified PG 67-22 asphalt binder. For this project, specific properties of each mixture were not of great interest.

Multiple mixtures were tested rather than a single mixture because mixture properties were not critical to screeding operations. Taking this approach allowed AC to be obtained from the plant at any time rather than waiting for testing days in which the plant was producing the same mixture (the quantities of AC obtained on any given day for this project's testing were not enough for the plant to justify producing a single mixture solely for this project). For each large repair test, AC was delivered to the test site in three approximately 10-ton loads spaced such that one load could be used prior to delivery of the next.

Table 4.3. Hot mix asphalt concrete mix design properties.

		AC1	AC2
Mix Designation		MT 9.5 mm	SC-1 Commercial Surface
Design Compaction Effort		65 N_{des}	—
NMAS (mm)		9.5	9.5
Percent Passing (%)	1.0 in. / 25.0 mm	100	100
	3/4 in. / 19.0 mm	100	100
	1/2 in. / 12.5 mm	100	100
	3.8 in. / 9.5 mm	98	94
	#4 / 4.75 mm	72	65
	#8 / 2.36 mm	53	44
	#16 / 1.18 mm	39	33
	#30 / 0.60 mm	32	24
	#50 / 0.30 mm	15	12
	#100 / 0.15 mm	7	8
	#200 / 0.075 mm	4.5	5.6
1/2 in. Crushed Gravel (%)		52	50
#8 Limestone (%)		7	0
#11 Limestone (%)		10	0
Coarse Sand (%)		10	25
RAP (%)		20	25
Hydrated Lime (%)		1	0
P_{AC} (%)		5.6	6.0
$P_{ba,\ mix}$ (%)		0.65	—
P_{be} (%)		4.95	—
G_{sa}		2.656	—
G_{sb}		2.556	—
G_{se}		2.598	—
G_{mm}		2.391	—
VMA		15.2	—
VFA		73.7	—
D/B Ratio		1.13	—

– *NMAS = nominal maximum aggregate size*
– *P_{AC} = asphalt binder content*
– *P_{be} = effective asphalt binder content*
– *G_{sb} = aggregate bulk specific gravity (g/cm³)*
– *G_{mm} = mixture maximum specific gravity (g/cm³)*
– *VFA = voids filled with asphalt*
– *RAP = reclaimed asphalt pavement*
– *$P_{ba,\ mix}$ = absorbed asphalt content, mix mass basis*
– *G_{sa} = aggregate apparent specific gravity (g/cm³)*
– *G_{se} = aggregate effective specific gravity (g/cm³)*
– *VMA = voids in mineral aggregate*
– *D/B Ratio = ratio of dust to effective binder content*

4.2 Field test site

Testing in this report was conducted at the ERDC Outdoor Pavement Test Facility, Vicksburg, MS, on one of two test sections (Figure 4.9). Large concrete repairs were conducted on a 75-by-150-ft concrete section composed of varying slab sizes (15 by 15, 20 by 20, or 25 by 25 ft) that were 15 in. thick. Small concrete repairs and large asphalt repairs were conducted on a different concrete test section that was 50 by 285 ft composed of 12.5-by-15-ft slabs that were 11 to 13 in. thick.

Figure 4.9. Aerial views of ERDC test sections.

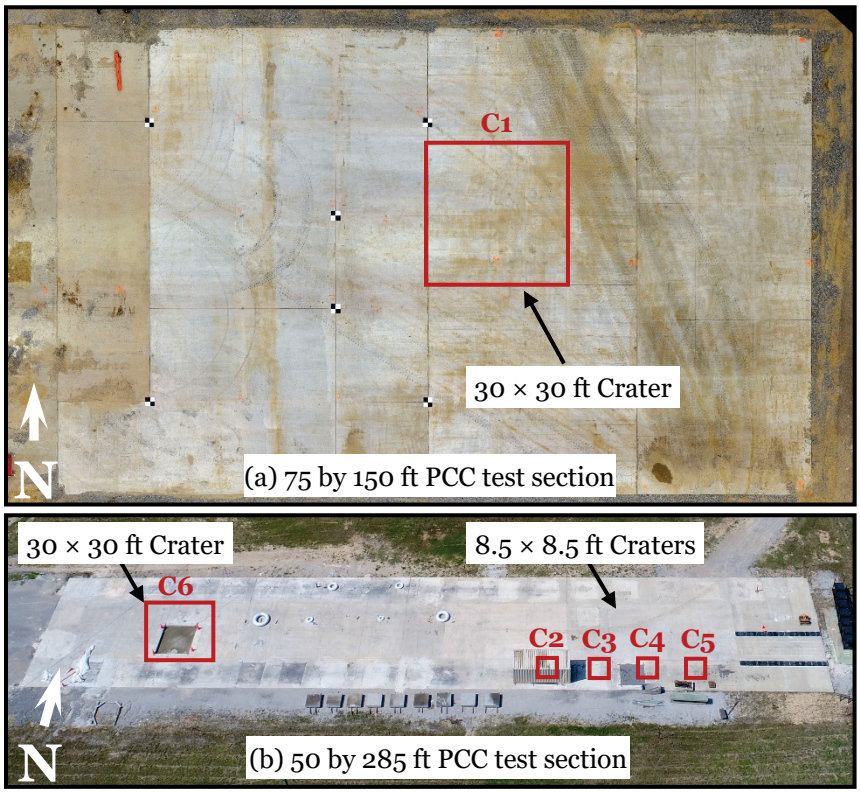

4.3 Test crater preparation

Five test craters were constructed and are detailed in Table 4.4. Test craters were produced from intact slabs using a CTL and a CTL wheel saw attachment as shown in Figure 4.10a. Saw-cut concrete was then broken and removed using a mini-excavator with breaker head and bucket attachments as shown in Figure 4.10b. Each crater was then excavated to a depth of 24 in. prior to backfilling.

Table 4.4. Crater properties for RADR screed testing.

Repair Material	Crater ID	Size (ft x ft)	Depth (in.)	Backfill Type	Backfill Thickness (in.)	Surface Thickness (in.)
RSC	C1	30 x 30 (Large)	24	Soil Cement	14	10
	C2	8.5 x 8.5 (Small)	24	Foam	14	10
	C3	8.5 x 8.5 (Small)	24	Foam	14	10
	C4	8.5 x 8.5 (Small)	24	Foam	14	10
	C5	8.5 x 8.5 (Small)	24	Foam	14	10
AC	C6	25 x 30 (Large)	22	FF	18	4

– *Note: crater C6 was reused for successive repairs; after a repair, only the surface was excavated, leaving the backfill, and the crater was used for the next repair test.*

Figure 4.10. Producing test craters.

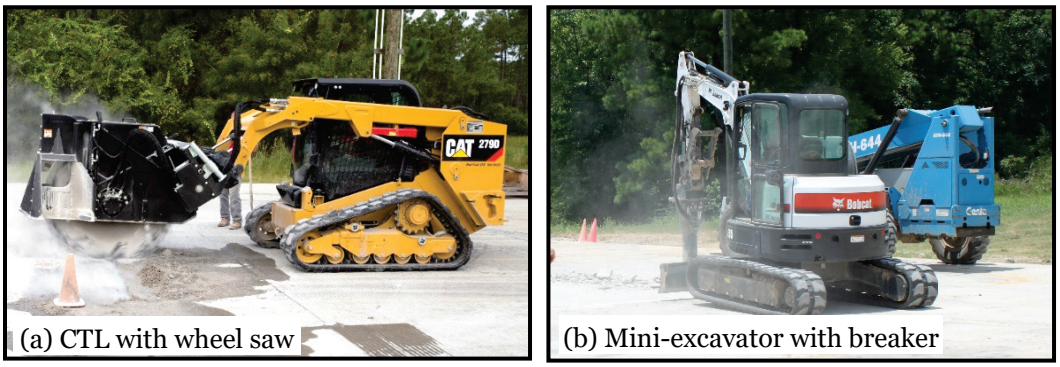

(a) CTL with wheel saw (b) Mini-excavator with breaker

Backfill materials varied because the craters used often overlapped with other projects with different objectives. C1 was also utilized for the large crater concrete repair project (Edwards, Bell, and Opperman 2021), and C2 to C5 were also utilized for the foam-in-a-bag backfill project (Gurtowski et al.[1]). This variety was acceptable since backfill material has negligible impact to screeding operations. Because these backfill processes are described in other reports, they are not described herein. The only pertinent item from these four craters is that C1 was formed into four 15-by-15-ft quadrants using plastic forms and form stakes prior to RSC placement as shown in Figure 4.11.

Figure 4.11. Plastic formwork for large crater C1.

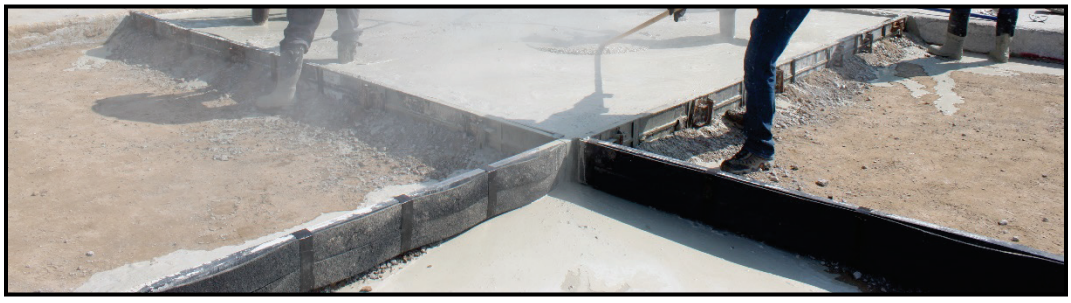

Large crater C6 was the only crater that did not overlap with another project, but C6, being used as a test bed for the different FF materials described in Section 4.1.1, was prepared somewhat differently than normal. To obtain additional data from a single backfill process,

[1] Gurtowski, L. A., M. Mejías-Santiago, J. M. Lalley, J. A. Sherburn, Z. B. McClelland, M. McKechnie, C. T. Bradley, and M. E. Glynn. Draft report. *Development and evaluation of instant structural materials for airfield damage repair*. ERDC TR. Vicksburg, MS: U.S. Army Engineer Research and Development Center.

the backfill was performed in two stages as illustrated in Figure 4.12. In the first stage, 8 in. of FF was placed using the dry method, and 10 in. of FF was placed using the wet method in the second stage.

Figure 4.12. Placement plan for large crater C6 backfill.

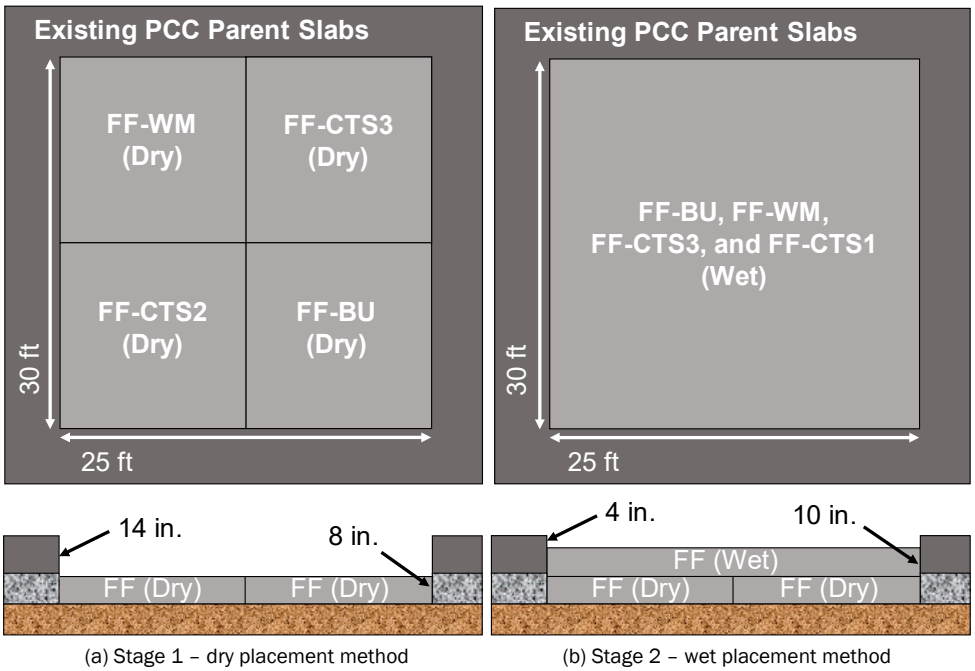

(a) Stage 1 – dry placement method (b) Stage 2 – wet placement method

For the dry placement method, four different FF materials were used where FF-BU, FF-WM, and FF-CTS3 were tested for properties as described in Section 4.1.1, and FF-CTS2 was used only as additional miscellaneous material but was not tested. These were separated into quadrants by 8-in. wooden forms (Figure 4.13a). FF was spread in each quadrant using the dry "slash-and-splash" method and then roughly leveled (Figures 4.13b and 4.13c). Water was metered on top of each lift with 120 gal. for lift 1 and 90 gal. for lift 2 (Figures 4.13d and 4.13e). These volumes were determined based on previous experience and measured using a flow meter. Quadrants 1 and 2 (FF-BU and FF-WM) were placed first; the following day, the forms were stripped and quadrants 3 and 4 (FF-CTS2 and FF-CTS3) were placed. Figure 4.13f shows the completed stage 1 backfill.

For the wet placement method, the same FF materials were tested with the exception that the additional miscellaneous material was FF-CTS1 rather than FF-CTS2. Figure 4.14 shows the overall backfill process using the simplified volumetric mixer (SVM) described in Section 4.4.3. Six supersacks of each FF material were used, one material at a time.

Material samples for Section 4.1.1 characterization were taken in the middle of each batch of six supersacks to give time for any remaining material from the previous batch to clear the SVM material bin.

Figure 4.13. Crater C6 flowable fill backfill–dry placement method (stage 1).

Figure 4.14. Crater C6 flowable fill backfill–wet placement method (stage 2).

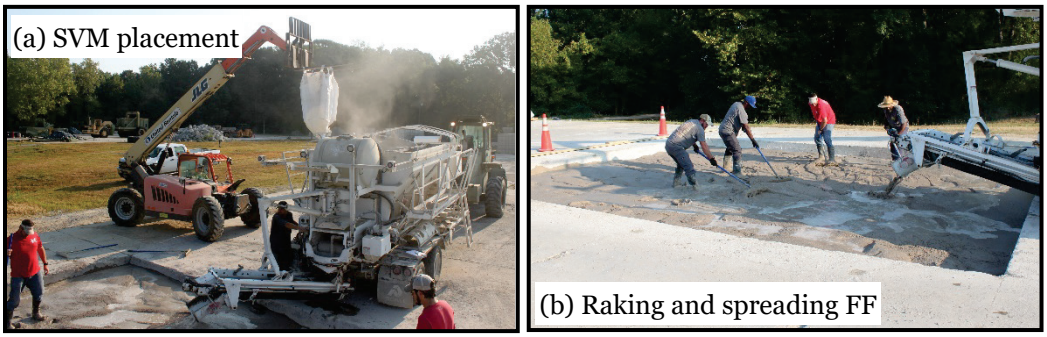

Leveling the final FF surface at the 4-in. depth was a challenge for such a large repair considering how quickly rapid-setting FF sets. This was accomplished by hand using rakes and floats. Figure 4.15a shows the final

completed backfill surface, which was surveyed using a rod and level setup (Figure 4.15b) to determine the backfill surface profile (99 survey points).

Figure 4.15. Final crater C6 backfill profile and surveying.

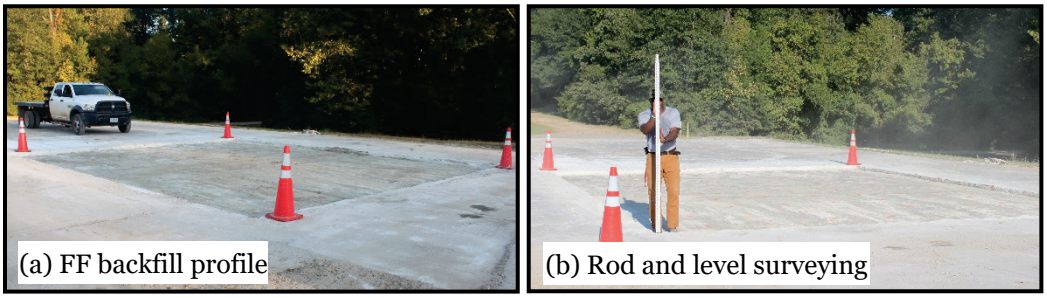

Figure 4.16 shows the backfill depth was not a uniform 4 in. but instead averaged 3.2 in. and was approximately 1.25 in. shallower in the center area than around the perimeter. Standard deviation was 0.61 in., yielding a coefficient of variation (COV) of 19%. As shown in Figure 4.14b, the SVM chute discharged the bulk of its material near this center area, and it had to be raked to the far edges. This inadvertently led to more material in the center and was compounded by the rapid set times, which made it difficult to adequately level once the material began to set.

Figure 4.16. Crater C6 surface profile showing depth (in.).

4.3	4.0	3.6	3.6	3.1	3.1	3.2	4.1	4.0
4.2	3.4	3.5	3.4	3.3	3.4	3.3	3.6	4.3
3.9	3.0	2.9	3.0	2.6	3.0	3.2	3.2	4.1
3.1	3.2	2.8	2.3	2.0	2.6	2.8	3.1	3.6
3.4	3.2	2.8	2.3	1.9	2.3	2.5	3.0	3.9
3.4	3.1	2.7	2.3	2.3	2.5	2.5	2.8	3.7
3.2	3.2	2.9	2.4	2.4	2.8	2.7	3.2	3.9
3.4	2.8	3.2	2.6	2.6	2.3	2.5	3.7	3.6
3.6	3.3	3.5	3.0	2.5	2.0	2.3	3.6	4.1
3.7	3.9	3.9	3.8	2.6	2.2	2.5	3.2	3.4
4.2	4.6	4.4	3.6	2.9	3.2	2.9	3.7	3.5

Avg Depths:	3.7 in.	3.1 in.	2.6 in.	3.7 in.
Roll-Down:	1.5 in.	1.25 in.	1.0 in.	1.5 in.

The dotted lines in Figure 4.16 indicate the approximate locations of longitudinal joints separating the three paving lanes. Average depths were determined along each of these longitudinal lines, as this is needed to set

screed bar grade for proper roll-down. Both are shown in Figure 4.16 where roll-down was approximately determined using the general rule that approximately 3/8-in. roll-down is required per 1-in. depth.

4.4 Equipment

Various pieces of heavy equipment were used throughout this project. This equipment either belonged to ERDC or was rented for the project.

4.4.1 Compact track loader

Figure 4.17 shows a Caterpillar 277C CTL, or skid steer, that was used primarily during AC repairs to transfer AC from the stockpile to the crater. It was also frequently used for cleanup tasks. These CTLs are rubber-tracked machines with high-flow hydraulics and quick-connect fittings that are used extensively in modernized ADR processes because they are versatile and efficient for many purposes. While there are many CTL attachments that may be used during RADR operations, the only attachment used in this project was a bucket attachment.

Figure 4.17. Caterpillar 277C compact track loader.

4.4.2 Telehandlers

Figure 4.18 shows two telehandlers utilized in this project for screeding operations. Key specifications are provided in Table 4.5. The Caterpillar TL1055C was the primary telehandler used throughout the project for most repairs. The TL1255D was used for the large RSC repair of crater C1 and was borrowed from another group at ERDC due to the TL1055C being down for repairs at the time. The primary difference between the two is that the TL1255D has a max capacity of 12,000 lb compared to 10,000 lb for the TL1055C. With the boom fully extended, the capacities are 3,500 and 2,500 lb, respectively.

It is worth noting that the Genie GTH-1256 AF is the unit that has been fielded as part of the USAF RADR major repair kit. While the non-military version (GTH-1256) has a 12,000 lb capacity, the Air Force version (GTH-1256 AF) has a 10,000 lb capacity. Neither Genie model was utilized in this project, but discussion of the Genie unit is provided in Chapter 7.

Figure 4.18. Caterpillar telehandlers.

Table 4.5. Telehandler specifications.

Specification	CAT TL1055C	Genie GTH-1256 AF
Power (hp)	142	142
Max Travel Speed (mph)	20.4	20.5
Overall Height (ft)	8.42	8.33
Wheelbase (ft)	12.00	11.46
Operating Weight (lb)	34,160	34,361
Max Lift Height (ft)	55	55
Max Forward Reach (ft)	43	42
Max Lift Capacity (lb)	10,000	12,000
Max Load at Max Height (lb)	5,000	5,000
Max Load at Max Reach (lb)	2,500	3,500

4.4.3 Simplified volumetric mixer

Figure 4.19 shows the tow-behind simplified volumetric mixer (SVM) manufactured by ProAll International Mfg. Inc. It is pre-calibrated for both rapid-setting FF and concrete and is towed with a vehicle capable of pulling at least 20 tons (typically a dump truck). Key components of the SVM are a single dry material hopper (approximately 7 yd^3 capacity), a conveyor belt feed system, a water pump to meter mix water at a fixed pump speed, one 400-gal. water supply tank, a washout tank, and a replaceable mixing auger mounted in a discharge boom at the rear of the mixer. The SVM is also equipped with two retractable catwalk platforms, a bin entry platform, a replacement auger, and two supersack piercing points.

Material consistency (i.e., *w/c* ratio) is controlled by adjusting a strike-off gate that changes dry material thickness on the conveyer belt feeding the

mixing auger. Gate settings range from 1 to 12. Raising the gate (i.e., increasing the gate setting) introduces more dry material to the auger and, thus, lowers *w/c* ratio, and vice versa. Typical gate settings during production for rapid-setting FF and concrete range from 4 to 8.

Figure 4.19. Simplified volumetric mixer.

Note that during equipment maintenance performed by the manufacturer prior to this work, the strike-off gate system was disassembled, serviced, and reassembled. When the gate was reassembled, the gate-setting indicator dial was not aligned properly. This was discovered once the SVM was loaded with material for backfilling crater C6 when the dial read 4.75 rather than 0. This offset should be noted but was not of great concern to the project since gate settings are frequently adjusted during placements to adjust mixture consistency until it appears visually suitable. The main implication is that care should be taken in comparing gate settings in this report to those of other reports as they may be reported differently.

4.4.4 Double drum vibratory roller

A CASE DV210 double drum vibratory steel wheel roller was used for AC compaction in this project (Figure 4.20). Table 4.6 provides key specifications. This size roller was used to relate to the original asphalt screed work conducted by ARA[1]. Only the steel wheel roller was used for this project; a pneumatic roller was not used.

[1] Pullen, A. B., C. L. Wilbur, C. Ishee, and J. Hall. 2016. Draft report. *Rapid airfield damage repair asphalt concrete placement: Development of prototype asphalt concrete screeds*. Vicksburg, MS: U.S. Army Engineer Research and Development Center.

Figure 4.20. Double drum steel wheel roller.

Table 4.6. Double drum vibratory roller specifications.

Specification	CASE DV210
Power (hp)	99
Operating Weight (lb)	22,928
Max Travel Speed (mph)	6.8
Wheelbase (in.)	136
Drum Diameter (in.)	51
Drum Width (in.)	67
Static Linear Load (lb/in.)	169
Centrifugal Force per Drum - low (lb)	17,310
Centrifugal Force per Drum - high (lb)	24,729
Nominal Amplitude – High (in.)	0.028

4.5 Crater repair methods

Table 4.7 summarizes the RADR screed test plan. Based on findings of Cox and Hoffman (2019), primary focus was on large repairs, with large asphalt repairs being of greater interest than large concrete repairs. The screed was also used for several small concrete repairs performed as part of a separate project; this was primarily for validation purposes.

Table 4.7. RADR screed test plan by crater ID.

Repair Material	Repair ID	Crater ID	Size (ft x ft)	Surface Thickness (in.)
RSC	R1	C1	30 x 30 (Large)	10
	R2	C2	8.5 x 8.5 (Small)	10
	R3	C3	8.5 x 8.5 (Small)	10
	R4	C4	8.5 x 8.5 (Small)	10
	R5	C5	8.5 x 8.5 (Small)	10
AC	R6	C6	25 x 30 (Large)	4
	R7	C6	25 x 30 (Large)	4

4.5.1 Concrete repairs

All concrete repairs at the Outdoor Pavement Test Facility were conducted with RSC placed with the SVM. This section discusses the repair process with respect to placing and screeding RSC; any previous crater preparation work (e.g., backfill and formwork) was discussed in Section 4.3.

Before or during each pour, the screed operator positioned the screed on the opposite side of the crater from the SVM (Figures 4.21a and 4.21b). Preferably, the screed should be positioned on the downhill side of the crater so that it can "push" material uphill as it screeds, but this positioning is not always feasible depending on crater location.

Figure 4.21. Overview of concrete repair process.

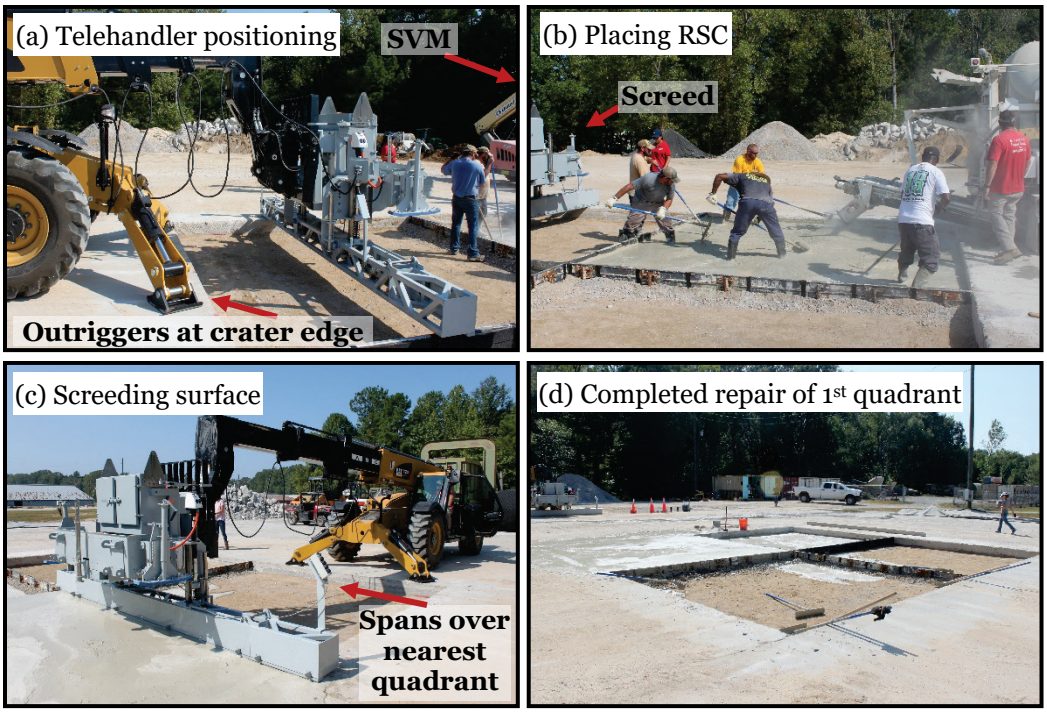

For large repairs, the SVM must be placed directly next to the quadrant being poured, so positioning the telehandler on the opposite side means the screed will span over the nearest quadrant and screed the far quadrant (Figure 4.21c). Since this means the telehandler must boom out over 30 ft, the screed should be parked fairly close to the edge of the crater with the outriggers down (Figure 4.21a). The operator should also boom the screed out partially to ensure proper alignment with the crater (as opposed to at an angle). Small repairs do not require the same

level of detail when positioning the screed since the telehandler does not have to extend its boom out nearly as far.

Once positioned, the outriggers should be used to take all weight off the front tires and to level the telehandler from side to side. The spotter should then assist the operator in leveling the screed from front to back by adjusting the fork tilt angle. For a large repair where one end of the screed bar must follow formwork, especially if plastic forms are used, the spotter may wish to raise the formwork side of the screed bar as shown in Figure 3.11. This better ensures that, when the screed is lowered and the suspension system is engaged, most of the down pressure is on the outside end of the screed bar, and minimal down pressure is applied to the formwork. Once these adjustments are made, the screed is considered set.

During each pour, a ground crew used concrete rakes to distribute RSC around the crater, building up slightly more material on the side of the repair from which screeding would begin (Figure 4.21b). Once the SVM operator believed sufficient RSC had been placed, the SVM was stopped, and screeding began with the assistance of a spotter (Figure 4.21c). Detailed information regarding operation and use of the screed during the screeding process is provided in Chapter 5.

Following screeding, the screed was used to push any excess RSC several feet past the repair to facilitate easier cleaning using the bucket of a CTL and shovels. In some cases, minor handwork with trowels was performed to clean the repair edges. Meanwhile, the screed was moved to a washout area to be pressure washed. Figure 4.21d shows the completed first quadrant of repair R1.

4.5.2 Asphalt repairs

All asphalt repairs at the Outdoor Pavement Test Facility were conducted with either AC1 or AC2 placed in crater C6. This section discusses the repair process with respect to placing, screeding, and compacting AC; any previous crater preparation work was discussed in Section 4.3.

Before each lane of a large repair was paved, the screed operator positioned the screed next to the crater (Figure 4.22a). The two outside lanes were always paved first, and the middle lane was paved last. In contrast to large crater concrete repairs where the screed skips the nearest quadrant and screeds the far quadrant, large asphalt repairs require

screeding of the entire 30-ft crater length at one time. This means the telehandler must be parked slightly further back from the crater (approximately 4 to 5 ft) so that the screed can take off from the existing pavement (Figure 4.22b).

Figure 4.22. Overview of asphalt repair process.

Alignment of the screed is also more critical for large asphalt repairs than for concrete repairs due to the use of various attachments like the end gates. It is necessary to line up straight with the crater, position the end gates, and then extend the screed out in a dry run to make sure the screed follows the side of the crater through all 30 ft. A few attempts were generally necessary to align the screed correctly; these steps took only a few minutes.

Once positioned, the outriggers should be used to take all weight off the front tires and to level the telehandler from side to side. The spotter should then assist the operator in leveling the screed from front to back by adjusting the fork tilt angle. The AGCS/MGCS ride track is then laid out on the backfill in the crater. Grade control devices are then set to the proper grade height for roll-down (nominally 1.5 in. for a 4-in.-thick repair), and all retaining pins are removed. At this point, the screed is considered set as shown in Figure 4.22b. Step-by-step details regarding screed setup are provided in Chapter 5.

Asphalt mix was delivered to the site by dump truck and dumped in a single pile on the concrete test section (Figure 4.22c). Each load of approximately 10 tons provided sufficient material to pave one 9-ft lane with excess material remaining. Mix temperatures were measured from the time mix was delivered.

As soon as possible, a CTL with a bucket was used to transfer mix from the pile to the crater. Because the RADR screed has no mechanism (e.g., augers) to distribute the mix laterally, the CTL operator side-loaded each bucket by scooping into the pile at an angle (Figure 4.22d). By alternating left- and right-side loads, mix was more evenly dispersed from left to right within the paving lane (Figure 4.22e). Additionally, after a load was placed in the crater, it was back-bladed by angling the CTL bucket down and dragging it backwards across the crown of the pile. This is denoted as the pre-strike-off. This helps to keep asphalt piles in the crater from building too large and spilling over the top of the screed bar during screeding.

Figure 4.23 provides an illustration of the placement process in three lanes. Diagrams on the far left illustrate CTL placement and back-blading of loose mix, middle diagrams illustrate the lane after screeding, and far-right diagrams illustrate the lane after compaction.

Figure 4.23. Illustration of asphalt placement in three paving lanes.

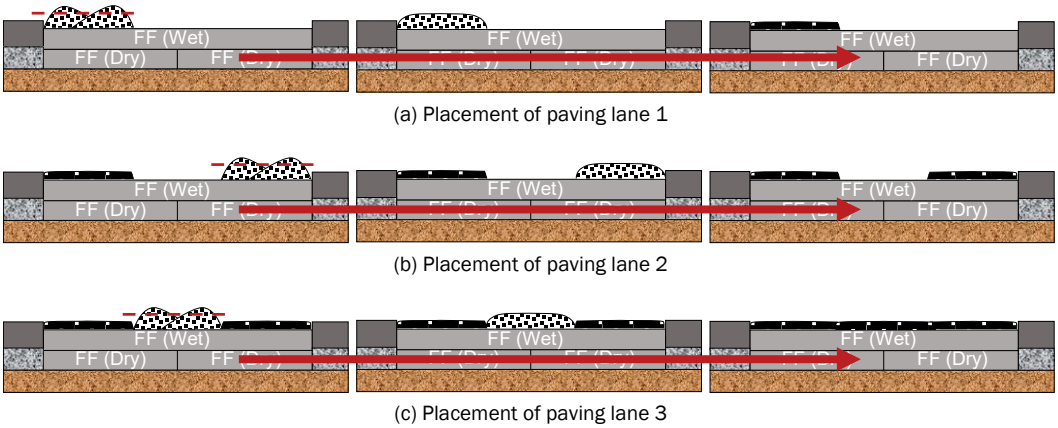

(a) Placement of paving lane 1

(b) Placement of paving lane 2

(c) Placement of paving lane 3

Once the active paving lane was filled with several CTL bucket loads of mix, screeding began (Figure 4.22f). As the screed was advanced, two ground men with shovels stood on either side of the screed to help ensure a full head of material was maintained across the entire screed width, redistributing mix if necessary (Figure 4.22f). Simultaneously, the CTL operator continued ferrying additional mix to the screed. As the screed approached the end of the crater, the CTL operator slowed his tempo accordingly while remaining close with a bucket of mix in the event the ground men needed an additional shovel or two of mix.

Behind the screed, another ground man was simultaneously working to clean excess material from the start of the paving pull as well as the joint face. Using a lute, he tamped the joint face to promote a uniform clean edge (Figure 4.22g). All other edges, such as around the perimeter of the crater, were also tamped with a lute to ensure that the roll-down material was folded back inside the repair before compaction (Figure 4.22h).

Following screeding, the screed was used to push the excess head of material several feet from the crater where the CTL could more easily scoop it up and remove it. Additional cleaning and other minor handwork with shovels and lutes were generally necessary to remove excess material from the repair area prior to compaction. Figure 4.24 shows the cleanup process as well as a paving lane after cleanup that is ready for compaction.

Figure 4.24. Excess asphalt cleanup prior to compaction.

Compaction began as soon as other equipment cleared the area and excess mix was removed (Figure 4.25). The initial roller pattern used was the same as that used in the ARA screed work[1], which subjected the repair to 0.5 static passes (initial) followed by 2.5 vibratory passes (intermediate) followed by 4 static passes (finish). One pass was defined as a pair of forward and backward passes. Figure 4.26a illustrates this pattern. Since the lane width required two compaction lanes, all initial roller passes were applied before any intermediate passes, and all intermediate passes were applied before any finish passes. This pattern is similar to that in the Interim RADR TTPs (USAF-AFCEC 2019) except that 4 static passes with a steel-wheel roller were used at the end rather than 2 passes with a pneumatic roller followed by 3 passes with a steel-wheel roller.

During compaction of the first paving lane of repair R6, excessive check cracking and lateral shoving were observed, which can be indicators of over-rolling. As a result, the decision was made to continue all other compaction efforts with a modified roller pattern (Figure 4.26b) as follows: 0.5 static passes (initial), 1.5 vibratory passes (intermediate), and

[1] Pullen, A. B., C. L. Wilbur, C. Ishee, and J. Hall. 2016. Draft report. *Rapid airfield damage repair asphalt concrete placement: Development of prototype asphalt concrete screeds*. Vicksburg, MS: U.S. Army Engineer Research and Development Center.

2 static passes (finish). This considerably reduced check cracking and lateral shoving and did not appear to have a negative impact on pavement density as discussed in Chapter 8.

Figure 4.25. Asphalt compaction.

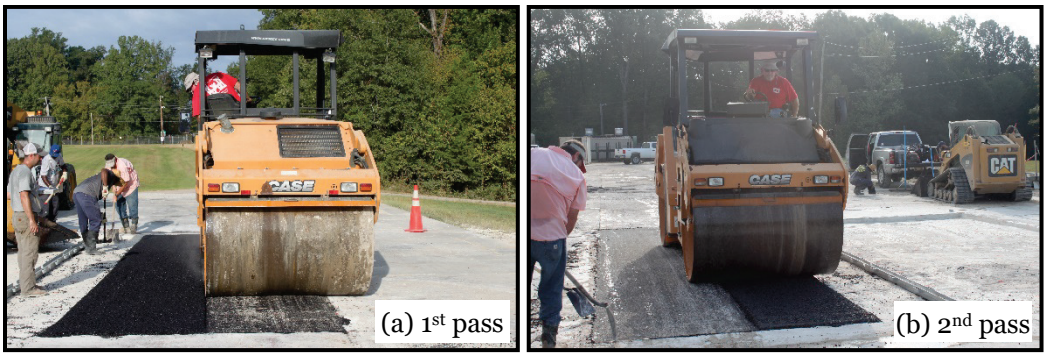

Figure 4.26. Roller pattern for asphalt compaction.

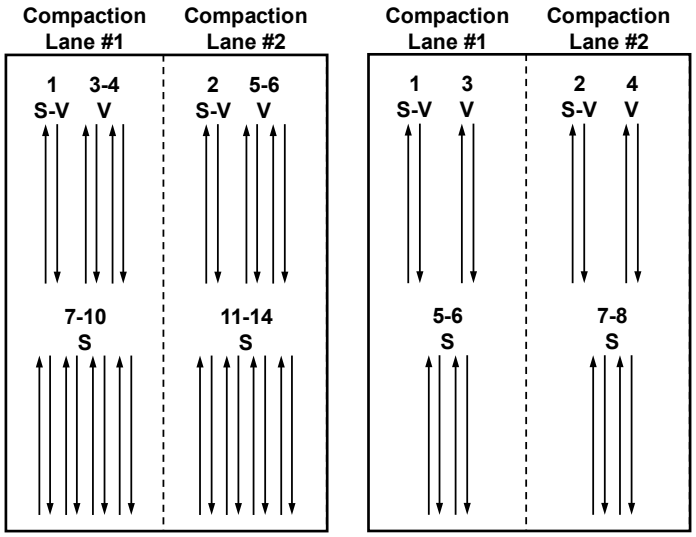

(a) Initial roller pattern (b) Modified roller pattern

Following compaction, the free edge of a paving lane, or the longitudinal joint, almost always experienced some degree of lateral shoving. While the modified roller pattern alleviated this to some extent, particularly with respect to mat thickness near the free edge, some shoving still occurred (Figure 4.27a). With such large single lift thicknesses of 4 in., this is not surprising; however, a wandering joint is much more difficult to match when paving the adjacent lane, especially with the simplified RADR screed relative to a conventional paver that has hydraulically adjustable end gates.

The cutoff wheel described in Section 3.4.6 was designed and fabricated in response to the longitudinal joint challenges. Once both outside lanes were

completed, the cutoff wheel was used to trim the free edges (Figure 4.27b). Figures 4.27c and 4.27d show a joint after it was cut and after the cut material was removed, respectively. The trimmed joints helped promote better density at the joint and also created a clean vertical face and straight joint that was much easier to match with the adjacent lane.

Figure 4.27. Cutting back asphalt longitudinal joints.

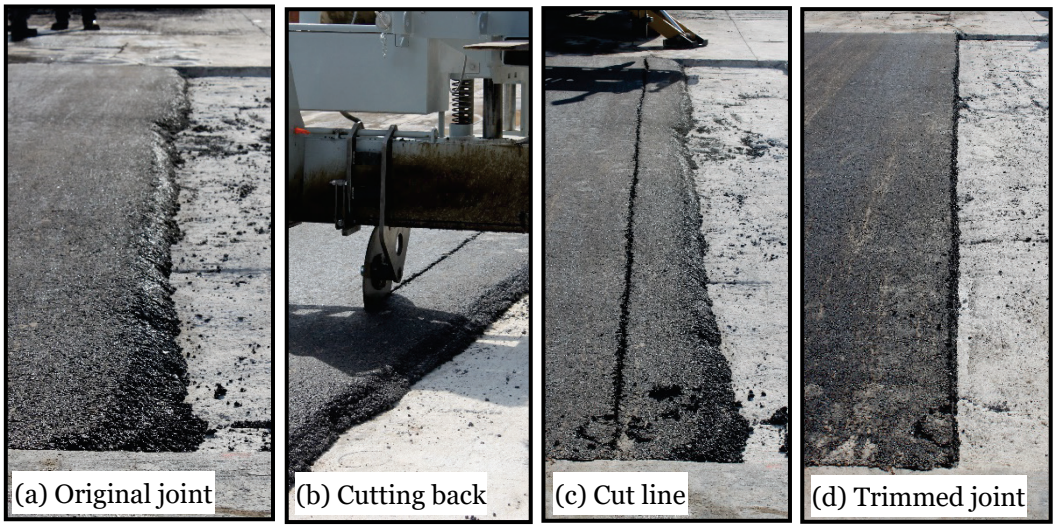

4.6 Data collection

Data recorded throughout this project was used to evaluate performance of the RADR screed. The screed itself was assessed for physical characteristics such as size and weight as well as design simplicity and versatility. Much of this assessment was based on user feedback.

Timing data and other pertinent notes, such as asphalt mix temperatures, were recorded during repairs. Of particular interest with timing was the overall time required to perform screeding as well as the number of screed passes conducted.

Finished repairs were evaluated by visual inspection, surface profile survey measurements, and, for asphalt repairs, core samples. Visual inspections sought to identify any extreme roughness issues, cracking, segregation or tearing, and any other notable distress.

4.6.1 Surface profile surveys

Rod and level surveys, illustrated in Figure 4.15, were used to determine surface profiles. Figure 4.28a shows the survey point layout for the large

concrete repair R1, which included five longitudinal profiles and three transverse cross sections where point spacing was 1 ft. While not shown, the survey layout for small concrete repairs R2 to R5 was similar but with only three longitudinal profiles and one cross section each.

Figure 4.28. Survey point layout illustration for large repairs.

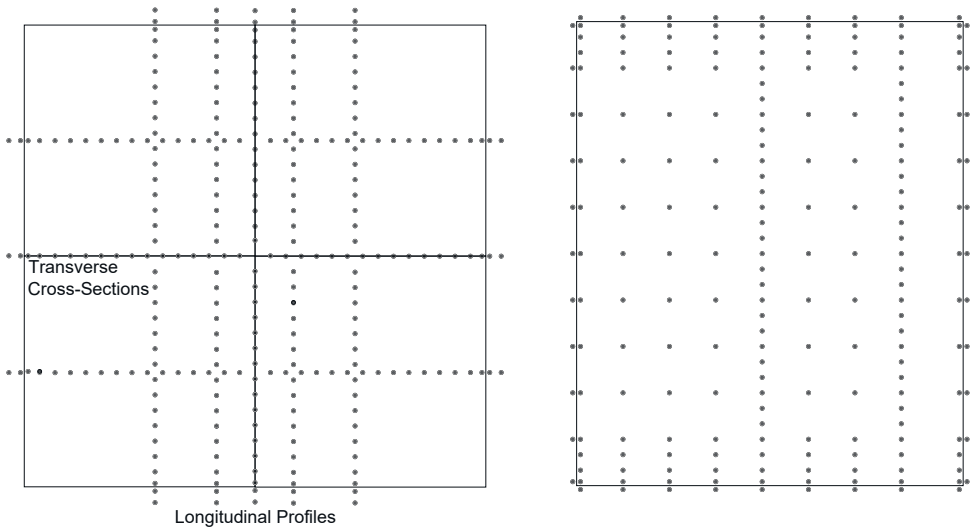

(a) Typical large concrete repair (b) Typical large asphalt repair

Figure 4.28b shows the survey layout for large asphalt repairs R6 and R7, which was essentially a 3-ft grid layout except for certain areas where a 1-ft spacing was used. The 1-ft spacing was used for the first and last 3 ft of the repair (longitudinal direction) because these areas often exhibited irregular dips or bumps where the roller transitioned from concrete to asphalt or vice versa. Additionally, two longitudinal profiles within each repair were measured at 1-ft intervals to provide greater resolution; the two profiles selected were those that were the lowest and the highest. Figure 4.28b shows two longitudinal profiles like this, but note that the profiles selected differed between repairs R6 and R7.

For both concrete and asphalt repairs, survey points around the perimeter of the repair on the existing pavement were used to establish a baseline plane that would represent the target for a perfectly flush repair. For RQC assessments, the differences between actual repair elevations and the theoretical flush plane were determined at each survey point and used to create elevation deviation surveys and produce RQC statistics.

For both small concrete and small asphalt repairs (large repairs were not included), the Interim RADR TTPs (USAF-AFCEC 2019) state that RQC

checks should be performed using line-of-sight (LOS) profile measurements as described in TO 35E2-5-1 (USAF 1992). TO 35E2-5-1 primarily focuses on large crushed-stone crater repairs with foreign object debris (FOD) covers (i.e., legacy repairs); while it does describe the general procedure for conducting LOS measurements, some extrapolation is required to apply the technique to RADR repairs. However, it can be generally concluded that a repair must be within ±0.75 in. of the surrounding existing pavement to be considered a flush repair. If a repair is not flush, then the chain of command must be notified, and the correct course of action will be advised.

Note that the Interim RADR TTPs do not state a flush repair is required; they simply state that an RQC check should be performed in accordance with TO 35E2-5-1. The objective in TO 35E-2-5-1 is a flush repair; however, if the repair is not flush, TO 35E2-4-1 is referenced with respect to determining the allowable RQC for that specific repair. A review of documentation indicates that TO 35E2-4-1 was superseded by Engineering Technical Letter (ETL) 13-3 (USAF-AFCEC 2013), which has in turn been superseded by Air Force TTP 3-32.12 (USAF-AFCEC 2016). TTP 3-32.12 states that RQC checks are required only for legacy repair methods because the new RADR methods are considered semi-permanent and are repaired flush with the surrounding pavement.

While flush small repairs are fairly simple to accomplish with RADR methods, a gap in guidance exists with respect to large repairs. The interim RADR TTPs focus mostly on small repairs and state that guidance for large asphalt repairs is forthcoming, and while the TTPs do provide information on large concrete repairs, RQC checks are not discussed. While TTP 3-32.12 (USAF-AFCEC 2016) may state that RADR methods provide flush repairs, it is the understanding of the authors that this is primarily in reference to small repairs, not large repairs, which are much more challenging to finish flush even with RADR methods. As a result, this report attempts to establish RADR repair quality categories that mesh with existing RQC definitions described in TTP 3-32.12 and other related references (collectively referred to as the RQC manuals).

The reason for creating this stand-alone quality category terminology is that determination of allowable RQC is dependent on many variables including repair location, repair spacing relative to other repairs, repair length, environmental factors, aircraft type, aircraft operation, and more. These variables are outside the scope of this work. The goal with the quality category

system is to utilize those fixed variables that pertain only to the repair itself. These include maximum repair height, maximum sag, and repair slope.

Table 4.8 lists proposed Quality Categories A through E for up to a 4.0-in. bump. Category A essentially describes a flush repair where the entire repair is ±0.75 in. relative to the existing pavement. For non-flush repairs, the maximum bump allowances increase in 1.0-in. increments, while the maximum sag and repair slope requirements are constant for all repair qualities.

Table 4.8. Proposed RADR repair quality categories.

Quality Category	Max Bump (in.)	Max Sag (in.)	Max Repair Slope (%)
A	Flush (+0.75)	Flush (-0.75)	5.0
B	1.0	-2.0	5.0
C	2.0	-2.0	5.0
D	3.0	-2.0	5.0
E	4.0	-2.0	5.0

-- Maximum repair slope in a landing touchdown zone is 3.4%.

In TTP 3-32.12 (USAF-AFCEC 2016), *maximum bump* is defined as the highest point along an LOS measurement. *Maximum sag* is defined as the difference in elevation of the lowest point and the average elevation of the two highest points on either side of the sag. The maximum repair slope is not explicitly defined though it was interpreted as the difference in elevation between two points divided by the distance between those points. A minimum distance between points of 1 ft was used in this report to determine maximum repair slope. Note that during analysis, no violations of the maximum repair slope criteria were found, even for the landing touchdown zone case, so maximum repair slope is not discussed further in this report. It was not found to be a difficult metric to satisfy with RADR methods, even for large repairs.

As a final note, it is worth the reminder that LOS measurements are typically done with stanchions rather than a rod and level. The stanchion method will inevitably be much more subjective than true surveying equipment. While results in this project are expected to have minimal error, it is possible that a repair could be assessed slightly differently if evaluated using stanchions (e.g., an area of a repair that is near +0.75 in. could be called Category A/flush or possibly Category B, depending on the observer).

4.6.2 Asphalt coring

Cores (6-in. diam) were cut from asphalt repairs R6 and R7 for air void (V_a) determination following ASTM D6752 (2017a) and D2041 (2011) for bulk and maximum specific gravities, respectively. V_a measurements were used to verify whether or not reasonable compaction was achieved using the set roller patterns. They were also used to determine whether or not trimming the joints with the cutoff wheel was effective at increasing joint density.

Figure 4.29 demonstrates the general layout of cores from large asphalt repairs (marked in orange paint). Ten cores were taken from each repair. Six cores were taken from the repair mat with two each from the three paving lanes. These were taken at the approximate midsection of the repairs. Two joint cores were taken from either side of each longitudinal joint within a few inches of the joint. The location along the joint at which these cores were taken was selected to be the average representation of the entire joint length.

Figure 4.29. Coring layout for large asphalt repairs.

5 Operation and Use of the RADR Screed

This chapter outlines detailed steps for the operation and use of the screed. This could be considered a supplement to Section 4.5, in which crater repair methods were discussed broadly; this chapter focuses primarily on the screeding aspects of a repair. The intent of this chapter is to provide a bridge between the format of a typical research report and the step-by-step format of TTPs. The chapter is divided into concrete repair and asphalt repair with each section discussing screed operation in detail as well as in a simplified numbered list format.

5.1 Connecting the screed and telehandler

5.1.1 Detailed description

In order to connect the screed to the telehandler, the telehandler forks should be fully inserted into the screed fork pockets until the telehandler mast just slightly bumps the screed's crash rack. The screed should then be picked up off the ground so that it is fully supported by the telehandler.

The cam action draw latches (Figure 3.14) are then adjusted to the proper length and used to secure the screed to the telehandler. The top of the screed crash rack may not touch the telehandler mast; this might happen if the telehandler forks are worn and no longer at 90°. No attempt should be made to remove this gap by using the cam action draw latches as they were not intended to support this weight. The latches should be adjusted to provide a slight resistance when latching. This adjustment is sufficient to ensure the screed stays securely on the forks. Lastly, the clevis pins are inserted into the cam action draw latches.

With the screed lifted off the ground, the three support legs (Figure 3.10) may be pinned in the raised position.

The power cord (Figure 3.15) is then clipped to each telescoping segment of the telehandler boom using the attached magnets. The end with alligator clamps is attached to the telehandler battery and routed out from under the engine cover. Magnets should be used to clip the cord in strategic locations to ensure the cord will remain clear of the telehandler's front tires, especially during turning. The other end of the power cord should be plugged into the screed's power port. Lastly, the slack in the

power cord should be adjusted so that movement of the telehandler boom up and down or in and out is not restricted by the cord.

5.1.2 Simplified steps

1. Fully insert forks into fork pockets and pick up screed.
2. Fasten screed to telehandler using cam action draw latches.
   a. Adjust latch length to provide slight resistance when latching.
   b. Do not overstress latch by attempting to remove gap between screed and telehandler mast.
   c. Insert clevis pins into latches.
3. Raise and pin the three support legs.
4. Connect the power cord.
   a. Connect clips to battery terminals.
   b. Run cord out from under engine cover.
   c. Plug cord into screed.
   d. Use magnets to clip cord to telehandler boom.
      (1) Make sure cord does not interfere with telehandler tires during steering.
      (2) Distribute slack in cord evenly so boom movement is not restricted.

5.2 Concrete repair

5.2.1 Detailed description

5.2.1.1 Screed configuration

For a large repair, the only task required to configure the screed is to fold down the extension wings (Figure 3.8) to extend the screed bar length from 12 ft to 17 ft. The wings should be pinned in position from the back side of the screed bar using the 1-in.-diam pins. Lastly, insert the clevis pin for retention. For a small repair, the wings are not needed.

The control pendant and post (Figure 3.16) should be relocated near the end of the screed bar so that it is within reach from the existing pavement. Two clevis pins are used to secure the post to the screed bar truss. The post may be placed on either side of the screed for easier access.

No other attachments are needed for concrete repairs. Other attachments may remain in the storage locations on the screed frame or be removed and set to the side.

5.2.1.2 Telehandler positioning

Prior to the start of placement, the telehandler/screed operator should park the telehandler on the opposite side of the crater from the SVM. The preferred equipment arrangement is that the SVM be positioned on the uphill side of the repair and the telehandler be on the downhill side so that the screed can "push" material uphill as it advances.

Alignment of the telehandler and screed with the repair is important, particularly for large repairs, as illustrated in Figure 5.1. If the telehandler boom is not parallel with the repair, the screed will drift to the left or right as it is advanced, potentially losing contact with the existing pavement, which is the screed's grade reference. During the alignment step, it is helpful to boom the screed out across the crater (keeping the screed lifted in the air) as this makes it quickly evident whether the telehandler is adequately aligned.

Figure 5.1. Illustration of telehandler alignment with large concrete repair.

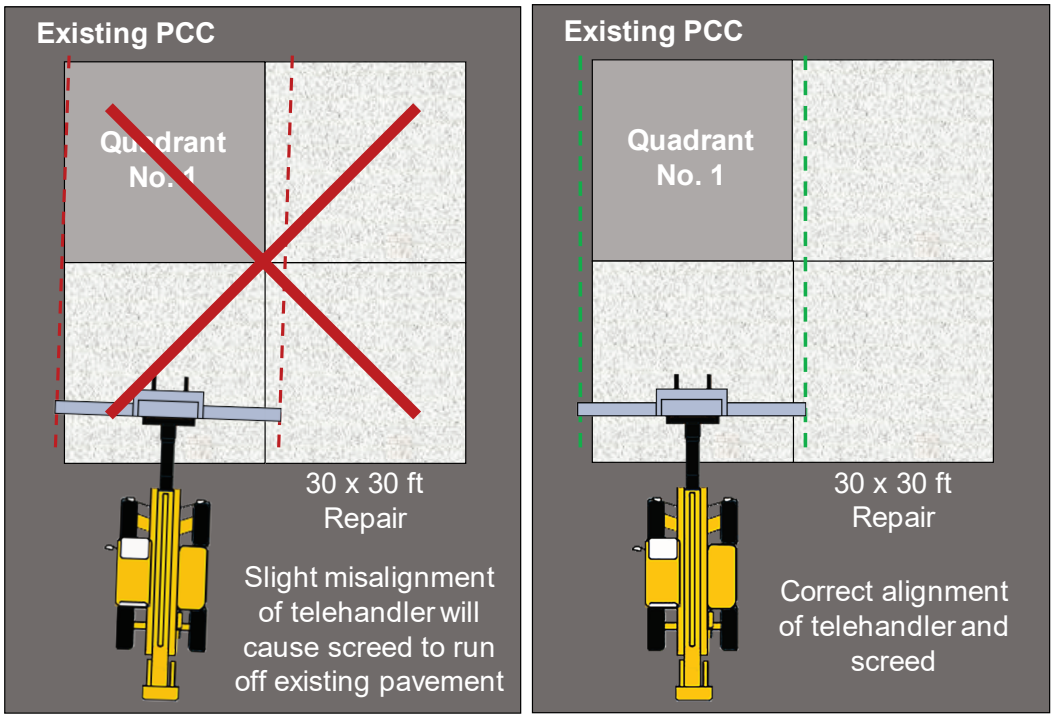

(a) Incorrect alignment (b) Correct alignment

Once aligned, the telehandler should be parked such that the outriggers, when down, are within several inches (e.g., 4 in.) of the edge of the crater (Figure 4.21a). This minimizes the boom distance required to fully span to the far side of the crater. The outriggers should be lowered to take all weight off the front tires and to level the telehandler from side to side.

Note that there is no need to lift the front end of the telehandler excessively off the pavement with the outriggers. Some have previously suggested that doing so will enable the boom angle to be lowered to where it is level so that the operator only has to extend the boom and never adjust its angle. As shown in Figure 5.2, lifting the front end higher only decreases the boom angle with respect to the telehandler chassis. Its angle relative to the pavement does not change.

Figure 5.2. Illustration of telehandler outrigger deployment.

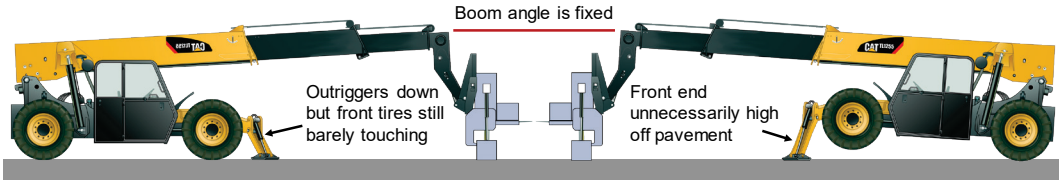

(a) Sufficient outrigger position (b) Unnecessary outrigger position

5.2.1.3 Screed leveling

Once the telehandler is positioned, the screed should be leveled from front to back by adjusting the fork tilt. The spotter observes the level indicators on the side of the screed (Figure 3.17) and relays the necessary adjustments to the operator.

For a large repair where plastic forms are used to partition the repair into four quadrants, care should be taken to avoid accidentally applying excessive down force from the screed bar during screeding as this could crush the forms. To help prevent this problem, the formwork side of the screed bar can be raised several inches using the electric jack on that side as was shown in Figure 3.11. When the travel spring on the existing concrete side of the screed bar is compressed during screeding, minimal load will be applied to the formwork on the other end.

5.2.1.4 Screeding

Once the SVM operator determines sufficient RSC has been placed, the spotter turns on the screed's vibrators using the control pendant and signals the operator to lower the screed to the grade control references (i.e., existing pavement or formwork).

The operator should lower the screed until the travel springs are partially compressed to about their midpoint as shown in Figure 3.12. For a small repair, both springs will be evenly compressed, and the

operator can visually monitor the depth indicators as he advances the screed. The operator may not need much assistance from the spotter except for signaling when to stop.

For a large repair, the operator can still monitor the travel spring depth indicators as he advances the screed, but large repairs require more overall attention, and the operator will need to rely more heavily on the spotter. If the screed bar was rolled to keep load off the forms as discussed in the previous section, the operator should lower the inside end of the screed bar until it makes contact with the forms. At that point, the outside travel spring should be partially compressed like normal due to the roll in the screed bar. The operator should attempt to keep the outside travel spring depth indicator at a constant position throughout screeding as this will in turn mean the inside end of the screed bar stays in contact with the formwork without overloading it. If possible, the spotter should remain on the formwork side of the repair since this is the more critical side. The spotter should signal the operator to make any adjustments and also when he has reached the end of the repair and can retract the screed.

More than one pass of the screed is possible and may be necessary. This is driven by several factors. For example, the spotter may realize during screeding that there is not enough RSC and call the SVM operator to add more. Also, depending on the consistency of the RSC, it can flow under the screed bar while screeding; this can be furthered by the vibrators (though the vibrators are helpful for overall consolidation and finish). Oftentimes, a second pass is sufficient as the RSC consistency has stiffened enough by the time the second pass is performed. Once all passes have been conducted, the spotter should switch off the vibrators.

5.2.1.5 Cleanup

Once screeding is complete, the screed should be cleaned immediately before the RSC hardens significantly. This can generally be done whenever the SVM is cleaned. Wash-down of the screed is quick since RSC typically contacts only the lower portion of the screed bar. This should be performed in a washout area with a pressure washer.

Once cleaned, the screed is ready to be moved into position for the next crater or for the next quadrant of a large repair.

5.2.1.6 Non-screeding tasks

In addition to actual operation of the screed, other side tasks are required. During screeding, ground men may use rakes to push RSC up to the screed to fill in any low areas. If the repair is too low overall, more RSC may need to be added to the repair. After screeding, any excess RSC can be cleaned from the pavement with a CTL and rakes and shovels. Some repairs may require minor finishing hand work with trowels around the edges of the repair.

5.2.2 Simplified steps

1. Configure the screed.
   a. For a large repair, fold extension wings down; secure with 1-in. pins and clevis pins.
   b. Relocate control pendant and post to either end of screed bar. Pin post in place.
2. Position the telehandler (less critical for small repairs).
   a. Position telehandler on opposite side of crater from SVM. Plan repair so that screed pushes material uphill, if possible.
   b. Align telehandler so that boom is parallel with repair.
   c. Holding screed in the air, boom out partway to ensure proper alignment. Adjust if necessary.
   d. Park telehandler so that outriggers are about 6 in. from crater edge.
   e. Lower outriggers to take weight off front tires and level telehandler from left to right.
3. Level the screed.
   a. Adjust fork tilt to level screed using the swinging level indicators.
   b. To minimize damage to formwork for a large repair, roll screed bar by raising formwork end 3-4 in. using an electric jack.
4. Screeding.
   a. Once repair is filled with RSC, switch on vibrators.
   b. Small repairs.
      (1) Lower screed to pavement and partially compress travel springs.
      (2) Advance screed, keeping travel springs partially compressed at all times.
      (3) Spotter may assist operator with adjustments as needed.
      (4) Spotter should signal operator to stop once screed has pushed 1-2 ft beyond repair.
   c. Large repairs.

(1) Lower inside end (formwork side) of screed bar to contact formwork; if screed bar was properly rolled (Step 3b), this should result in partial compression of outside travel spring.
(2) Advance screed, keeping outside travel spring at initial compression level.
(3) Spotter should focus on formwork side of repair and assist operator with adjustments.
(4) Spotter should signal operator to stop once screed has pushed 1-2 ft beyond repair.

d. Additional passes can be performed following Step 4b or 4c.
e. Once screeding is complete, switch off vibrators.
f. Lift and retract screed.

5. Cleanup.
   a. Move screed to washout area and wash off RSC with pressure washer.
   b. Wash screed at same frequency as the SVM.
   c. Once screed is cleaned, it is ready for the next repair.
6. Non-screeding tasks.
   a. Use rakes to push RSC up to screed in low areas.
   b. Add additional RSC if necessary to fill crater fully.
   c. Clean excess RSC from pavement with CTL, rakes, and shovels.
   d. Perform finish hand work with trowels around repair edges as needed.

5.3 Asphalt repair

5.3.1 Detailed description

5.3.1.1 Screed configuration

Screed-bar extension wings should be folded to accommodate end-mount attachments. A grade control device should be mounted on each end. For a large repair, these should be a grade control ski on the outside end of the screed bar and either the AGCS or MGCS on the inside end. For a small repair, two grade control skis can be used, but one ski with either the AGCS or MGCS will also work. All end-mount attachments mount by hooking over the hanger shaft and pinning at the bottom as shown in Figure 3.18.

End gates should be mounted to the front of the screed bar and spaced at the desired repair width. These mount by hooking over the mounting rail

on top of the screed bar, followed by latching around the sacrificial wear plate underneath the screed bar using cam action latches.

The control pendant and post should be located on either side of the screed wherever most convenient. Two clevis pins are used to secure the post to the screed bar truss. Ride track sections should be removed from the storage bin and laid in the crater for later alignment. Other attachments may remain in the storage locations on the screed frame or be removed and set to the side.

A release agent will greatly ease cleanup efforts and should be applied to the screed bar and end gates prior to screeding.

5.3.1.2 Telehandler positioning

Prior to paving a repair lane, the telehandler/screed operator should park the telehandler longitudinally at the edge of the crater. Screeding direction is not overly important except for large repairs where the grade control ski should be oriented to the outside of the repair so it can ride on existing pavement. For large repairs, outside lanes should be paved first.

Alignment of the telehandler and screed with the paving lane is important, particularly for large repairs, as illustrated in Figure 5.3. If the telehandler boom is not parallel with the crater, the screed will drift left or right as it is advanced, and the end gates will not follow the repair edges as intended. Multiple attempts at correct alignment may be necessary and generally take only a few minutes. Alignment should be checked by setting the outside end gate on the edge of the repair and booming out the full distance of the repair with the screed lifted a few inches off the pavement. The end gate should deviate from the repair edge no more than 1 in.

Once aligned, the telehandler should be parked such that the screed bar is over existing pavement within 1 ft of the edge of the crater. This minimizes the boom distance required to fully span to the far side of the crater. The outriggers should be lowered to take all weight off the front tires and to level the telehandler from side to side. As illustrated in Figure 5.2, there is no need to excessively lift the front end of the telehandler with the outriggers.

Figure 5.3. Illustration of telehandler alignment with large asphalt repair.

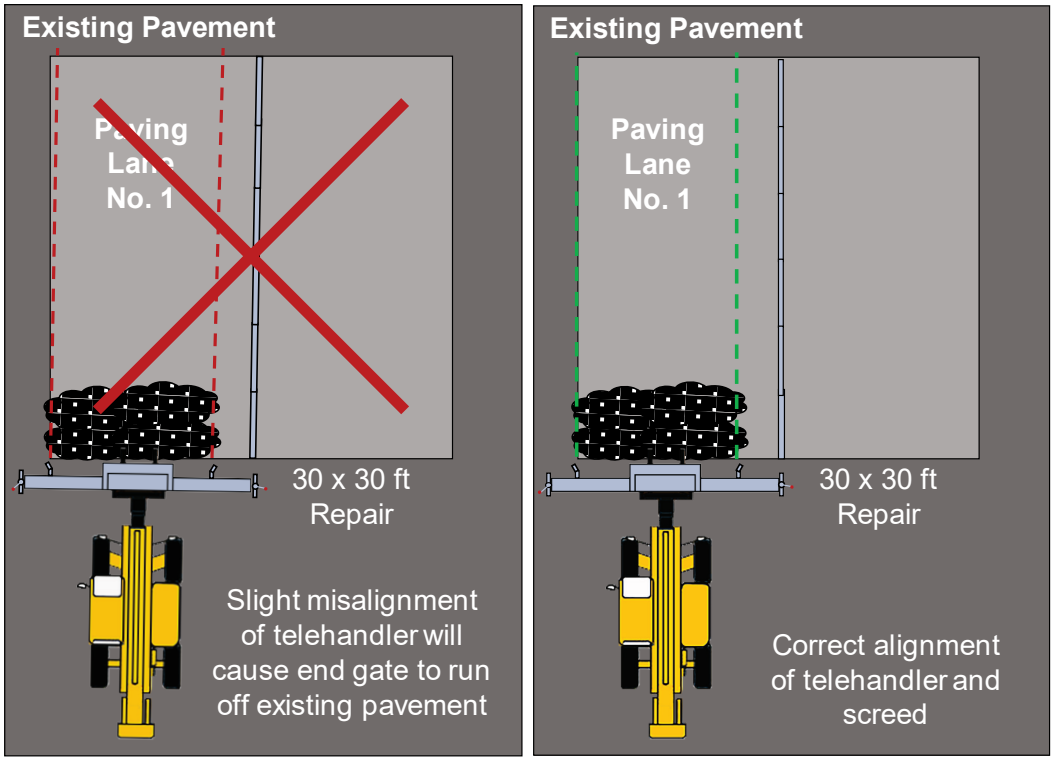

(a) Incorrect alignment (b) Correct alignment

5.3.1.3 Ride track alignment (large repair only)

Once the telehandler is positioned, the ride track should be laid out in the crater to match the path of the AGCS or MGCS. To start, enough track pieces should be laid out in a roughly straight line along the approximate AGCS/MGCS path, starting with the first section and ending with the last section with the AGCS release tab.

The screed should then be boomed out over the crater, holding it 2-3 in. above the ride track. As the AGCS/MGCS passes over the ride track, the track should be shifted left or right so that it is centered. Once the screed has been boomed all the way to the other side of the repair, it can be retracted the same way so that the spotter can verify the track is correctly aligned and make final tweaks if needed.

5.3.1.4 Screed leveling

Once the ride track is laid out and aligned, the screed should be leveled from front to back by adjusting the fork tilt. The spotter observes the level indicators on the side of the screed (Figure 3.17) and relays the necessary adjustments to the operator.

Further leveling adjustments will likely be necessary during screeding of large repairs. The screed tends to pitch forward as illustrated in Figure 5.4 due to the boom's sagging over long distances and the load of pushing the asphalt pile. It is important to keep the screed fairly level for asphalt repairs because if it pitches too far forward, it will affect the end gates and grade heights. Therefore, the screed should be periodically leveled during screeding. As an additional measure, it may be helpful during initial leveling to start with the screed pitched backward slightly (less than 1 tick on the level indicator).

Figure 5.4. Illustration of screed roll due to telehandler boom sag.

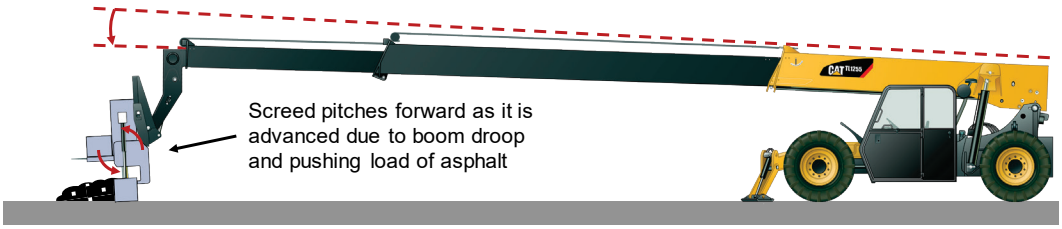

5.3.1.5 Pre-screeding

Prior to screeding, the spotter should set the grade height and configure all attachments. First, the operator should set the screed on the pavement and compress the travel springs slightly. Inside and outside grade control devices should then be set to the proper roll-down factor of approximately 3/8-in. per 1 in. repair thickness (i.e., 1.5 in. for 4-in. repair).

Grade control skis are straightforward to set. Adjust the leveling jack until the ski is set at the proper height (e.g., 1.5 in.). Using the aluminum stepped gauge block in the toolbox, verify the gap between the screed bar and pavement is correct. Lock the leveling jack handle in place using the clevis pin.

The MGCS, if used, is set somewhat similarly to the skis except that there are two leveling jacks to adjust. Set both at the proper height (e.g., 1.5 in.), and verify using the stepped gauge block. Lock both jack handles by flipping them over into the locking ring.

The AGCS, if used, requires the most, though not difficult, steps for setup. First, fully raise the leveling jack. Second, remove the orange retention pins and allow the wheels to drop freely to the pavement. Third, engage the wheel lock levers (this engages the pawl with the gear rack so that the

wheels cannot freely slide back up). Fourth, adjust the leveling jack until the proper height (e.g., 1.5 in.) is achieved; verify with the gauge block. Lock the jack handle by flipping it over into the locking ring.

Note that once the AGCS is set, the screed should not be lifted off the pavement. The AGCS wheels will extend if the screed is lifted but will not retract when the screed is set down. The AGCS will lose its grade height set point and will have to be reset following the steps in the previous paragraph.

Also, if the AGCS is being used for a repair in which the automatic grade adjustment is not needed (e.g., small repair), the AGCS can be treated more like the MGCS. In this case, the retention pins are not removed, disabling the up-and-down wheel movement, and grade height is set by the leveling jack alone.

End gate retention pins should be removed. This allows the end gates to drop to the pavement and freely float across the pavement surface.

5.3.1.6 Screeding

Once the CTL operator has placed sufficient AC in front of the screed, the spotter turns on the vibrators using the control pendant and signals the operator to begin advancing the screed. The operator should monitor the travel spring depth indicators as the screed is advanced to make sure partial compression of the springs is maintained. He should make boom angle adjustments as necessary.

For a large repair, the spotter should monitor several items at three key stages of the process: (1) transition into the crater, (2) during screeding, and (3) transition out of the crater.

As the screed transitions into the crater, the spotter should first monitor the inside end gate. As it falls into the crater, the spotter should remove any AC from under the end gate so that it can come to rest on the FF base. Second, the spotter should monitor the inside grade control as it transitions into the crater. If using the MGCS, the spotter must manually lower the leading MGCS wheel to the ride track, followed by the trailing MGCS wheel. Grade height should be checked after this transition to ensure it was maintained. If using the AGCS, the spotter does not need to do anything except monitor the transition to ensure it takes place with no issue.

During screeding, the spotter should periodically check the level of the screed. If it begins to pitch too far forward, the nose of the end gates may bite into the existing pavement and FF base. Grade control devices will also be affected. If the screed approaches 1 tick mark out of level, the spotter should signal the operator to adjust the fork tilt. Note: hydraulic sensitivity should be turned down on the telehandler to enable fine adjustments to the fork tilt and prevent unintentional large adjustments.

As the screed transitions out of the crater at the far end of the repair, the spotter should closely monitor the inside end gate, signaling the operator to stop advancing the screed before the end gates contact the crater wall. The end gate should then be raised and pinned to clear the crater edge. Inside grade control should also be monitored. If using the MGCS, the wheels must be manually raised to allow the screed to exit the crater. If using the AGCS, the spotter needs only to monitor the transition to ensure it takes place with no issue.

The screed should be used to push the remaining AC pile 1-2 ft beyond the repair to facilitate cleaning with a CTL. Vibrators are then switched off. The screed is lifted off the pavement, and if the AGCS was used, the wheel lock levers are disengaged, and the wheels are raised and pinned. The outside end gate is also raised and pinned. The screed can then be retracted.

It is preferable to complete the screeding in one pass. If a second pass is required and it is for a large repair, the entire screeding process must be restarted in order to reset the inside grade control device.

5.3.1.7 Cleanup

Once screeding is complete, the screed may require cleaning. Release agent is sprayed to break down AC, and shovels are used to remove it. The screed should be moved to a non-active area for cleanup so that release agent does not deteriorate active pavement.

5.3.1.8 Non-screeding tasks

The CTL operator should ferry AC to the crater with alternating left- and right-side loaded buckets. Rather than dumping AC out of the bucket from several feet high, the CTL operator should hold the bucket near the ground and roll the AC out. This prevents inconsistent consolidation and minimizes variations in the final grade of the repair. After the bucket is placed, the CTL

operator should back-blade across the top of any large piles to spread the AC. As the screed gets close to the end of the pull, the CTL operator should remain close with a full bucket in case additional AC is needed.

Two ground personnel, working in front of the screed on either side, should monitor the head of AC material in front of the screed. Shovels should be used to redistribute AC to any low areas to make sure the screed maintains a full head of material across its width.

A third ground person, working behind the screed, should use a lute to clean up and tamp the paving lane edges. This includes at the start of the paving pull and on the sides behind both end gates, especially the inside joint face of a large repair. Luting should not be used to broadcast AC across the mat; it should be used only in a tamping manner to ensure the roll-down is folded back inside the repair before compaction.

After screeding, excess AC should be quickly removed from the pavement using a CTL and shovels so that compaction can start immediately. Compaction should follow the defined rolling pattern. Between passes, ground men should use shovels to trim any excess AC that shoves out from the repair.

5.3.1.9 Joint trimming (large repair only)

After the two outside lanes of a large repair are paved, the joints can be trimmed back using the cutoff wheel. The cutoff wheel is front-mounted and hangs lower than any other attachment, meaning no other attachments need to be adjusted or removed for joint trimming.

As in Section 5.3.1.2, the telehandler should be aligned parallel to the repair so that the joint is trimmed uniformly down the repair length. Prior to trimming, the screed should be boomed across the repair while being held in the air to verify correct alignment.

Trimming a minimum of 3 in. from the top of the joint face is recommended; more may be trimmed as needed. The spotter guides the operator to bring the cutoff wheel to the edge of the repair and lower it through the lift of asphalt. The operator advances the screed, ensuring it cuts through the full depth of asphalt. Once the cut is made, ground men remove trimmed AC with shovels.

5.3.2 Simplified steps

1. Configure the screed.
   a. Fold extension wings (if necessary).
   b. End-mount grade control devices; secure with 1-in.-diam pins and clevis pins.
      (1) For a small repair, use two grade control skis or one ski and the AGCS or MGCS.
      (2) For a large repair, use a grade control ski on the outside end and the AGCS or MGCS on the inside end.
   c. Front mount end gates at desired repair width; secure underneath the screed bar with cam action latches.
   d. Position control pendant and post to either end of screed bar where convenient. Pin post in place.
   e. Remove ride track sections.
   f. Spray release agent on screed bar and end gates.
2. Position the telehandler (less critical for small repairs).
   a. Position telehandler next to crater edge in the longitudinal direction. For large craters, pave outside lanes first, keeping grade control ski on outside of lane.
   b. Align telehandler so that its boom is parallel with repair.
   c. Reposition outside end gate to match longitudinal repair edge.
   d. Holding screed in the air, boom out full distance of repair; end gate should deviate less than 1 in. from repair edge. Adjust if necessary.
   e. Park telehandler so that screed bar is about 1 ft from crater edge.
   f. Lower outriggers to take weight off front tires and level telehandler from left to right.
3. Align ride track (large repair only).
   a. Lay out overlapping track sections in approximate position, making sure first and last sections are in place.
   b. Boom screed full length of crater with screed 2-3 in. above track.
   c. Shift track left or right to follow AGCS/MGCS wheels.
   d. Verify alignment is correct while retracting screed.
4. Level the screed.
   a. Adjust fork tilt to level screed using the swinging level indicators.
   b. Note that adjustments will likely be required during screeding.
5. Pre-screeding.
   a. Compress travel springs slightly.
   b. Establish screed bar grade height at 3/8-in. per 1 in. of repair thickness (i.e., 1.5 in. for 4-in. repair).
      (1) Grade control skis:

(a) Adjust leveling jack to achieve grade height.
(b) Verify grade height with gauge block.
(c) Lock jack handle in lock ring with clevis pin.
(2) MGCS (if used):
(a) Adjust both leveling jacks to achieve grade height.
(b) Verify grade height with gauge block.
(c) Flip handles over into locking rings to secure.
(3) AGCS (if used):
(a) Fully raise leveling jack.
(b) Remove wheel retention pins and allow wheels to drop.
(c) Engage wheel lock levers.
(d) Adjust leveling jack to achieve grade height.
(e) Flip handle over into locking ring to secure.

c. Remove end gate retention pins and allow gates to drop.

6. Screeding.
   a. Once sufficient AC is placed in front of the screed, switch on the vibrators (spotter) and begin advancing screed (operator).
   b. Monitor travel spring depth indicators and adjust boom angle as necessary to maintain partial compression.
   c. Screed transition into crater (large repair only).
      (1) Remove AC from under inside end gate as it falls into crater so that it can rest on FF base.
      (2) If MGCS is used, manually lower leading wheel to ride track as it enters crater, followed by trailing wheel.
      (3) If AGCS is used, simply monitor transition to ensure no issues.
   d. Leveling during screeding (large repair only).
      (1) Level screed if level indicators approach 1 tick from level.
      (2) Turn telehandler hydraulic sensitivity down to enable fine adjustments.
   e. Screed transition out of crater (large repair only).
      (1) Stop screed advancement just before inside end gate contacts crater edge. Raise and pin end gate to clear edge.
      (2) If MGCS is used, manually raise the leading wheel then the trailing wheel to allow screed to transition out of crater.
      (3) If AGCS is used, simply monitor transition to ensure no issues.
   f. Use screed to push AC pile 1-2 ft beyond repair for CTL cleanup.
   g. Once screeding is complete, switch off the vibrators.
   h. Lift screed off pavement. If AGCS was used, disengage wheel lock levels and raise and pin wheels. Raise and pin outside end gate.
   i. Retract screed.

7. Cleanup.
   a. Release agent applied before screeding should minimize cleanup required. If additional cleaning is needed, spray more release agent and use shovels to remove built up AC.
   b. Once screed is cleaned, it is ready for next repair.
8. Non-screeding tasks.
   a. CTL operator.
      (1) Transfer AC to crater with alternating left- and right-side loads.
      (2) Do not dump loads from several feet off ground. Instead, hold bucket near ground and roll AC out of it.
      (3) Back-blade the crown of any large piles to spread the AC.
      (4) Near end of screeding, remain close with full bucket in case additional AC is needed.
   b. Two ground personnel work in front of screed on either side using shovels to make sure consistent head of material remains in front of full width of screed.
   c. One ground person works behind screed with lute cleaning edges, tamping joint face (inside of large repair), and folding back roll-down inside repair.
   d. Clean excess AC using CTL and shovels.
   e. Compact lane following defined rolling pattern.
   f. During compaction, trim any excess AC that shoves out from repair.
9. Joint trimming (outside lanes of large repair only).
   a. Mount cutoff wheel on front mounting rail of screed.
   b. Align telehandler parallel with repair so that joint cut is straight. Boom screed out over repair to verify proper alignment.
   c. Trim 3 in. from top of joint face (minimum); trim more if necessary.
   d. Cut full depth of asphalt for full repair length.
   e. Remove trimmed AC with shovels.

6 RADR Screed Test Results

This chapter presents results from the seven crater repairs (R1 to R7) conducted using the RADR screed. The repairs conducted for this project overlapped with two other projects, as discussed in Section 4.3; consequently, results are grouped as follows: R1 (large concrete repair), R2 to R5 (small concrete repairs), and R6 to R7 (large asphalt repairs).

As discussed in Cox and Hoffman (2019), small crater repairs do not present nearly the challenge that large repairs do. Further, large concrete repairs are considerably simpler from a screeding perspective than large asphalt repairs.

The test plan for this project recommended performing at least one large concrete repair to validate that the new RADR screed is as adequate as the ASTH for large concrete repair. It recommended the bulk of the project effort be spent on evaluating the new RADR screed for large asphalt repairs, as this area was the least refined. Small repairs were not in the initial test plan; however, the opportunity to use the RADR screed for repairs in another project was taken to provide additional data.

6.1 Large concrete repair

Table 6.1 provides placement data for repair R1 by quadrant. This repair began at 09:05 with loading the SVM with RSC and was completed at 14:18 (313 min). Assuming quadrants were placed one after the other with no cleanout time for the SVM, the time required for loading the SVM, pouring, and screeding would have been approximately 155 min (2.58 hr).

Table 6.1. Repair R1 placement data.

Quadrant	SVM Pour Time (min)	Screeding Time (min)	Screed Passes	Ambient Temp (F)	RH (%)	Notes
Q1	14	5	2	85	65	Pass 1 approx. halfway, Pass 2 full-length
Q2	15	4	2	88	60	Additional RSC was added between passes
Q3	17	4	2	93	47	—
Q4	15	3	3	95	41	Additional RSC was added between passes
Quadrant Avg	15.3	4.0	2.3	88	53	—

– Gate setting varied, but 7.5 was most frequent

Concrete pour time with the SVM averaged about 15 min, and screeding time averaged 4 min. These operations generally did not overlap. For all quadrants, more than one screed pass was performed. The most common

reason multiple passes were required was that more RSC was added to the repair. It was also observed that RSC, if on the wetter side, would flow under the screed, which has been a common observation with other screeds in the past as well. The solution to this is simply additional screed passes, assuming they can be applied quickly enough. There were no issues applying these additional passes with respect to the RSC set time, and more passes could have been applied if necessary.

Figure 6.1 shows an overall view of the completed repair R1. Visually, the repair appeared reasonable with no major defects except those shown in Figure 6.2. In Figure 6.2a, a small transverse bump, which was the result of a second screed pass across only part of the repair, is visible in quadrant 4 (Q4). Rather than starting at the beginning, the second pass was started from the middle of the repair, leaving a slight bump.

Figure 6.1. Repair R1 overview photographs.

Figures 6.2b and 6.2c show the transverse joint between Q2 and Q4 where the expansion material that was fixed to the Q2 joint face was snagged during screeding and pulled into Q4 slightly. The total length of this defect was 1-2 ft. This could be prevented by ensuring expansion material is sufficiently recessed below the surface just slightly so that it cannot be snagged during screeding.

Figure 6.3 shows a survey map of the final surface where values shown are the deviation (in.) from a flush repair at a particular location within the repair. The color scale is formatted so that dark red colors represent the highest elevations and dark blue colors represent the lowest elevations. The total range of the scale is from -1.4 in. to 1.4 in., as this spans all observed

data. Lastly, the midpoint of the color scale (white) occurs at the 50th percentile mark and does not necessarily correspond with a 0.0 in. deviation.

Figure 6.2. Repair R1 detail photographs.

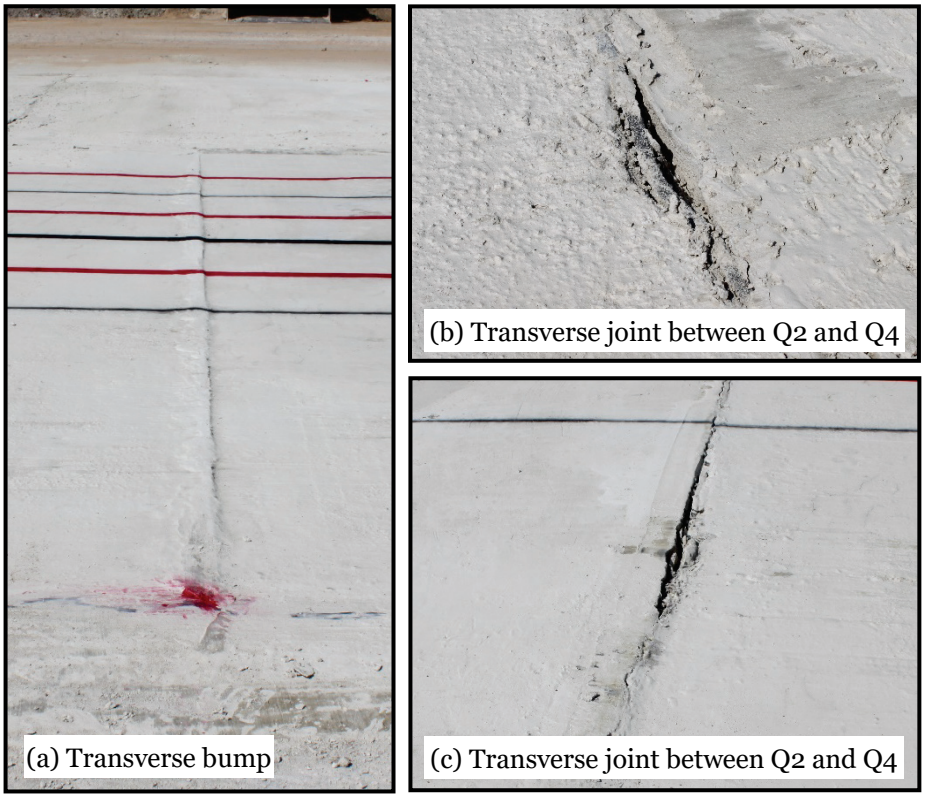

Figure 6.3 shows that there are two particularly low areas along the centerline in quadrants 1 and 2. This is most likely a result of the plastic forms being pushed down during screeding, which is somewhat visible in Figure 6.4. As can be seen in Figure 6.3, the screed produced a very flush repair in other areas, such as around the perimeter, where the screed had a solid grade reference to ride. For quadrants 3 and 4, the screed used the inside edges of quadrants 1 and 2, respectively, as the grade reference, but since these areas were low, some of this depression was transferred to quadrants 3 and 4.

Table 6.2 summarizes the survey data in Figure 6.3 by quadrant as well as overall. The average elevation of the entire repair is -0.46 in., which is within the ±0.75 in. requirement for a flush repair; however, by definition, the repair would not be considered flush due to the individual areas that exceed ±0.75 in. The maximum bump is 0.36 in., but the maximum depression is -1.27 in. Table 6.2 also shows that, of all the survey points, approximately 22% were lower than -0.75 in.

Figure 6.3. Repair R1 surface profile survey map.

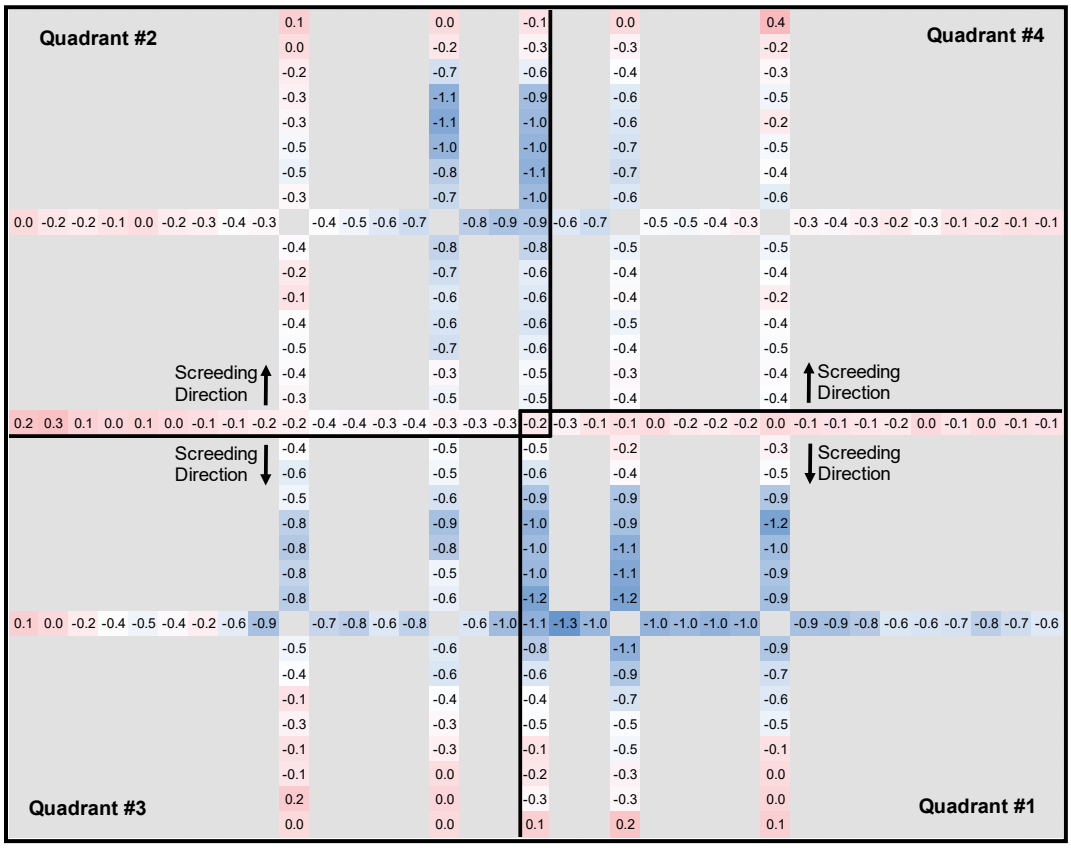

Figure 6.4. Dip in R1 quadrant 1 surface due to sagging forms.

Since there could be an unusually high or unusually low outlier in the maximum and minimum numbers that would be misleading of the overall repair, a 95% confidence interval (CI) was calculated for each quadrant and the entire repair to provide a more representative assessment. The

lowest CI was for Q1 where the screed was riding on the forms and was -1.33 to 0.25 in. (±0.79 in.). The Q2 CI was not quite as low due to adjustments made to the screed (the screed bar was rolled as discussed in Sections 4.5.1 and 5.2.1.3), but it was still lower than that of Q3 and Q4.

Table 6.2. Repair R1 survey results (by quadrant).

Statistic		Q1	Q2	Q3	Q4	Overall
Deviation (in.)	Avg	-0.54	-0.42	-0.45	-0.38	-0.46
	S.D.	0.40	0.33	0.31	0.20	0.34
	Min	-1.27	-1.10	-0.95	-0.70	-1.27
	Max	0.24	0.29	0.17	0.36	0.36
95% CI (in.)		-1.33 to 0.25	-1.06 to 0.22	-1.05 to 0.15	-0.77 to 0.02	-1.12 to 0.20
95% CI Tolerance (in.)		± 0.79	± 0.64	± 0.60	± 0.39	± 0.66
Percent Non-Flush (%)	> +0.75 in.	0.0	0.0	0.0	0.0	0.0
	< -0.75 in.	38.0	17.7	22.2	0.0	21.9
Quality Category		B	B	B	A	B

-- *95% confidence interval tolerance represents the tolerance that would include 95% of the repair relative to the average overall deviation (e.g., -0.54 in. for Q1), not with respect to a flush repair (i.e., 0.0 in.). The purpose of this metric is to show the overall tolerance for comparison to the ±0.75 in requirement.*

Over the entire repair, the 95% CI was -1.12 to 0.20 in., which was ±0.66 in. of the average -0.46 in. elevation. This suggests that repair R1 was too low by approximately 0.5 in. However, from a smoothness perspective, the repair being ±0.66 in. of the average elevation suggests that, had the elevation been flush on average, it would have met the ±0.75 in. criteria.

Because RQC manuals effectively assume that all RADR repairs will be flush by default yet this repair was not, it is worthwhile to consider this further. If a repair is not flush, RQC manuals then categorize it primarily on the maximum bump (e.g., 1 in., 2 in.) while also specifying a maximum sag allowance. These values are determined by evaluating at least five longitudinal lines across the width of the repair similar to the five longitudinal lines in Figure 6.3.

The Figure 6.3 longitudinal lines were analyzed according to the RQC methodology, and results are shown in Table 6.3. RQC manuals require the maximum peak to be less than a specified allowable limit (e.g., 1 in., 2 in.) and the sag (difference between max peak and max valley) to be less than 2 in. Repair R1 sag values ranged from 0.99 to 1.25 in., which are well within the 2-in. sag limit. It is worth noting that repair R1 is considered non-flush not due to an excessive bump (i.e., > +0.75 in.) but due to an excessive depression (i.e., < -0.75 in.).

Table 6.3. Repair R1 survey results (by longitudinal profile line).

Statistic	L1	L2	L3 (CL)	L4	L5
Avg Deviation (in.)	-0.34	-0.54	-0.64	-0.54	-0.43
Peak Avg (in.)	0.15	0.00	0.00	0.10	0.05
Valley (in.)	-0.84	-1.10	-1.15	-1.15	-1.15
Sag (in.)	0.99	1.10	1.15	1.25	1.20

– Peak Avg is the average height, relative to a flush repair plane, of two peaks on either side of a sag.

– Valley is the maximum depth below the flush plane and between two peaks.

– Sag is the total change in height from the peak avg to the valley.

Unfortunately, the results of repair R1 make the RADR screed appear as if it does not provide a flush repair. However, it is the opinion of the authors that this is not an accurate representation of the RADR screed. It is also helpful to recall that this is the result of one repair, and results are likely to improve over time with additional experience.

Additionally, the statement in RQC manuals that RADR processes provide flush repairs is predominantly speaking to small repairs, in which case the RADR screed easily provides flush repairs as shown in the subsequent section. When it comes to large repairs, there is less experience with RSC, particularly from a screeding and flushness standpoint. For comparison, survey data from six other large repairs performed for a different project are analyzed herein. Four utilized the traditional mag bar screed, and two utilized the ASTH.

Figure 6.5 shows an example survey map for a mag bar repair, and Figure 6.6 shows an example survey map for an ASTH repair. For mag bar repairs, it is more common to observe bumps (i.e., above the flush plane). This is most likely because manually screeding a large repair by pulling a mag bar is a physically taxing exercise, and it is often difficult, especially if the RSC consistency is thick, to screed it flush with the grade control references. Figure 6.5 shows a maximum bump of 1.2 in., which would be considered a non-flush repair by RQC standards. The Figure 6.5 repair would fall into a Category C repair as defined in Section 4.6.1.

The ASTH exhibits similar challenges to the RADR screed in that it is used on a telehandler, which provides more potential down force than a technician can physically exert. While this generally prevents bumps (above flush plane) from being a factor, it can lead to depressions for large repairs where forms are used since this grade control reference is not as rigid as existing pavement. Figure 6.6 shows a maximum depression of 0.8

in., which would be considered non-flush by RQC standards; this repair would classify as a Category B repair as defined in Section 4.6.1.

Figure 6.5. Example mag bar surface profile survey map.

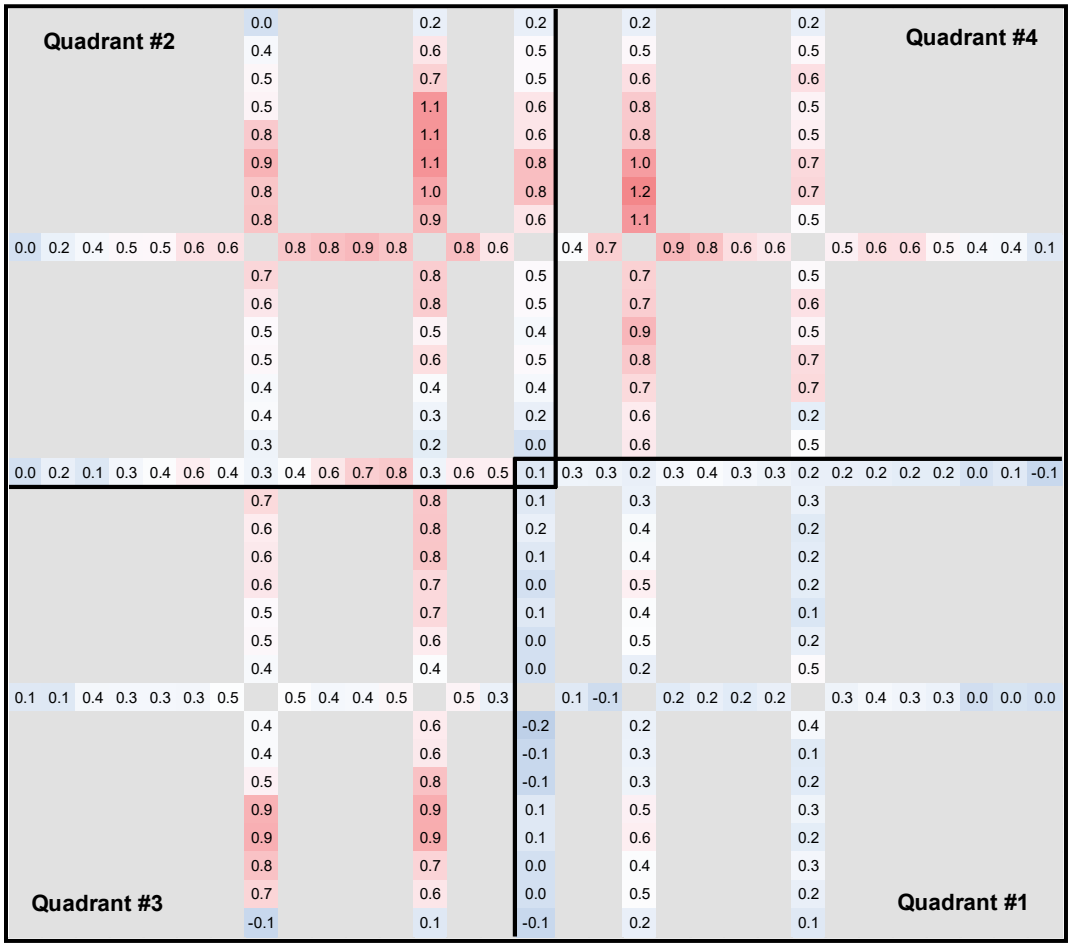

Table 6.4 shows summary data similar to that of Table 6.2 but for the four mag bar repairs and two ASTH repairs. Overall, it can be seen that the mag bar yielded high quality repairs most of the time in that three of the four repairs were flush (Category A) and one was a Category C. The ASTH yielded Category B repairs in both cases.

Figures 6.7 and 6.8 graphically present survey data for all three screeds collectively. It is evident that the overall spread of data is fairly similar for each screed, but the average is shifted in each case. On average, the RADR and ASTH screeds yielded repairs that were slightly low (below zero), while the mag bar yielded repairs that were slightly high (above zero).

Figure 6.8 also shows 95% CIs for each screed when all repairs made with a given screed are considered collectively. It shows that each screed is similar from a practical perspective, providing a finish that is about ±0.6 in. from the average elevation. This indicates that, for the most part, obtaining a relatively smooth, flat finish is not an issue with any of the screeds.

Figure 6.6. Example ASTH surface profile survey map.

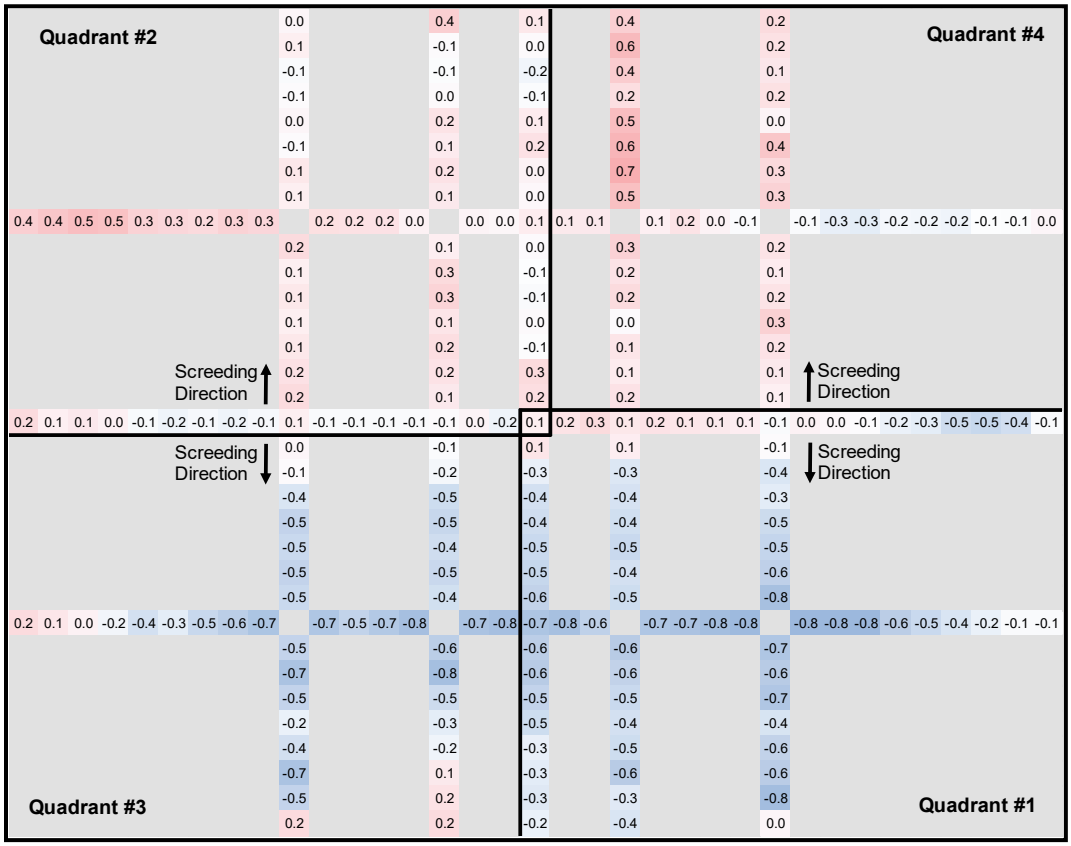

Table 6.4. Supplemental mag bar and ASTH survey data for large concrete repairs.

Statistic		Mag Bar Repair No. 1	Mag Bar Repair No. 2	Mag Bar Repair No. 3	Mag Bar Repair No. 4	ASTH Repair No. 1	ASTH Repair No. 2
Deviation (in.)	Avg	0.28	0.02	0.44	0.17	-0.15	-0.14
	S.D.	0.20	0.17	0.28	0.26	0.29	0.34
	Min	-0.14	-0.34	-0.24	-0.43	-0.71	-0.84
	Max	0.71	0.42	1.18	0.72	0.84	0.67
95% CI (in.)		-0.11 to 0.68	-0.30 to 0.35	-0.10 to 0.99	-0.33 to 0.67	-0.71 to 0.41	-0.81 to 0.54
95% CI Tolerance (in.)		± 0.40	± 0.32	± 0.55	± 0.50	± 0.56	± 0.68
Percent Non-Flush (%)	> +0.75 in.	0.0	0.0	15.9	0.0	0.8	0.0
	< -0.75 in.	0.0	0.0	0.0	0.0	0.0	4.0
Quality Category		A	A	C	A	B	B

– *95% confidence interval tolerance represents the tolerance that would include 95% of the repair relative to the average overall deviation (e.g., 0.28 in. for Mag Bar Repair No. 1), not with respect to a flush repair (i.e., 0.0 in.). The purpose of this metric is to show the overall tolerance for comparison to the ±0.75 in requirement.*

Figure 6.7. Histogram comparing screed elevation deviations.

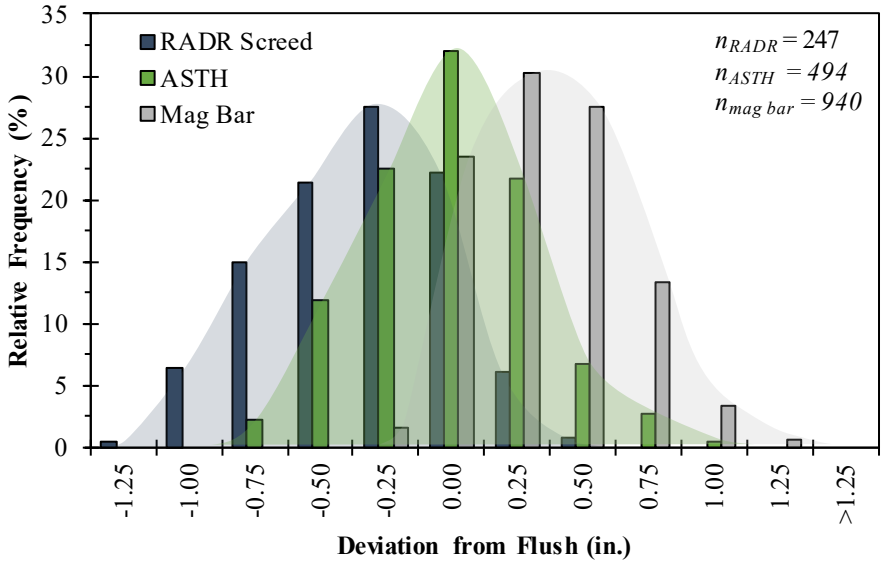

Figure 6.8. Box and whisker plot comparing screed elevation deviations.

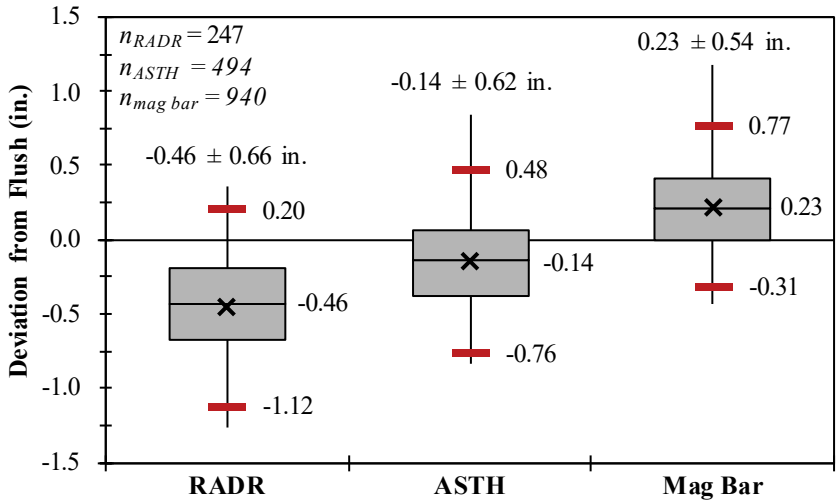

When comparing the RADR screed to the ASTH or the mag bar with the data available, it is important to note the data set size differences. The RADR screed has the smallest data set available with only one repair being performed (247 total survey points), meaning it is the least representative of the three data sets. The mag bar data set, at four repairs (940 total survey points) is the most representative data set. Without significant replication, care should be taken in making any strong statements regarding the RADR screed's ability to provide a flush repair. Other factors besides just the screed come into play as well such as how securely the forms were set.

To the knowledge of the authors, this depth of RQC analysis has not been performed for other large repairs within the RADR program, most likely because small repairs are much more common and are generally assumed to produce flush repairs. Given the data available, the primary takeaway from survey comparisons herein should be that all screeds considered have the ability to provide reasonable repairs. The practical reality is that, even with RADR equipment, materials, and techniques, it will be more difficult to achieve a flush repair for large repairs than for small repairs. To be certain that flush repairs will be achieved every time, additional training, preparation, and care will be necessary.

While the data in this section suggests that a mag bar provides the best finish in terms of a flush repair (most Category A repairs in Table 6.4), it is important to keep the personnel fatigue factor in mind. The mag bar is a physically taxing screed to use and, over time with successive back-to-back repairs, will likely yield increasingly more variable repairs. Even if the RADR screed repeatedly provides slightly low or recessed repairs, there is virtually no fatigue factor associated with its use, meaning repairs are more likely to remain consistent over time.

6.2 Small concrete repair

Of the three types of repairs described in this report, the least amount of information is presented for small concrete repairs as these are comparatively very straightforward repairs. Timing data is not presented. Survey data is presented, and the primary focus is on final finish quality.

Figure 6.9 shows photographs of repair R2 as an example of the final surface for a small repair. The left photo was taken prior to cleaning the surrounding pavement while the repair was still somewhat green, which makes the surface quality more visible.

Figure 6.9. Example overview photographs of small repair (R2 shown).

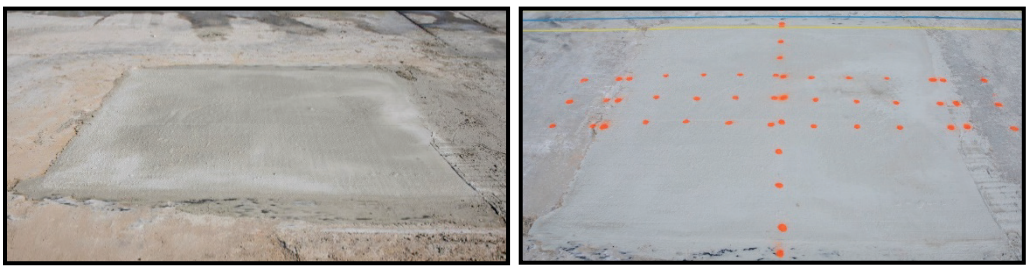

Table 6.5 presents a survey summary, and Figure 6.10 graphically presents the survey maps as before. All repairs easily classified as flush, or Category A, repairs in that not a single survey point exceeded the ±0.75 in. criteria. The maximum deviation (bump) of any repair was 0.60 in., and the minimum deviation (depression) of any repair was -0.51 in. The overall average 95% CI tolerance was ±0.35 in., which was roughly half that of the large repairs. This clearly illustrates the point that flush repairs are much more easily achieved for small repairs than for large repairs.

Table 6.5. Repair R2 to R5 survey results.

Statistic		R2	R3	R4	R5	Avg
Deviation (in.)	Avg	0.21	-0.09	0.12	-0.04	0.05
	S.D.	0.21	0.19	0.13	0.19	0.18
	Min	-0.12	-0.51	-0.11	-0.36	-0.27
	Max	0.60	0.36	0.46	0.24	0.41
95% CI (in.)		-0.20 to 0.62	-0.47 to 0.29	-0.13 to 0.37	-0.41 to 0.32	-0.30 to 0.40
95% CI Tolerance (in.)		± 0.41	± 0.38	± 0.25	± 0.37	± 0.35
Percent Non-Flush (%)	> +0.75 in.	0.0	0.0	0.0	0.0	0.0
	< -0.75 in.	0.0	0.0	0.0	0.0	0.0
Quality Category		A	A	A	A	A

– *95% confidence interval tolerance represents the tolerance that would include 95% of the repair relative to the average overall deviation (e.g., 0.21 in. for R2), not with respect to a flush repair (i.e., 0.0 in.). The purpose of this metric is to show the overall tolerance for comparison to the ±0.75 in requirement.*

Figure 6.10. Surface profile survey maps for repairs R2 to R5.

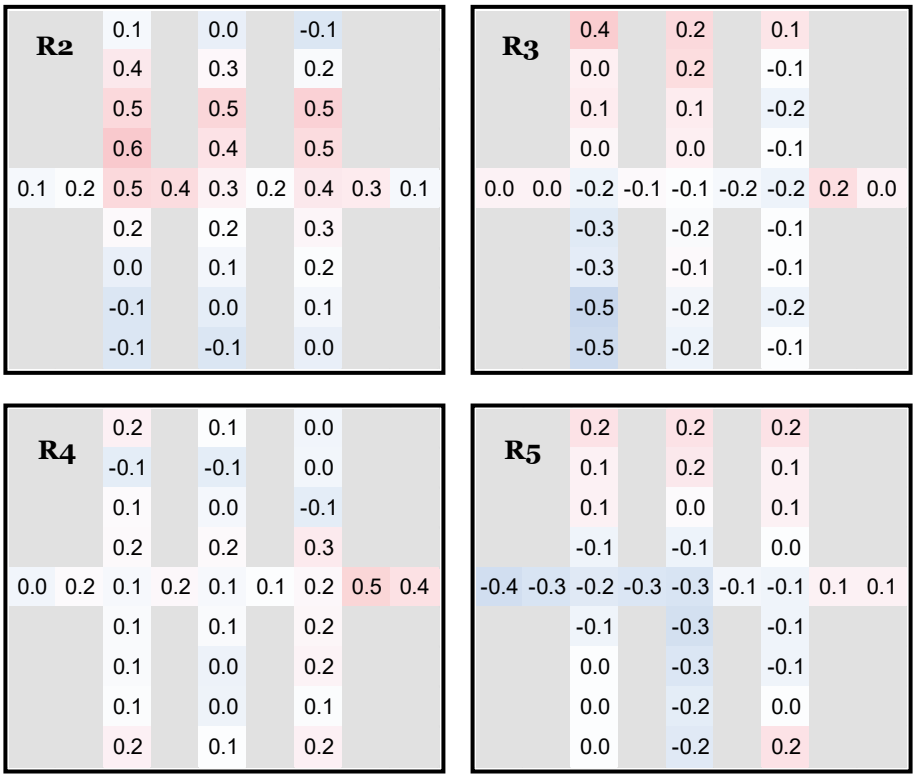

6.3 Large asphalt repair

Figure 6.11 presents timing data for repairs R6 and R7 by paving lane. Because the repair process did not involve AC production through Bagela BA 10000 asphalt recyclers, full timing data of each entire repair was less relevant since timing factors such as waiting on trucks to arrive from the asphalt plant are not normally a concern. Instead, each lane was timed starting when the CTL first scooped into the AC pile and ended once compaction was finished. Times required to complete an entire repair were then estimated by combining individual lane times with other adjustments to account for transition time between lanes.

Figure 6.11 shows that, on average, 4 min were required to charge the crater with enough AC mix that the screed had a sufficient head of material to push. This required several CTL trips between the AC pile and crater. Once screeding began, the CTL continued to deliver mix to the screed. Total screeding time averaged 11 min, meaning the screed was advanced at approximately 3 ft/min. The transition between screeding and compaction averaged 4 to 5 min. During this time, the screed was cleared from the area, excess AC was removed, final cleanup and tamping were performed around the paving lane, and the roller was positioned. Compaction time averaged 13 min. Overall time for each lane averaged 34 min.

Figure 6.11. Repairs R6 and R7 timing data.

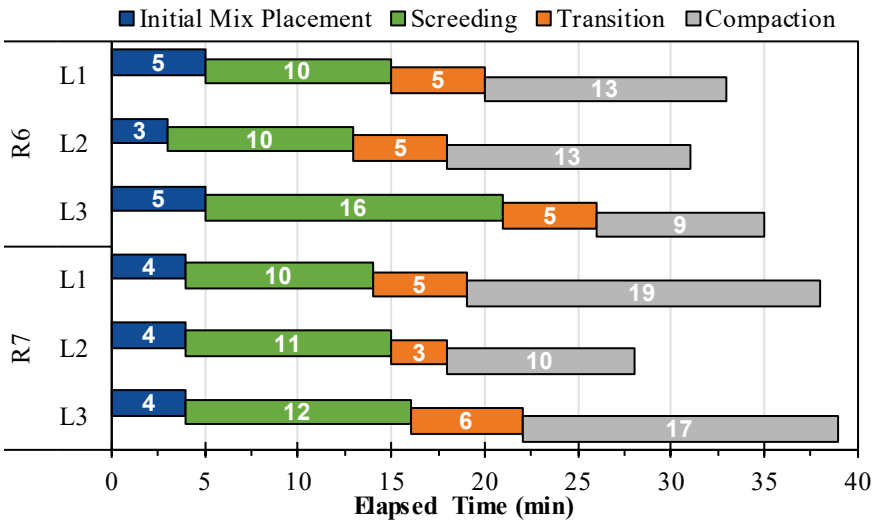

Individual lane times were combined to estimate total repair time from the start of the first lane, L1, to the end of compaction for the final lane, L3. For repair R6, the total time required, if there was no overlap in the

repair process, was 119 min (1.98 hr). However, in normal RADR operations where there is a steady supply of AC, it would be possible to begin paving L2 while L1 is compacted. This approach would have required 106 min (1.77 hr). For repair R7, the same two corresponding time requirements would have been 110 min (1.83 hr) and 91 min (1.52 hr), respectively. This shows there was a slight improvement in time with additional experience, and overall, these repair times are reasonable for a large repair compared to other past repair experiences.

For repair R7, recall that the joints of L1 and L2 (outside lanes) were cut back prior to paving L3. The addition of this trimming step increased total repair times to 130 min (2.17 hr), assuming no overlap in the process, and 111 min (1.85 hr), assuming L1 compaction and L2 paving started at the same time. In the latter case, joint trimming would have been performed on both joints after L2 was compacted. While trimming joints increases repair time slightly, it is believed that this helps produce a better quality repair overall and should be performed when possible.

Figure 6.12 plots all temperature measurements from repairs R6 and R7. Initial temperature readings were taken from AC stockpiles using dial thermometers, and all other readings were taken with a handheld infrared (IR) thermometer at the surface of a paving lane. IR temperature measurements can be variable, and surface temperatures can be misleading, especially during compaction due to the roller's water spray. This issue is somewhat evident at later times in Figure 6.12.

Figure 6.12. Repairs R6 and R7 temperature data.

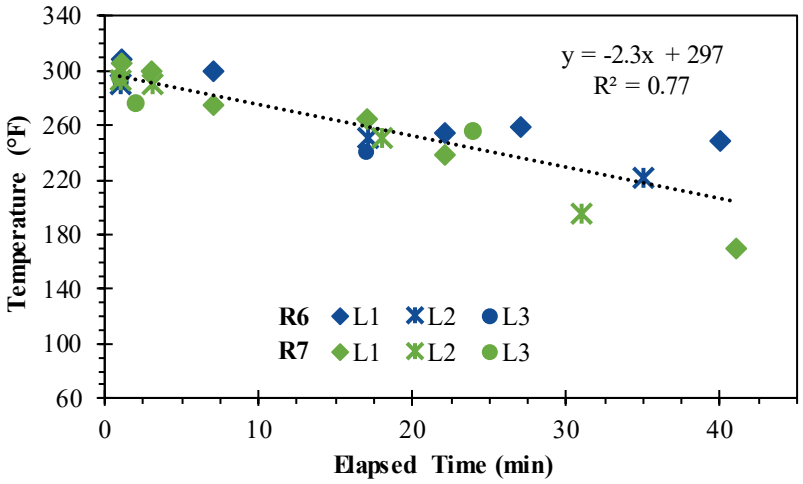

Overall, mix temperatures, when delivered, averaged about 300°F, which is not unreasonable considering the mix was trucked nearly an hour to the site. As a result, temperatures at the end of compaction were often lower than what is ideally preferred. However, this would be much less of an issue for normal RADR operations where AC is produced on site and Bagela production temperatures are generally higher (e.g., 320 to 350°F).

Table 6.6 provides information related to the screed setup, compaction, and lane width measurements. For R6, the AGCS grade height was adjusted for each lane to account for the variations in the FF surface as discussed in Section 4.3 and shown in Figure 4.16. For comparison, the AGCS grade height in R7 was fixed at 1.5 in. as if the FF surface was consistently 4 in. deep. The first case (R6) constitutes a more thorough approach but requires the FF surface to be surveyed (not necessarily by rod and level but perhaps stanchions). The second case (R7) is less thorough but is a simpler approach for the repair personnel. Both were attempted to investigate tradeoffs.

Table 6.6. Repairs R6 and R7 parameters and dimensions.

Repair	Lane	Grade Ht, ski (in.)	Grade Ht, AGCS (in.)	Rolling Pattern	End Gate Width (ft)	Final Width (ft)	Trimmed Width (ft)
R6	1	1.50	1.13	Initial	8.25	9.50	n/a
	2	1.50	1.25	Mod	8.25	9.00	n/a
	3	1.50	1.13	Mod	6.50	6.50	—
R7	1	1.50	1.50	Mod	9.00	9.66	8.50
	2	1.50	1.50	Mod	8.83	9.66	8.25
	3	1.50	1.50	Mod	8.33	8.33	—

– 1 additional vibratory and 1 additional static pass applied to R7, L3 to compact patch of AGCS marks

As discussed in Section 4.5.2 and illustrated in Figure 4.26, the rolling pattern was adjusted after R6, L1 because it was felt the mix was being over-rolled. Lane width data illustrates this as well; the final lane width measured 9.50 ft despite the end gate width being set at 8.25 ft. This excessive lateral movement created other issues as discussed subsequently in the survey results. The modified roller pattern minimized lateral movement in remaining lanes.

In addition to over-rolling, other factors may have contributed to the excessive lateral movement of R6, L1. These could include temperature or lift thickness (t) to nominal maximum aggregate size (NMAS) ratio. A 9.5 mm NMAS mix was used in this project because it was readily available, but at a 4-in. lift thickness, this yields a t/NMAS ratio of over 10. Other

ARA work has utilized a 12.5-mm NMAS mix, which still yields a somewhat high *t*/NMAS ratio of 8. Typical *t*/NMAS ratio recommendations are between 3 and 6, meaning a 19-mm NMAS mix may be more appropriate. It is not a guarantee that all mixes will exhibit issues with large *t*/NMAS ratios, but that can be one potential factor to consider.

Figure 6.13 shows completed repairs R6 and R7. Visually, both repairs looked reasonable aside from a few minor areas; however, R7 was an overall better repair due, at least partly, to the trimmed joints. R6 joints were noticeably lower quality. Minor scuffing was caused by the grade control devices riding on the freshly placed, and still warm, outside lanes. These issues and others encountered during the repairs are discussed further in the following paragraphs.

Figure 6.13. Repair R6 and R7 overview photographs.

During placement and screeding, the CTL operator sometimes placed excess AC in front of the screed that spilled beyond the width of the inside end gate as shown in Figure 6.14. This left a minor amount of raking and cleanup that was required behind the screed. However, the end gates performed their role of leaving a clean vertical face, and they helped kick out excess AC to the side making it easier to rake while the ground man was tamping the joint face.

Figure 6.14. Excess AC overflowing RADR screed inside end gate.

To screed a 30-ft square repair, the telehandler must extend its boom approximately 35 ft due to the setback distance from the crater when it is positioned. At this distance, the CAT TL1055C telehandler payload capacity is around 3,000 lb. Recall that the RADR screed in the asphalt configuration weighed 3,575 lb. Though the telehandler was able to push the screed the full repair distance and then still lift it off the ground, it could not then retract the screed because the sagging boom was in a bind. Since no other adjustments to the screed weight could be made at the time, a different telehandler was simply used to support the screed and take some of the weight off the CAT TL1055C (Figure 6.15). Once the screed was retracted about 5 ft, the CAT TL1055C was able to continue retracting the load by itself.

Figure 6.15. Second telehandler assisting with lifting screed.

During R6, L3, the screed was positioned such that the grade control ski rode on the adjacent L2 lane that had just been placed and was the hotter of the two outside lanes. Although it did not cause any major damage, the ski caused surface scuffing at several points as it slid across L2 (Figure 6.16). The scuffing and minor amount of dislodged AC were

partially corrected during compaction; however, a visible scuff mark remained even after compaction as is visible in Figure 6.17a.

Figure 6.16. Scuffing from grade control ski during repair R6.

Figure 6.17 shows details of the final compacted R6 surface. The joints between the two outside lanes and L3 were adequate but not ideal. Because of the waviness of the L1 and L2 joints after compaction, a single end gate width setting for L3 was not adequate to match the joints. The R6 joints would probably not pose any immediate performance issues, but they would be expected to deteriorate under traffic at a faster rate than a properly matched joint.

Figure 6.17. Scuffing and joints on completed repair R6.

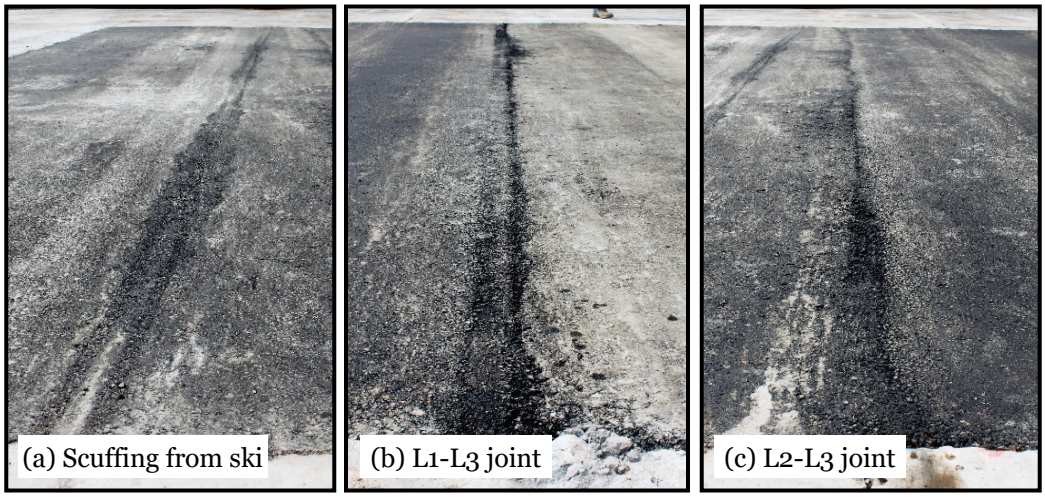

Figure 6.18 shows a noticeably visible depression at the end of R6, L1. As this lane was over-rolled and shoved laterally, it thinned out the lift near the free edge. With each additional pass, this became more exaggerated near the end of the lane where the roller transitioned on and off the repair. Depressions like these were much less of an issue once the roller pattern was modified.

Figure 6.18. Depression at end of repair R6, L1 from over-rolling.

Figure 6.19 shows pavement surface differences between the initial and modified rolling patterns. The surface of R6, L1 exhibited considerable check cracking, which is an indicator that the mix was over-rolled. Once the rolling pattern was modified, check cracking was no longer an issue.

Figure 6.19. Detail of repair R6 pavement surface.

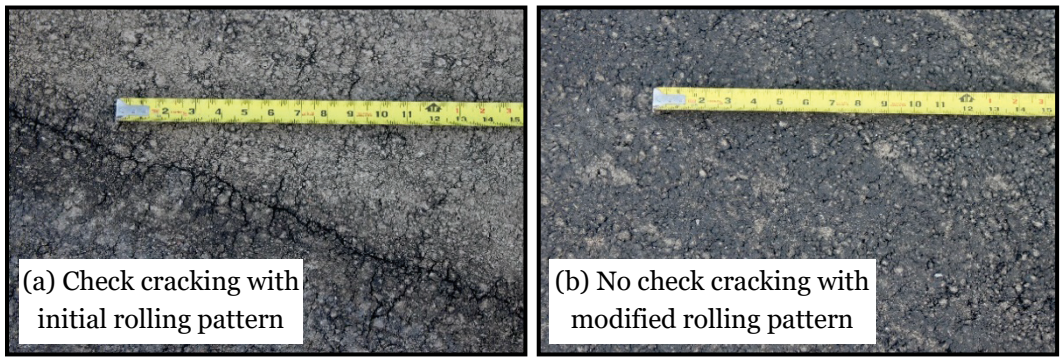

Figure 6.20a shows the screed setup prior to placing R7, L3 where the joints were trimmed. In contrast to repair R6, the end gates for R7 were easily set to the lane width and exhibited no issues matching the joints. Figure 6.20b shows the joints were barely visible once compacted. Not only does this yield a repair that will perform better and last longer, it reduces the likelihood of FOD generation at the joint.

Figure 6.20. Effect of trimming joints on repair R7.

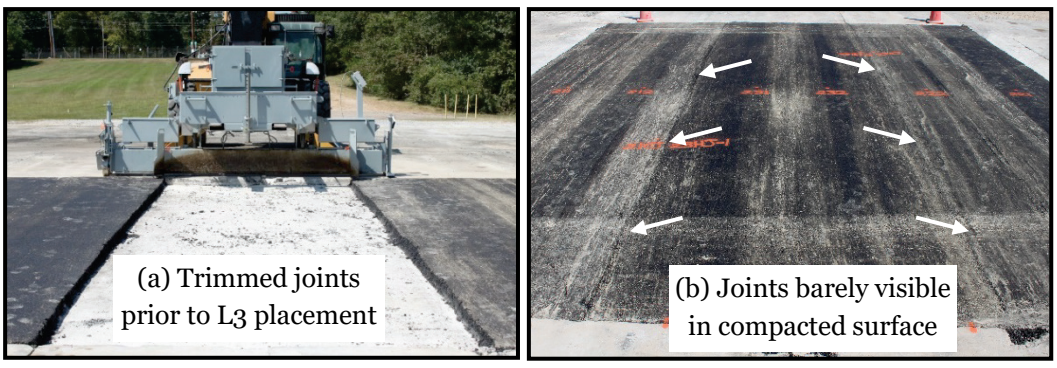

Because the grade control ski scuffed the surface of L2 during repair R6, screeding was performed from the opposite direction for R7, L3. The purpose of this was to investigate how the AGCS would ride on the hotter lane (L2) in comparison to the grade control ski. It was believed the AGCS might fare better since its wheels would roll across the surface rather than skid across it like the ski. Figure 6.21 shows that some minor tracking still occurred, but it did not appear to damage the pavement in any meaningful way. The only exception was one location where the screed was stopped momentarily and the wheels sank into the pavement slightly under the screed's weight. These depressions were isolated to one location and are shown in Figure 6.21c prior to compaction.

Figure 6.21. Tracking from AGCS during repair R7.

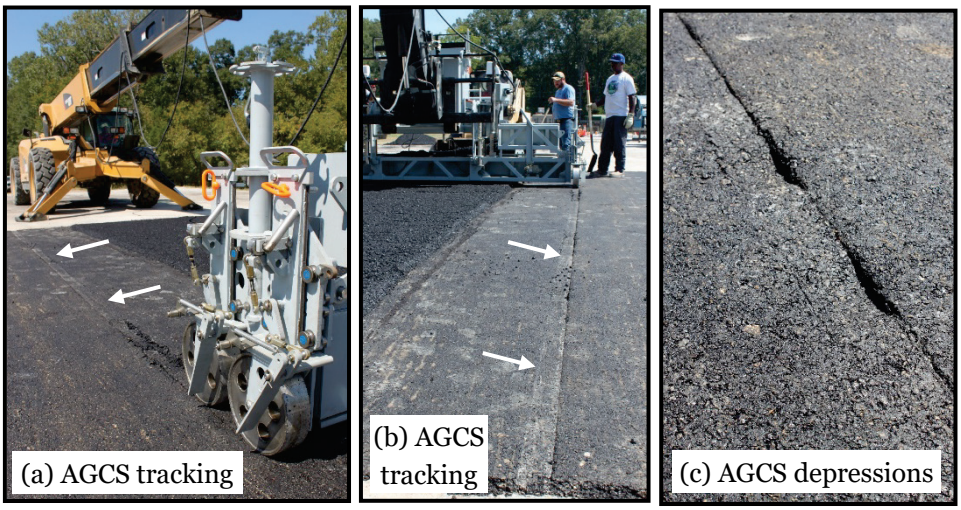

Figure 6.22 shows the areas where grade control devices left marks in the final R7 surface. Figure 6.22a shows that the tracking left by the AGCS is still visible but much less noticeable after compaction. Similarly, Figure 6.22b shows the depressions made by the AGCS wheels were partially corrected during compaction but are still present and more visible than the rest of the AGCS tracking.

The grade control ski rode on the colder outside lane (L1) for R7. No obvious marks were visible during screeding or immediately after compaction; however, viewing the repair early the next day when the light angle from the sun was low revealed very slight scuffing as shown in Figure 6.22c. This mark was almost undetectable at any other time and did not appear to cause any damage to the repair.

Figure 6.22. Tracking and scuffing on completed repair R7.

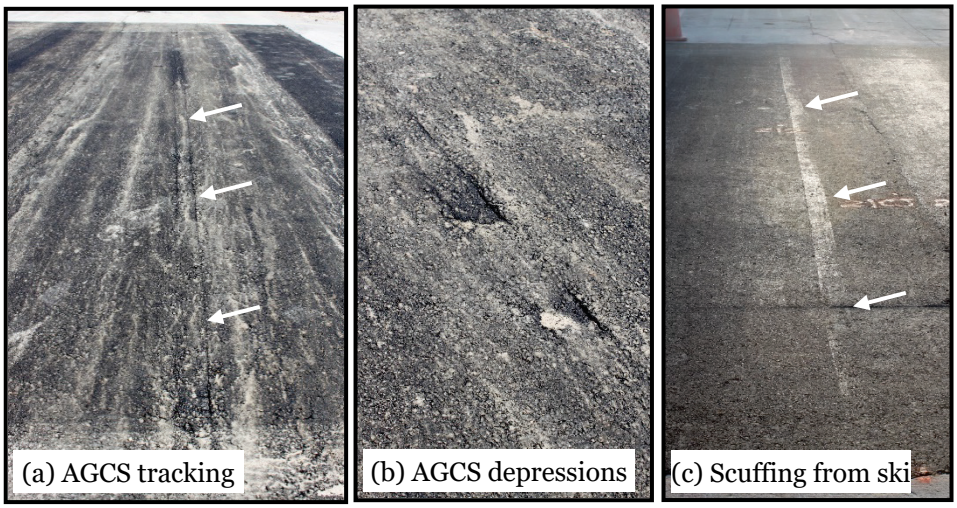

Because the fixed roll-down factor of 1.5 in. was used for repair R7, it was expected that the overall repair elevation, particularly in the middle, might be slightly high. Due to the slight bow wave of asphalt pushed in front of the roller during compaction, this slight overfilling of material tended to build up near both ends of each paving lane. Because this could also be encountered during future RADR operations, the use of two static transverse roller passes applied at each end of the repair was investigated as a possible way to mitigate bumps. This technique was effective; however, it created a slight ridge in the mat along the inside edge of the roller drum. This bump is visible in Figure 6.23 but was well under 0.5 in.

Figure 6.23. Transverse compaction of repair R7.

Figures 6.24 and 6.25 show survey maps of the final surface elevations for repairs R6and R7, respectively. Recall from Section 4.6.1 that asphalt survey data was collected primarily on a 3-ft grid; however, longitudinal point spacing was reduced to 1 ft in the last 3 ft on both ends of the repair to capture dips and bumps associated with the roller

transitioning on and off the repair. Additionally, two longitudinal lines were surveyed at a 1-ft spacing; the two lines were chosen to represent the lowest and the highest longitudinal lines across each repair.

For repair R6 (Figure 6.24), the lowest area of the repair corresponded to the inside edge of L1 where the excessive lateral movement occurred. This was especially pronounced near the west end of the repair as previously discussed (Figure 6.18). This dip was carried across the repair through L3 as well.

Figure 6.24. Repair R6 surface profile survey map.

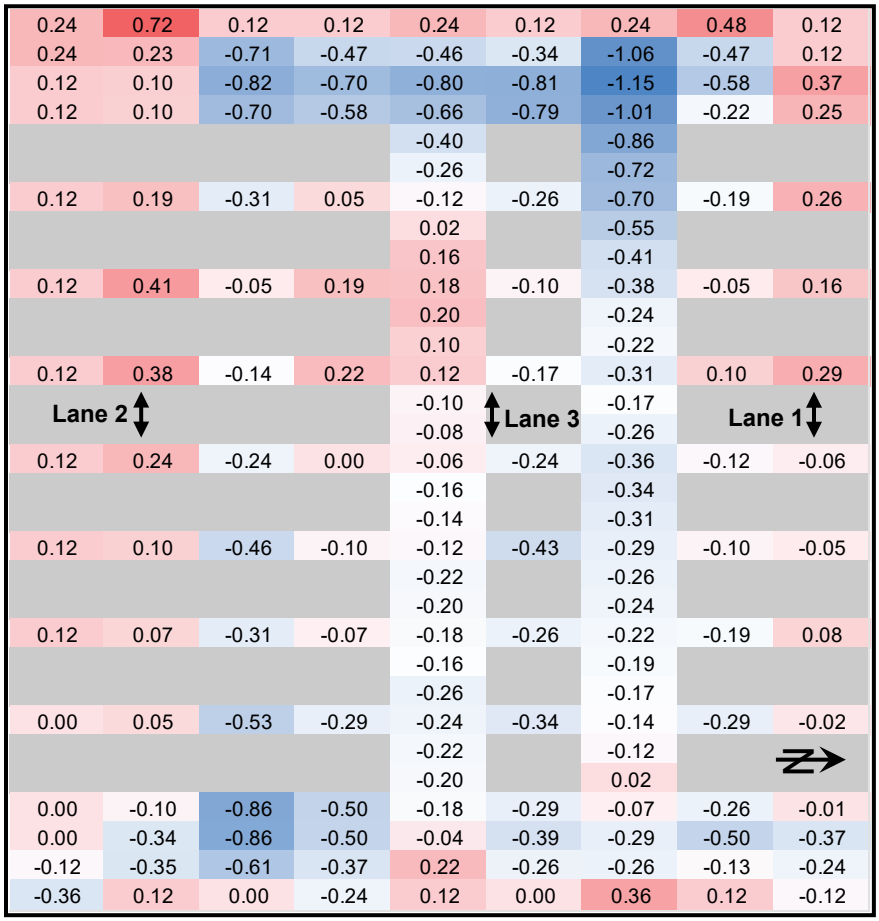

For repair R7 (Figure 6.25), the lowest areas of the repair corresponded to the ends where the transverse roller passes were applied (Figure 6.23). Even though these areas were the lowest of the repair, they were still nearly flush with the existing pavement. Overall, R7's elevation was high. As discussed previously, this was somewhat expected because of the fixed 1.5-in. roll-down factor, and not surprisingly, Figure 6.25 exhibits some similarities to Figure 4.16, which plots the FF surface elevations.

Figure 6.25. Repair R7 surface profile survey map.

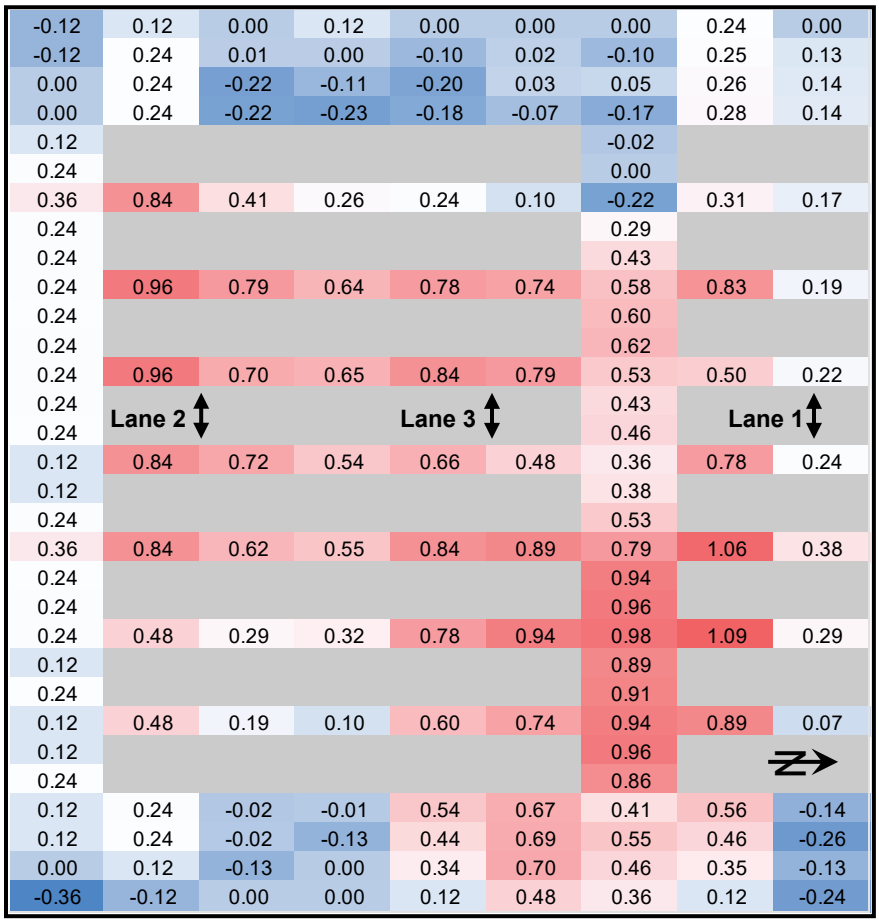

Table 6.7 summarizes the survey data in Figures 6.24 and 6.25 by lane as well as overall. The average overall elevations are -0.17 and 0.32 in. for R6 and R7, respectively, which is within the ±0.75 in. requirement for a flush repair. However, like the large concrete repairs, by definition, the repair would not be considered flush due to the individual areas that exceeded ±0.75 in. For R6, the maximum bump is only 0.72 in., but the maximum depression is -1.15 in.; of all survey points, 6% were lower than -0.75 in. For R7, the maximum depression was only -0.36 in., but the maximum bump was 1.09 in. with 16% of the survey points exceeding 0.75 in. Overall, both repairs classified as Category B repairs as defined in Section 4.6.1.

Somewhat similarly to that of the large concrete repair R1, the RADR screed produced a 95% CI tolerance around ±0.65 in. for both large asphalt repairs. All factors considered, it is actually a meaningful finding that the overall smoothness tolerance for R6 and R7 was similar to that of R1. Aspects that complicate large asphalt repairs compared to large concrete repairs include the following factors. For large asphalt repairs,

the screeded surface is not the final surface because compaction is required; therefore, even if the surface was screed perfectly, compaction introduces new opportunity for error. Further, proper screed elevation depends on proper operation of grade control devices, but even if they work as designed, any imperfections in the FF base will be translated to the asphalt surface (unless tedious grade control adjustments are made throughout screeding). Given these factors, it is actually somewhat impressive that repairs R6 and R7 yielded similar CI tolerances as R1.

Table 6.7. Repairs R6 and R7 survey results.

Statistic		R6 L1	R6 L2	R6 L3	R6 Overall	R7 L1	R7 L2	R7 L3	R7 Overall
Deviation (in.)	Avg	-0.20	-0.11	-0.18	-0.17	0.39	0.24	0.35	0.32
	S.D.	0.33	0.35	0.26	0.32	0.36	0.29	0.36	0.34
	Min	-1.15	-0.86	-0.81	-1.15	-0.26	-0.36	-0.23	-0.36
	Max	0.48	0.72	0.24	0.72	1.09	0.96	0.94	1.09
95% CI, CI (in.)		-0.86 to 0.45	-0.79 to 0.57	-0.68 to 0.32	-0.79 to 0.46	-0.32 to 0.1.10	-0.33 to 0.81	-0.36 to 1.06	-0.35 to 1.00
95% CI Tolerance (in.)		± 0.65	± 0.68	± 0.5	± 0.63	± 0.71	± 0.57	± 0.71	± 0.67
Percent Non-Flush (%)	> +0.75 in.	0.0	0.0	0.0	0.0	23.0	9.8	15.6	16.2
	< -0.75 in.	6.6	5.0	6.5	6.0	0.0	0.0	0.0	0.0
Quality Category		B	B	B	B	B	B	B	B

– *95% confidence interval tolerance represents the tolerance that would include 95% of the repair relative to the average overall deviation (e.g., -0.20 in. for R6, L1), not with respect to a flush repair (i.e., 0.0 in.). The purpose of this metric is to show the overall tolerance for comparison to the ±0.75 in requirement.*

Figure 6.26 presents histograms of R6 and R7 survey data to show the distribution of elevations. Alternatively, Figure 6.27 presents a profile view of each repair by lane. These plots help visualize how little of each repair was out of tolerance with respect to flush repair requirements.

Figure 6.26. Repair R6 and R7 elevation histogram.

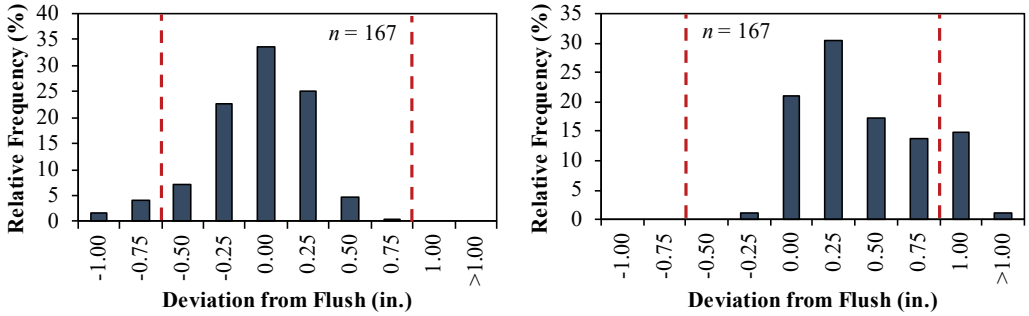

(a) Repair R6

(b) Repair R7

Figure 6.27. Profile view of repairs R6 and R7 elevations by lane.

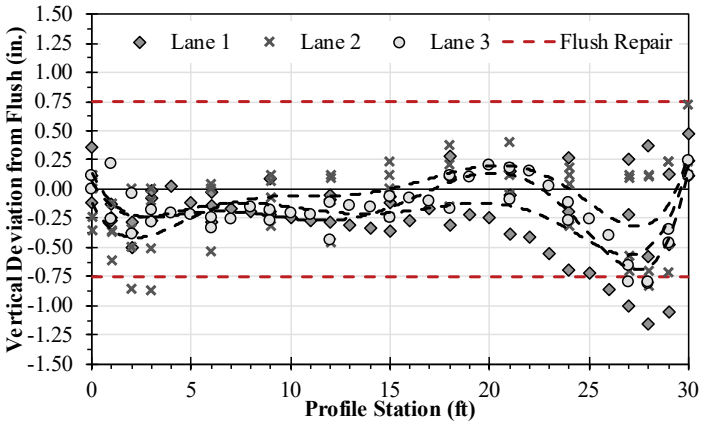

(a) Repair R6

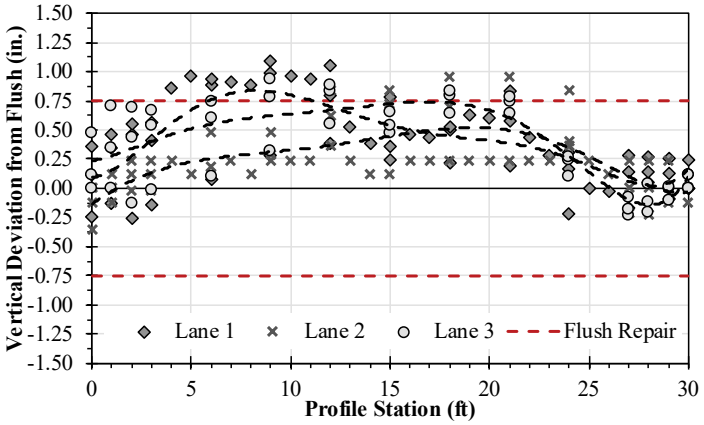

(b) Repair R7

Had R6, L1 been compacted using the modified roller pattern like all other lanes, it is possible that the dips in R6 would have been avoided, and R6 would have been a flush repair. If anything, R7 illustrates the importance of selecting a roll-down factor to match the actual lift thickness; use of a default roll-down factor is not sufficient.

With respect to roll-down factors, Figure 6.28 plots deviation from flush vs. roll-down factor ratio (roll-down factor divided by lift thickness) for repair R7. This plot was possible because the R7 roll-down factor was fixed at 1.5 in., meaning the roll-down factor ratio varied. Repair R6 was not included because roll-down factor ratio was not varied.

Figure 6.28 shows that roll-down factor ratios ranged from approximately 0.40 to 0.58, which resulted in repair surfaces that were 0.1 to 0.5 in. high. Extending the trendline to the x-axis (i.e., perfectly flush), Figure 6.28 suggests that the 3/8-in. per 1-in. lift thickness guideline (i.e., roll-down

factor ratio of 0.375) stated in Section 5.3.1.5 will provide a flush repair. R6, paved at the 0.375 roll-down factor ratio, further supports this; aside from the depressions caused by over-rolling, R6 was very close to flush on average as shown in Figure 6.26. Note that Jackson and Hall (2014) suggested a roll-down factor ratio of 0.44; based on the testing herein, this would have produced a repair approximately 0.15 in. high on average.

Figure 6.28. Flushness vs. roll-down factor ratio for repair R7.

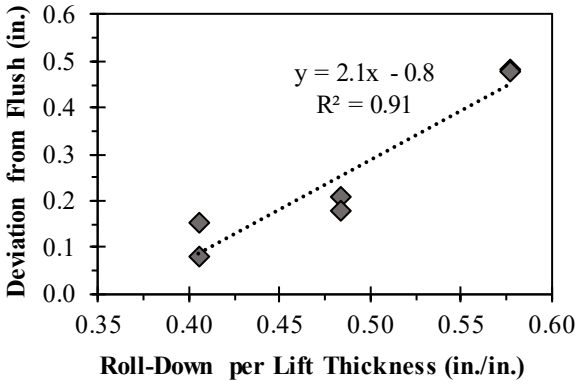

Figure 6.29 presents air void data measured on cores taken from each repair. Each value in Figure 6.29 is the average of two cores. Values representing joints are the average of one core from either side of the joint and within a few inches of the joint. General locations where cores were cut are represented in the figure as well.

Figure 6.29. Air void data for repairs R6 and R7.

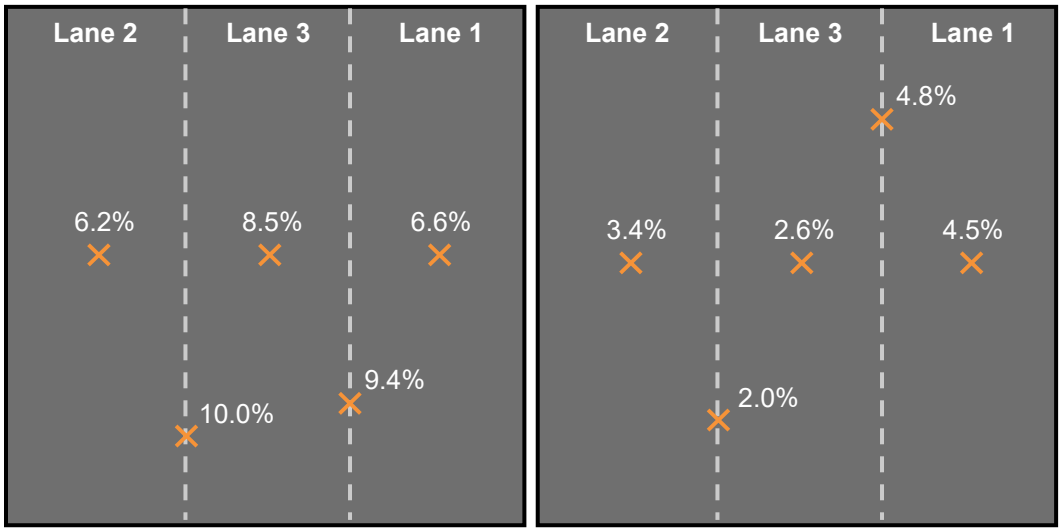

(a) Repair R6 (b) Repair R7

Mat air voids were fairly reasonable for R6, though 8.5% V_a in L3 is higher than desired. Mat air voids were unexplainably low for R7 (cores were retested at a later date and confirmed there were no testing discrepancies); it is difficult to achieve this level of compaction, especially with a single roller type. Note that in-place density did not suffer when the roller pattern was modified to half the passes of the initial pattern. This is another indicator that the initial roller pattern was over-rolling the mix.

Lastly, note the difference in joint air voids between R6 and R7. For R6, air voids at the joints are roughly 2.5 to 3.5% greater than air voids throughout the mat. In contrast, joint air voids for R7 are effectively the same as those of the mat. This further supports the use of the cutoff wheel to trim joints. Not only does a trimmed joint produce a more visually appealing repair, it helps in achieving better compaction at the joint, which will extend the repair's lifespan.

7 Discussion of Results

This chapter discusses overall findings and lessons learned from development and use of the new RADR screed. The focus of this chapter is on high-level discussion of strengths of the RADR screed, key areas of concern for moving forward, and also general observations of large repair processes.

7.1 RADR screed strengths

The RADR screed is the result of multiple years of testing and evaluation of different equipment options, including purpose-built pieces of equipment fabricated in-house or by various vendors under contract. Given the years of effort invested in this concept, the RADR screed is fairly close to successfully providing all the features and attributes required to perform both large and small repairs with either asphalt or concrete. This particular attribute sets the RADR screed apart from previous screed designs that were dedicated to one material type or the other or perhaps worked efficiently only for small repairs but not large repairs.

For small repairs, the RADR screed is fully capable. Small repair screeding, however, does not set the RADR screed apart from other cheaper and lighter alternatives since many other screed options can perform small repairs. The primary key advantage of the RADR screed over others for small repairs, specifically concrete, is that it will not suffer from the fatigue factor. Other screed options are physically taxing on repair teams and become more difficult to use with each successive repair.

For large concrete repairs, the RADR screed offers several advantages relative to the current mag bar screed. It requires virtually no manual labor to operate. The fatigue factor exists for the mag bar screed even for small repairs and is amplified exponentially for large repairs. The RADR screed is faster than the mag bar. In addition to reducing repair times, which has value, it affords the opportunity to make multiple screed passes before the RSC sets. Since RSC tends to flow under the screed bar when fluid, multiple passes are often needed in order to perform a flush repair.

For large asphalt repairs, the RADR screed fills a void that has existed in the search for a suitable screed. Previous screed options have been either too small or too simple to repeatedly perform quality repairs without extreme care by the repair team, or they have essentially been small

asphalt pavers, which affects deployability and increases requirements for training and operator skill level. The RADR screed was able to perform reasonable quality repairs in a manageable time, which is notable since large asphalt repair is the least developed RADR method of the four types.

In addition to the RADR screed's strengths with respect to each type of repair in comparison to the corresponding screed normally used, the overwhelming strength of the RADR screed is its versatility to perform all repair types investigated. This cannot be said of other screeds previously tested. Overall, the RADR screed was considered successful on technical fronts.

7.2 RADR screed areas of concern

7.2.1 Weight and telehandler capacity

The most obvious issue with the RADR screed in its current form is its weight as noted in Section 3.1 and again in Section 6.3 (Figure 6.15). To some degree, a heavy screed has value as this gives it the necessary mass and strength to handle the heavy load of pushing the asphalt pile for large repairs. It is also worth noting that screed weight played a factor for large asphalt repairs only when trying to retract the boom after a lane was placed. While weight was problematic, it did not affect the actual screeding operation (i.e., booming the screed out). Nonetheless, the weight was significant enough to cause some functional issues and needs to be addressed.

Because of the weight issue, the RADR screed in its current form should be thought of as a 95% design version rather than a 100% design version. The recommended course of action would be to address weight reduction as a design revision during the transition to production. Weight reduction should not be difficult to achieve by economizing strategic components of the screed frame and screed bar. For example, wall thickness of certain tubing components could be reduced without negatively impacting screed utility and strength. Some plate components, (e.g., ¼-in. plate on the front of the screed bar) could be replaced with thinner plate. The design could be modified to correct the screed frame's compatibility with telehandler masts, eliminating the 325-lb fork pocket extension adapter.

While weight reduction should be considered in future screed builds and should be achievable fairly easily, it is necessary to understand the impacts of the screed's weight as currently designed. Figure 7.1 shows the load chart for the CAT TL1055C used in this project. On the load chart, the

screed sits at approximately the 5-ft mark on the x-axis when the screed is positioned at the edge of a crater. Total boom distance required is approximately 31 ft to screed a 30-ft crater and exit the far side; this corresponds to the 36-ft mark on the x-axis of Figure 7.1. As indicated by red arrows, the telehandler has a capacity around 3,000 lb at this distance. Thus, it seems reasonable that the telehandler was borderline in terms of handling the 3,575-lb screed (in the asphalt configuration).

Figure 7.1. CAT TL1055C load chart.

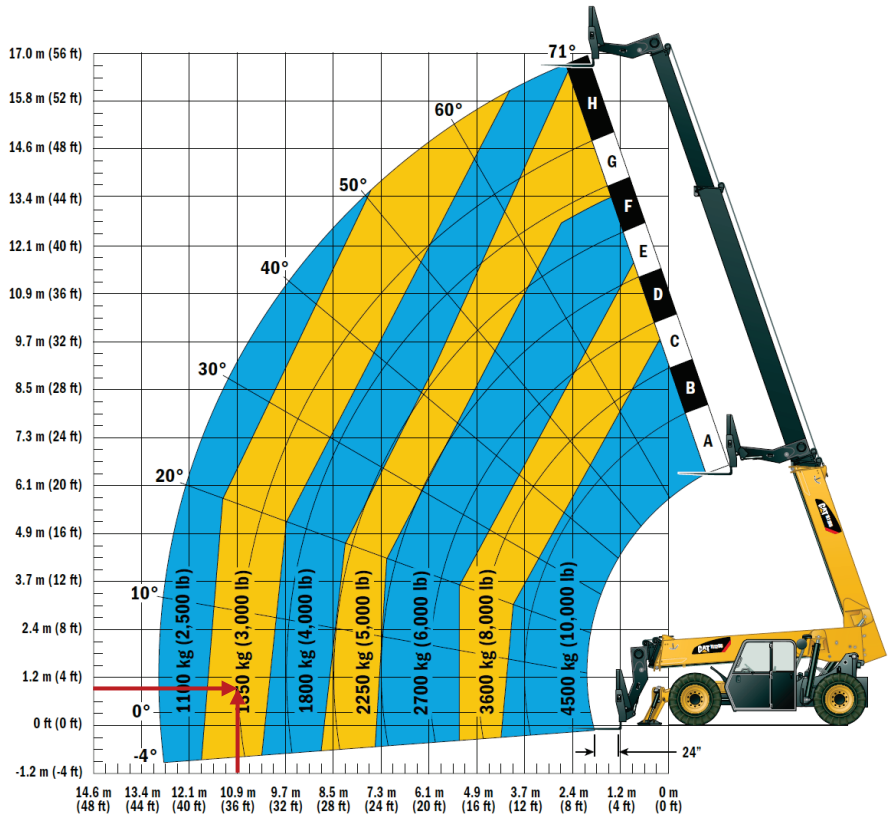

Because the Air Force has fielded the Genie GTH-1256AF in the RADR major repair kit rather than the CAT TL1055C, Figure 7.2 presents the load chart for the Genie model, which is also a 10,000-lb capacity telehandler. Note the GTH-1256AF is sometimes mistaken for a 12,000-lb telehandler due to the "12" in its model number; however, the specifications clearly indicate 10,000-lb capacity (the non-Air Force version, GTH-1256, is in fact a 12,000-lb machine). At the same boom distance required to screed a 30-ft crater, the GTH-1256AF capacity is just under 3,000 lb. Note that the point of load determination on the x-axis differs from 36 ft to 34 ft between Figures 7.1 and 7.2 due to differences in the "zero" position of

each x-axis. Overall, the Genie lift appears to have several hundred pounds less capacity at this distance when compared to the CAT.

Figure 7.2. Genie GTH-1256AF load chart.

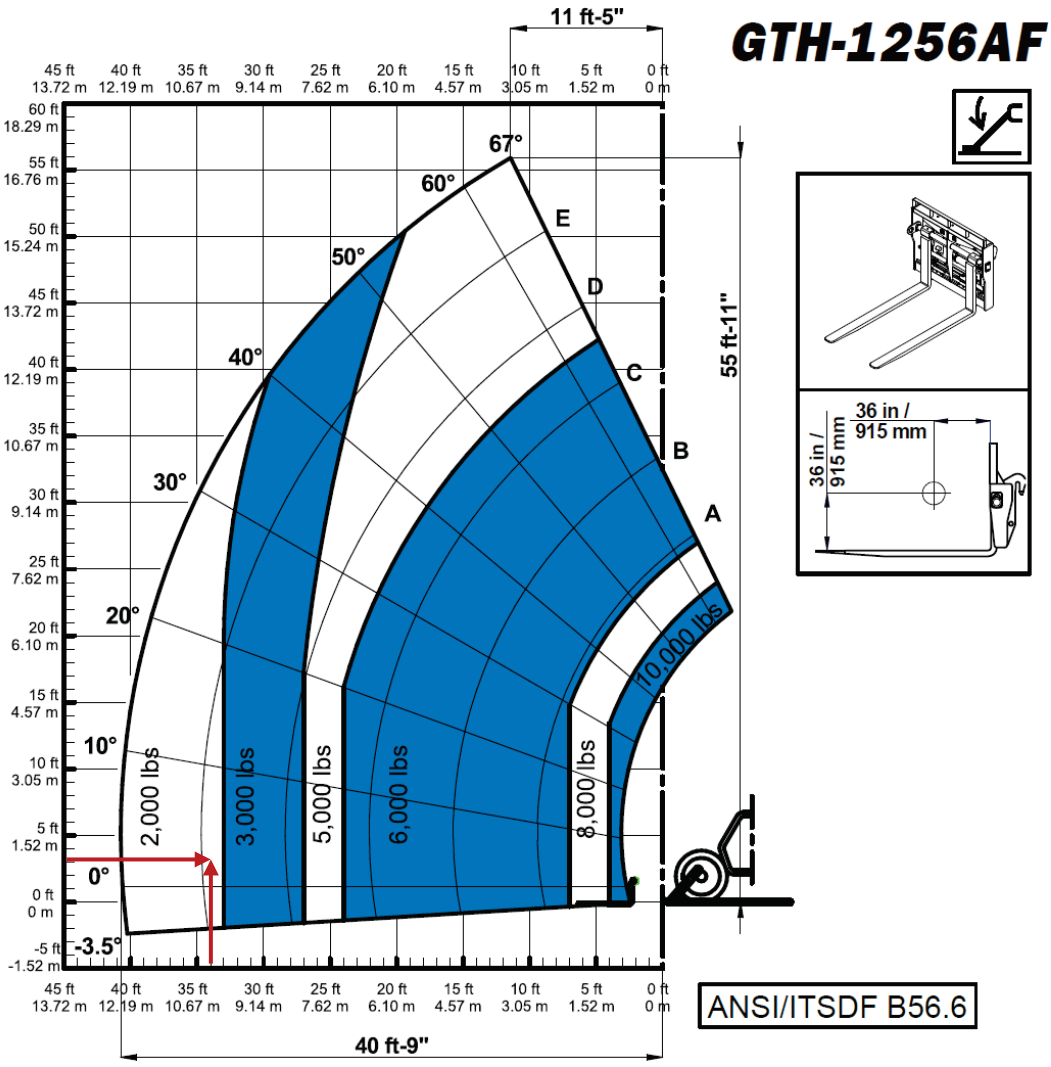

To ensure the RADR screed could be utilized, approximately 600 lb for the CAT lift and perhaps 800 lb for the Genie lift would need to be removed. Eliminating the fork pocket extension adapter would immediately eliminate 325 lb. This leaves an additional 300-500 lb that needs to be trimmed. Discussion with the vendor that built the RADR screed suggests this should be possible.

7.2.2 Large repair finish quality

Large repair methods are less established than small repair methods. As a result, large repairs were the primary interest of this project, and this section documents some of the key challenges observed.

Flush repairs were not achieved for the large repairs performed in this project. Repairs were not necessarily far out of flush tolerances (0.4 in. at most), but they were out nonetheless. It is worth mentioning that a large number of rod-and-level survey points were collected, which provides a much more comprehensive assessment than the stanchion method typically used to assess a repair. If the same repairs were checked with the stanchion method, it is possible that some of the out-of-tolerance points might not have been located. They might have been missed altogether due to the measurement of fewer survey points or to reduced resolution with stanchions relative to a rod and level.

The difficulty in achieving flush repairs is not necessarily attributed to the RADR screed but to overall challenges with large repairs. It is expected that additional procedural refinement will help improve the success rate of flush repairs and minimize RQC issues. The primary concern for large concrete repairs is the potential to overload plastic formwork, and the primary concern for large asphalt repairs is accurate assessment of the FF profile, which is not guaranteed to be a uniform 4-in. depth. These are factors that can be monitored as additional experience with large repairs is gained in order to establish best practices.

Paving a large asphalt repair in multiple lanes is inevitable considering screed width limitations. In turn, this means that longitudinal joints will be present between lanes. Under the current RADR methods, it is difficult to match these joints when paving the adjacent lane; this negatively impacts the final repair surface, potentially with regard to RQC checks, but also with regard to FOD potential. The approach taken in this project to mitigate this issue was to cut back the joint similar to normal airfield construction practices. It is believed this practice will make it easier to perform large asphalt repairs and will produce longer lasting repairs.

8 Conclusions and Recommendations

The objective of this report was to design, build, and test a single integrated screed device that was based on lessons learned from the previous screed integration project (Cox and Hoffman 2019). Key goals for this screed were that it could be used for both small and large crater repairs with either asphalt or concrete and that it was to be operated by a telehandler with minimal personnel requirements (e.g., operator and spotter). This integrated screed device was denoted the RADR screed.

The RADR screed was designed and built in partnership with a commercial vendor and then tested at ERDC with full-scale field testing. Both large and small asphalt and concrete repairs were performed. The screed was considered a technical success in terms of meeting key objectives. The primary deficiency of the RADR screed is that its weight pushes the limits of a 10,000-lb capacity telehandler when its boom extends the approximately 35 ft required for a large repair. Specific conclusions and recommendations are provided in the following sections.

8.1 Conclusions

The following conclusions are presented based on testing and evaluation of the RADR screed.

1. Small repairs
    a. Small repairs were not originally included in the test plan because they did not pose any issues for the integrated screed studied in Cox and Hoffman (2019).
    b. Though not originally planned, the RADR screed was used for four small concrete repairs in this project when an opportunity arose. The RADR screed quickly provided flush repairs.
2. Large concrete repairs
    a. One large concrete repair was performed in this project.
    b. The RADR screed was efficient and allowed multiple passes to be applied before the RSC set.
    c. The final repair surface quality was reasonable with the only significant deficiency being an RQC issue.
    d. Overall, 22% of the survey points measured in the repair were outside the ±0.75-in. limits that define a flush repair. The 95%

confidence statistics show the repair was -0.46±0.66 in. with respect to the surrounding pavement.

e. Non-flush repairs are also common for other screeds including the traditional mag bar and the ASTH. Flush repairs are more challenging for large repairs regardless of the screed used.
f. The RADR screed yielded a non-flush repair largely due to the plastic formwork that does not provide a solid grade control reference for the screed. Measures implemented to control deformation of the forms were moderately successful.

3. Large asphalt repairs
   a. Two large asphalt repairs were performed in this project, each of which was paved in three lanes.
   b. From the beginning of mix placement in a paving lane to the end of compaction, each paving lane required an average of 34 min. Total screeding time for each lane averaged 11 min.
   c. All asphalt attachments performed well with no notable issues.
   d. At 3,575 lb in the asphalt configuration, the RADR screed was too heavy for the CAT TL1055C to retract the boom once the screed had been fully extended across a paving lane. Assistance was briefly needed from another telehandler to help retract the screed.
   e. Final repair surfaces were reasonable other than joint issues on the first repair and RQC deficiencies on both.
   f. The joints were lower quality on the first repair due to the challenge of matching untrimmed joints. This was successfully mitigated by trimming the joints with the cutoff wheel attachment. Trimmed joints were easier to match and yielded higher in-place densities.
   g. For the first repair, 6% of the survey points measured within the repair were outside the ±0.75-in. limits of a flush repair. The 95% confidence statistics show the repair was -0.17±0.63 in. with respect to the surrounding pavement. Low spots were mostly attributed to compaction issues.
   h. For the second repair, 16% of the repair was outside the ±0.75-in. flush-repair limits; 95% confidence statistics show the repair was 0.32±0.67 in. with respect to the surrounding pavement. This was mostly attributed to the use of a fixed 1.5-in. roll-down factor rather than adjusting the roll-down factor based on FF base depth. This illustrated the importance of checking FF base profiles and making adjustments to the roll-down factor if needed.
   i. Results indicate that a roll-down factor of 3/8-in. roll-down per 1-in. lift thickness would provide a flush repair on average.

8.2 Recommendations

Based on the testing conducted in this project with the RADR screed, the overall recommendation is to begin utilizing it for other RADR testing for the sake of training as well as identifying further refinement needs. Specific recommendations are as follows.

1. Small repairs
   a. No additional recommendations are required.
   b. The RADR screed functions as intended.
2. Large concrete repairs
   a. The technique of rolling the screed bar to take pressure off plastic forms should be practiced more as additional large crater repairs are performed. It should be determined whether this is a reliable means of consistently controlling dips on the formwork side of repairs.
   b. Plastic forms and their installation process should be assessed to determine whether formwork strength could be improved.
   c. Expansion board material, if pre-attached to formwork before the repair is performed, should be recessed below the tops of forms slightly so it is not snagged by the screed bar.
3. Large asphalt repairs
   a. The surface profile of the FF base should be assessed prior to asphalt paving in order to set proper roll-down factors for each paving lane (3/8-in. roll-down per 1-in. of lift thickness).
   b. The cut-off wheel should be used to trim longitudinal joints before paving the middle lane as this procedure aids in matching joints, improving joint density, and reducing FOD potential.
   c. The standard rolling pattern described in the Interim RADR TTPs should be evaluated. The standard pattern caused check cracking and excessive lateral shoving. The modified pattern (half the compactive effort) eliminated check cracking, minimized shoving, and still achieved reasonable density.
4. General
   a. The RADR screed should be considered for implementation.
   b. As efforts transition from initial prototype testing to production of units for fielding, specific focus should be given towards weight reduction. The RADR screed is currently 600-800 lb overweight depending on the telehandler used. Eliminating the fork pocket extension adapter will remove 325 lb. Remaining weight should be removed by strategically economizing components where logical.

Many components of the screed could be fabricated from thinner plate steel or tubing with reduced wall thickness.

c. Once the suggested modifications above are completed, a full-scale demonstration in which active-duty airmen are allowed to operate the screed is recommended. This will allow for feedback on screed design, training, and operation, as well as realistic timing data using troop labor.

References

American Society for Testing and Materials (ASTM). 2011. *Standard test method for theoretical maximum specific gravity and density of bituminous paving mixtures*. Designation D2041-11. West Conshohocken, PA: ASTM.

_____. 2016a. *Standard test method for ball drop on controlled low strength material (CLSM) to determine suitability for load application*. Designation D6024/D6024M-16. West Conshohocken, PA: ASTM.

_____. 2016b. *Standard test method for linear drying shrinkage of concrete masonry units*. Designation C426-16. West Conshohocken, PA: ASTM.

_____. 2016c. *Standard test method for preparation and testing of controlled low strength material (CLSM) test cylinders*. Designation D4832-16. West Conshohocken, PA: ASTM.

_____. 2017a. *Standard test method for bulk specific gravity and density of compacted asphalt mixtures using automatic vacuum sealing method*. Designation D6752-17. West Conshohocken, PA: ASTM.

_____. 2017b. *Standard test method for flow consistency of controlled low strength material (CLSM)*. Designation D6103-17. West Conshohocken, PA: ASTM.

_____. 2017c. *Standard test method for static segregation of self-consolidating concrete using column technique*. Designation C1610/C1610M-17. West Conshohocken, PA: ASTM.

_____. 2018. *Standard test method for compressive strength of cylindrical concrete specimens*. Designation C39/C39M-18. West Conshohocken, PA: ASTM.

Defense Logistics Agency (DLA). 2015a. *Detail specification: concrete capping material, rapid setting*. MIL-DTL-32536. Washington, DC: Department of Defense.

_____. 2015b. *Detail specification: flowable fill backfill material, rapid setting*. MIL-DTL-32537. Washington, DC: Department of Defense.

Bell, H. P., B. C. Cox, L. Edwards, L. I. Garcia, N. R. Hoffman, M. Mejías-Santiago, and J. L. Johnson. 2019. *Rapid airfield damage recovery technology integration experiment*. ERDC/GSL TR-19-8. Vicksburg, MS: U.S. Army Engineer Research and Development Center.

Carruth, W. D. 2019. *Evaluation of commercially available screeds for finishing of rapid-setting concrete*. ERDC/GSL TR-19-4. Vicksburg, MS: U.S. Army Engineer Research and Development Center.

Cox, B. C., and N. R. Hoffman. 2019. *Development of an integrated pavement screed for screeding asphalt or concrete crater repairs*. ERDC/GSL TR-19-39. Vicksburg, MS: U.S. Army Engineer Research and Development Center.

Cox, B. C., and T. A. Carr. 2018. *Camouflet repair alternatives*. ERDC/GSL TR-18-20. Vicksburg, MS: U.S. Army Engineer Research and Development Center.

Edwards, L., H. P. Bell, and M. Opperman. 2021. *Alternatives for large crater repairs using rapid set concrete mix®*. ERDC/GSL TR-21-16. Vicksburg, MS: U.S. Army Engineer Research and Development Center.

Jackson, C. J., and J. Hall. 2014. *Development of tactics, techniques and procedures to cap large crater repairs with hot-mix asphalt*. AFCEC-CX-TY-TR-2014-0025. Tyndall Air Force Base, FL: U.S. Air Force Civil Engineer Center.

United States Air Force (USAF). 1992. *Crushed-stone crater repair and line-of-sight profile measurement for rapid runway repair*. TO 35E2-5-1. Washington, DC: USAF.

USAF, Air Force Civil Engineer Center (AFCEC). 2013. *Engineering technical letter (ETL) 13-3: Minimum airfield operating surface selection and repair quality criteria*. ETL 13-3. Washington, DC: USAF.

_____. 2016. *Air Force tactics, techniques, and procedures: Minimum airfield operating surface (MAOS) selection and repair quality criteria (RQC)*. 3-32.12. Washington, DC: Department of Defense.

_____. 2019. *Interim tactics, techniques, and procedures (TTPs); interim process for rapid airfield damage repair (RADR)*. Rev 13.1. Washington, DC: Department of Defense.

Unit Conversion Factors

Multiply	By	To Obtain
degrees Fahrenheit	(F-32)/1.8	degrees Celsius
feet	0.3048	meters
gallons (U.S. liquid)	0.1336	cubic feet
inches	0.0254	meters
miles per hour	0.44704	meters per second
pounds (mass)	0.45359237	kilograms
square feet	0.09290304	square meters
square yards	0.8361274	square meters
yards	0.9144	meters

REPORT DOCUMENTATION PAGE

Form Approved
OMB No. 0704-0188

Public reporting burden for this collection of information is estimated to average 1 hour per response, including the time for reviewing instructions, searching existing data sources, gathering and maintaining the data needed, and completing and reviewing this collection of information. Send comments regarding this burden estimate or any other aspect of this collection of information, including suggestions for reducing this burden to Department of Defense, Washington Headquarters Services, Directorate for Information Operations and Reports (0704-0188), 1215 Jefferson Davis Highway, Suite 1204, Arlington, VA 22202-4302. Respondents should be aware that notwithstanding any other provision of law, no person shall be subject to any penalty for failing to comply with a collection of information if it does not display a currently valid OMB control number. **PLEASE DO NOT RETURN YOUR FORM TO THE ABOVE ADDRESS.**

1. REPORT DATE *(DD-MM-YYYY)*	2. REPORT TYPE	3. DATES COVERED *(From - To)*
September 2022	Final	

4. TITLE AND SUBTITLE

Evaluation of a Prototype Integrated Pavement Screed for Screeding Asphalt or Concrete Crater Repairs

5a. CONTRACT NUMBER

5b. GRANT NUMBER

5c. PROGRAM ELEMENT NUMBER

6. AUTHOR(S)

Ben C. Cox, Nolan R. Hoffman, and Thomas A. Carr

5d. PROJECT NUMBER
471376

5e. TASK NUMBER

5f. WORK UNIT NUMBER

7. PERFORMING ORGANIZATION NAME(S) AND ADDRESS(ES)

Geotechnical and Structures Laboratory
U.S. Army Engineer Research and Development Center
3909 Halls Ferry Road
Vicksburg, MS 39180-6199

8. PERFORMING ORGANIZATION REPORT NUMBER

ERDC/GSL TR-22-24

9. SPONSORING / MONITORING AGENCY NAME(S) AND ADDRESS(ES)

Headquarters, Air Force Civil Engineer Center
139 Barnes Avenue, Suite 1
Tyndall AFB, FL 32403-5319

10. SPONSOR/MONITOR'S ACRONYM(S)

11. SPONSOR/MONITOR'S REPORT NUMBER(S)

12. DISTRIBUTION / AVAILABILITY STATEMENT

Approved for public release; distribution is unlimited.

13. SUPPLEMENTARY NOTES

U.S. Air Force Rapid Airfield Damage Recovery (RADR) Program

14. ABSTRACT

Finishing, or screeding, the hot mix asphalt or rapid-setting concrete surface of a crater repair is important for rapid airfield damage recovery (RADR) since it determines the aircraft ride surface quality. The objective of RADR repairs is to expediently produce a flush repair, defined as ±0.75 in. of the surrounding pavement surface, with minimal logistical and personnel burden. Multiple screeds were previously evaluated; the most recent project proposed a prototype design of a telehandler-operated integrated screed for both small and large repairs using asphalt or concrete. This project's objective was to finalize the prototype design and fabricate and test the prototype RADR screed.

The prototype RADR screed was successful for small repairs (8.5×8.5 ft). Large repairs (30×30 ft) were generally successful with modest repair quality criteria (RQC) issues being the only notable deficiencies. Large concrete repair RQC issues were attributed to plastic formwork movement, and large asphalt repair RQC issues were attributed to compaction issues or improper roll-down factors. Methods to mitigate these factors were investigated but should be further evaluated. Overall, the RADR screed was successful from technical perspectives but, functionally, is 600-800 lb overweight. Weight reduction should be considered before entering production.

15. SUBJECT TERMS

Rapid airfield damage repair
Military bases
Equipment and supplies–Evaluation
Pavements
Asphalt
Concrete
Screeding
Finishing
Runways (Aeronautics)–Maintenance and repair

16. SECURITY CLASSIFICATION OF:			17. LIMITATION OF ABSTRACT	18. NUMBER OF PAGES	19a. NAME OF RESPONSIBLE PERSON
a. REPORT	b. ABSTRACT	c. THIS PAGE			19b. TELEPHONE NUMBER *(include area code)*
Unclassified	Unclassified	Unclassified	SAR	132	